Functional analysis of transcription factor *mScratch2* in cortical neurogenesis

Dissertation

for the award of the degree
Doctor rerum naturalium (Dr. rer. nat.)
Division of Mathematics and Natural Sciences
of the Georg-August-University Göttingen

submitted by
Vanessa Paul
from Menden (Germany)

Göttingen, September 2010

Thesis Advisor:
PD. Dr. Anastassia Stoykova

Doctoral Committee:

PD Dr. Anastassia Stoykova (1st Referee)	*Molecular Cell Biology, Max-Planck-Institute for biophysical Chemistry, Göttingen*
Prof. Dr. Tomas Pieler (2nd Referee)	*Developmental Biochemistry, Georg-August-University, Göttingen*
Prof. Dr. Klaus Armin Nave	*Neurogenetics, Max -Planck- Institute for Experimental Medicine, Göttingen*

Date of submission of thesis: September 30th, 2010
Date of oral exam: November 5th, 2010

Affidavit

I hereby declare that my doctoral thesis entitled "**Functional analysis of transcription factor *mScratch2* in cortical neurogenesis"** has been written independently with no other sources and aids than quoted.

……..

Vanessa Paul, Göttingen, September 2010

This work has been generated at the Max Planck Institute for Biophysical Chemistry - Karl-Friedrich-Bonhoefer-Institute - in Göttingen in the group of PD. Dr. Anastassia Stoykova (Molecular Developmental Neurobiology).

TABLE OF CONTENS

TABLE OF CONTENS IV

ABSTRACT VIII

1. INTRODUCTION 1

1.1 ORGANIZATION OF THE FOREBRAIN DURING DEVELOPMENT 1

1.1.1 Neural induction and formation of the mammalian telencephalon 1

1.1.2 Patterning and regionalization of the cerebral cortex 2

1.2 NEUROGENESIS IN MAMMALIAN NEOCORTEX 4

1.2.1 Cortical cell heterogeneity 4

1.2.2 Mechanisms of cortical layer formation 5

1.2.3 Cortical cell fate specification and differentiation 8

1.2.4 bHLH-TFs specify neural cell fates and regulate neuronal migration 10

1.3 THE TRANSCRIPTION FACTOR SCRATCH2 11

1.3.1 The superfamily of C_2H_2 zinc-finger transcription factors 11

1.3.2 Expression and functions of *Scratch* orthologs in vertebrates 13

1.4 SCOPE OT THE THESIS 14

2. RESULTS 15

2.1 EXPRESSION OF *mSCRT2* DURING EMBRYONIC AND POSTNATAL DEVELOPMENT 15

2.1.1 Expression in the mouse embryo 15

2.1.2 Down-regulation of *mScrt2* expression in the *Pax6*- deficient cortex 17

2.1.3 *mScrt2* expression in the perinatal and postnatal murine brain 18

2.1.4 *In-silco* analysis of alternative spliced mRNA isoforms of the mScrt2 gene 20

2.2 CONDITIONAL OVEREXPRESSION OF *mSCRATCH2* IN THE DEVELOPING CORTEX 22

2.2.1 Generation of a construct for conditional *mScrt2*-overexpression 22

2.2.2 Cre-recombinase mediated over expression of *mScrt2* in the developing cortex 24

2.2.3 *In-vivo* analysis of corticogenesis in *mScrt2* gain-of-function condition 27

2.3 INVESTIGATION OF THE MODE OF CORTICAL PROGENITOR DIVISION IN *SCRT2.2*-GOF BY CLONAL-PAIR ANALYSIS 34

2.4 ANALYSIS OF CORTICAL CELL MIGRATION AFTER FOCAL OVEREXPRESSION OF SCRT2.2 AND SCRT2.3 BY *IN-UTERO* ELECTROPORATION 38

2.5 ECTOPIC EXPRESSION OF *mSCRT2.2* IN EMBRYOS OF *XENOPUS LEAVIS* 44

2.6 CONDITIONAL KNOCKOUT OF *SCRT2* IN THE MOUSE 47
2.6.1 Generation of a construct for conditional knockout of *Scrt2* 47
2.6.2 Gene targeting in ES cells for generation of chimeric mice with a floxed *Scrt2* locus 50

3. DISCUSSION 53

3.1 Expression of the *mScratch* gene in the developing and adult brain suggests a role in the transition from cell proliferation to differentiation 53

3.2 TF *Scrt2* modulates the neuronal outcome of cortical neurogenesis 55

3.3 *mScrt2.2* promotes neurogenic versus proliferative division of cortical progenitors 57

3.4 mScrt2 influences cell migration in the developing cortex 59

3.5 Putative Scrt2-dependent mechanisms that could modulate the cortical neurogenesis and gliogenesis 61

4. METHODS 63

4.1 ANIMALS 63

4.2 HISTOLOGY 63
4.2.1 Cryo-conservation and sectioning of mouse brains 63
4.2.2 Cresylviolet (CV) staining 63
4.2.3 ß-galactosidase staining (whole mount) 64
4.2.4 ß-galactosidase staining (cryoslides) 64
4.2.5 Generation of DIG-labelled anti-sense RNA probes 64
4.2.6 *In-situ* hybridization on cryosections 65
4.2.7 Immunohistochemical staining (IHC) 66
4.2.8 Immunohistochemical staining (IHC) for goat-antibodies 67
4.2.9 Immuno-cytochemical staining (ICC) 67

4.3 GENERATION OF SCRT2 CKO-VECTOR BY RECOMBINEERING 67
4.3.1 Hybridisation of high-density filters (PAC library) 68
4.3.2 Generation of a conditional knock-out construct via recombineering 69
4.3.3 Gene targeting in mouse ES cells to produce chimeric mice 72
4.3.4 Southern blot 72

4.4 ANIMAL TREATMENTS 74
4.4.1 BrdU injections 74
4.4.2 *In-utero* electroporation 74

4.5 CELL CULTURE 75

4.5.1 Cortex dissection and dissociation 75
4.5.2 Clonal pair analysis and immuno-cytochemistry 76
4.5.3 Over expression *in-vitro* by transient cell transfection 76

4.6 MOLECULAR BIOLOGY 77
4.6.1 Extraction from genomic DNA from mouse cut-tails 77
4.6.2 Genotyping of mice 77
4.6.3 PCR 77
4.6.4 DNA electrophoresis and isolation from agarose gel 78
4.6.5 Isolation and -purification of plasmid-DNA from *E.coli* 78
4.6.6 Restriction enzyme digest of DNA 78
4.6.7 De-phosphorylation / blunting of linear DNA fragments 78
4.6.8 Measurement of nucleotide concentrations 78
4.6.9 Ligation 79
4.6.10 Preparation of electro-competent cells 79
4.6.11 Transformation of *E. coli* by electroporation 79
4.6.12 Total RNA isolation 80
4.6.13 cDNA synthesis 80
4.6.14 Total protein extraction and Bradford-measurement 80
4.6.15 Western blotting 80

4.7 EXPERIMENTS IN XENOPUS LEAVIS 81
4.7.1 Animals 81
4.7.2 Constructs 81
4.7.3 Embryo isolation 81
4.7.4 mRNA injection 81
4.7.5 Dexamethasone treatment 82
4.7.6 X-Gal staining 82
4.7.7 (Whole mount) – *in-situ* hybridisation 82

5. MATERIAL 83

5.1 KITS 83

5.2 BACTERIAL STRAINS 83

5.3 OLIGONUCLEOTIDES 84
5.4.1 Vectors 85
5.4.2 Anti-sense plasmids for ISH 85

5.4 ANTIBODIES 85
5.4.1 Primary Antibodies 85
5.4.2 Secondary antibodies (peroxidase-conjugated) 86

II. REFERENCES 87

III. SUPPLEMENT 99

INDEX OF FIGURES / TABLES 107

IV. ACKNOWLEDGEMENTS 109

V. CURRICULUM VITAE 110

ABSTRACT

The neocortex, a specific for the mammals layered structure that cover the forebrain, is characterized by an enormous cellular diversity as a result of several coordinated developmental processes that regulate the spatio-temporal generation of multiple neuronal and glial cell types. The origin of most of the cell types during corticogenesis is the pluripotent radial glia progenitors (RGPs) in the ventricular zone. RGPs are also the source of a second type of neurogenic progenitors, called intermediate progenitors (IPs). IPs have a role in the amplification of distinct neuronal fates, generated at particular developmental stages, predominantly influencing the generation and expansion of the upper cortical layer neurons, an evolutionary hallmark of higher species. In order to produce specific cell types in a appropriate number, the cell divisions of cortical progenitors must be precisely controlled to balance progenitor maintenance (proliferation) and neural differentiation.

Here, the first functional *in-vivo* study of the mammalian *Scratch2 (mScrt2)*, a newly identified member of the C_2H_2 zinc-finger transcriptional factors, is presented. The obtained findings could be summarized in the following:

1. *mScrt2* expression is CNS-restricted and specifically found at transition zones that contain proliferating and post-mitotic cells, confined to embryonic and postnatal regions, indicating a role in the promotion of neuronal differentiation. Additionally, evidence is presented for the presence of functionally different *mScrt2*-transcripts.

2. Conditional over expression of *mScrt2.2* in the developing cortex of generated transgenic mice revealed an increase in neuronal differentiation at early stages of neurogenesis and a severe reduction of cortical thickness at postnatal stages, mainly affecting the upper cortical layers. The mechanism behind could be partially determined by quantitative analysis of the mode of cortical progenitor divisions, that trend to undergo neurogenic divisions at the expense of IP generation and amplification, thus causing an early depletion of cortical progenitors and subsequent decrease in the number of cortical neurons.

3. The results suggests a role for *mScrt2* in the regulation of radial migration of neurons across the cortex by promoting the “multipolar migration” type, a mechanism that is assumed as a kind of arrest for a subpopulation of late-born neurons at the border subventricular/intermediate zone.

4. Ectopic *mScrt2* expression in *Xenopus leavis* embryos indicated that primary neurogenesis was influenced in a spatio-temporal specific manner, suggesting a conserved between mouse and frog function in the CNS-development.

In conclusion, by promoting the neurogenic mode of RGP-divisions and IPs, the mammalian *mScratch2* appears to modulate neuronal differentiation and migration in the developing cortex, with important consequences for the neocortical morphogenesis of the

adult brain. The results allow suggesting, that *mScrt2* is probably interfering with pro-neural bHLH transcription factors, and is acting in an evolutionary conserved *Pax6*-dependent genetic pathway, regulating the cortical neurogenesis.

1. INTRODUCTION

The nervous system is characterized by a considerable complexity that is reflected by its cellular diversity as well as the variety of functions it performs. The mammalian brain is the most complex organ evolved during evolution that receives inputs from sensory organs and transforms them into controlled motor activity and specific behavioural outputs. The cerebral cortex is the origin of higher cognitive functions, such as learning and memory.

The multi-functional brain develops at the anterior part of the central nervous system (CNS). The cerebral cortex (pallium) forms from the dorsal part of the telencephalon, the rostral-most vesicle formed after the closure of the neural tube early in the embryonic development. The cortex is subdivided into allocortex (medial pallium), an evolutionary older part and neocortex (dorsal, lateral pallium) that underwent the most rigorous changes during evolution. As a hallmark of the mammalian brain, especially in case of more "advanced" species such as primates, the neocortex is characterized by a big expansion, especially of the upper neuronal layers that form folds (gyri) and grooves (sulci). These changes are connected to an increasing complexity, reflected by enormous cellular diversity as a result of several coordinated developmental processes that include: neuroectoderm induction, proliferation, neuronal fate specification, differentiation, migration, maturation, axonal growth as well as guidance. A challenging mission in the field of developmental neurobiology is to itemize the molecular players behind the cellular mechanisms that play a role in generation and functioning of this complex structure, the mammalian neocortex.

1.1 ORGANIZATION OF THE FOREBRAIN DURING DEVELOPMENT

1.1.1 Neural induction and formation of the mammalian telencephalon

The origin of the CNS is the neuroectoderm, which is induced to form prior to gastrulation. In the mouse, the anterior visceral endoderm (AVE) is secreting the powerful morphogen Fgf8 to induce a pre-neural stage with anterior characteristics. According to the activation / transformation model, the neural fate is actually a “default state” of the ectoderm, being suppressed by BMP signalling between the ectodermal cells (reviewed in Meinhardt, 2001; Weinstein and Hemmati-Brivanlou, 1999). During gastrulation the neural fate is fully de-repressed and maintained by BMP-antagonists (activin, noggin, follistatin) emanated from the anterior part of the early involuting mesoderm (named the node in mouse, or the Spemann Organizer in amphibians (Spemann and Mangold, 2001), generating neural plate with anterior characteristic. Later on, secreted factors like Wnts, FGFs and retinoic acid (RA) from the later involuting mesoderm (the future notochord), posteriorize the caudal part of the neural tube that forms the spinal cord. As a result of complex interplay between distinct

signalling pathways, finally the anterior-posterior (AP) axis of the embryo and CNS is established. In mouse, the neural tube closes dorsally at around embryonic (E) day E8, forming three vesicles (prosencephalon, mesencephalon, rhombencephalon). Later, the prosencephalon subdivides to form the vesicles of the telencephalon and diencephalon (Fig. 1). The internal cavity of the neural tube gives rise to the ventricular system. Furthermore, the telencephalon regionalizes into the cortex (pallium) dorsally and into the basal ganglia (subpallium) ventrally. The specification of different cell fates in the forebrain is further achieved through extrinsic and intrinsic cues that determine a certain progeny fate in a given neuroepithelial compartment.

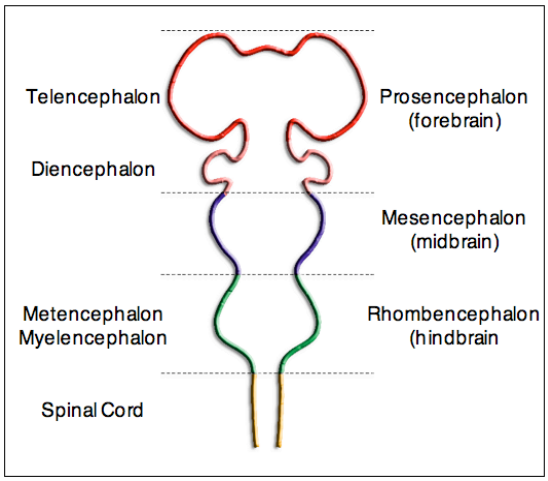

Figure 1: The primary brain vesicles. The three primary vesicles (right panel) get further subdivided as development continues (left panel).

1.1.2 Patterning and regionalization of the cerebral cortex

Patterning refers to a spatio-temporal order of neural differentiation. The cortical neurons are radially arranged into six layers and tangentially into functional areas that control distinct functions e.g. motor, sensory, visual and auditory functions. This process is mediated via a hierarchical order of intrinsic and extrinsic cell mechanisms.

The initial positional information along the AP and dorso-ventral (DV) axes of the developing telencephalon is given by morphogens and ligands secreted from inductive centres: the anterior neural ridge (Fgf8), the ventral prechordal mesendoderm (Shh), the dorsal roof plate (BMP4, Wnt3), the hem (Wnts, BMPs) in the medial wall and the antihem located at the border between the dorsal and ventral pallium (secreting the Wnt-antagonists, e.g. sFRP2).

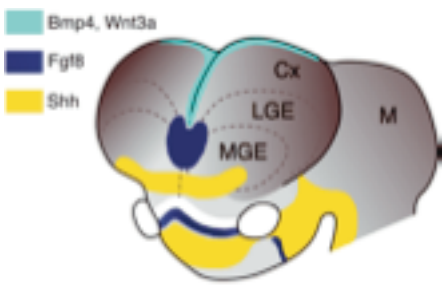

Figure 2: Inductive signalling centres in the telencencephalon. (anterior neural ridge (blue), ventral prechordal mesendoderm (yellow), dorsal roof plate (cyan). The hem (in medial wall) and the antihem at the pallial-subpallial border are not indicated in this schema.

The information of the combinatorial code of such positional cues is interpreted by a graded gene expression, specifying grid-like compartments in the telencephalic proliferative neuroepithelium (reviewed by Borello and Pierani, 2010;

Henke et al., 2009). The dorsal and the ventral part of the telencephalon are thereby specified by sets of regionally restricted, graded expression of distinct evolutionary conserved homeodomain transcription factors (HD-TFs) with important functions for progenitor proliferation, differentiation and acquisition of distinct cell fates (Schuurmans et al., 2004; Schuurmans and Guillemot, 2002; Sur and Rubenstein, 2005).

The neocortex is a mammal specific six-layered structure generated in the dorsal telencephalon. During development, the anlage of the prospective neocortex is marked already at stage E8.5 by the expression of TF *Pax6*, while the region of the prospective basal ganglia (medial and lateral ganglion eminences, MGE, LGE) is characterized by the expression of TFs *Gsh2* and *Nkx2.1* (Fig. 3; (Rallu et al., 2002). These pattern genes belong to two different classes of HD-TFs that cross-repress their expression, thus establishing a sharp boundary between the pallial and subpallial progenitor domains (named also the cortico-striatal border). Two members of the bHLH, TF *Ngn2* and *Mash1* show similar restricted expression confined to the progenitors in the ventricular zone (VZ) of the pallium and subpallium, respectively. Notably, the TF *Ngn2* was found to act as a direct *Pax6* downstream target, able to repress and restrict the regionalized expression of *Mash1* to the subpallium (Fode et al., 2000). Thus, the TF Pax6 plays a crucial role in regulation of a gene hierarchy to establish the cortico-striatal border even before the onset of neurogenesis in the developing telencephalon (Fig.3).

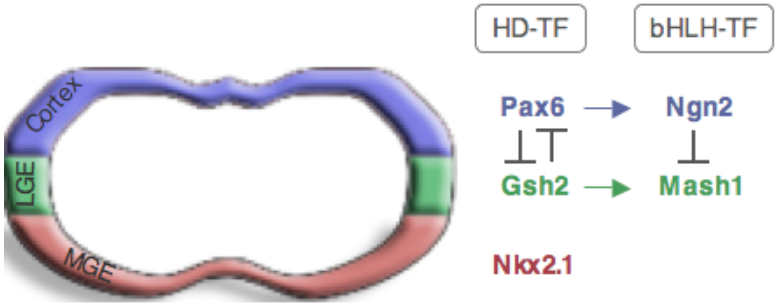

Figure 3: Patterning of the telencephalon. Along the dorso-ventral axis, the telencephlalon is subdivided into the cortex (pallium) and the basal ganglia (subpallium), composed of the lateral and medial ganglion eminences (LGE, MGE). The compartments of the neuroepithelium are specified by the restricted expression of HD-TFs, that cross-repress their expression and in turn regulate the expression of bHLH-TFs to establish the pallial-subpallial border (PSPB, modified from Rallu et al., 2002).

Recent evidences provided important new knowledge about the mechanisms of cortical area formation and area distribution along the AP-axis of the cortex (reviewed by Mallamaci and Stoykova, 2006; Muzio et al., 2002; O'Leary et al., 2007). Originally two models for the arealization of the neocortex have been proposed: the protomap theory (Rakic, 1988) assuming, that all information for establishment of the cortical areas is encoded by

intrinsic genetic programs in the progenitors and the protocortex theory (O'Leary, 1989), hypothesizing that the thalamo-cortical axons (TCA), connecting distinct sensory nuclei of the thalamus with their corresponding cortical areas provide the neocortex with activity-dependent area identity. Nowadays, the main view states that cortical functional arealization includes a complex interplay between intrinsically encoded "proto map" in the VZ, modulated by extrinsic environmental cues, including TCA, that stabilize the final area size and maintain the sharply bordered gene expression. Recent evidence indicate that cortical arealization and layer formation are interconnected processes, exemplified e.g. by the rather different thickness of one and the same layer in two adjacent cortical domains (Dehay and Kennedy, 2007). In addition, regional and layer specific expression of molecular determinants in post-mitotic neurons in the cortical plate (CP) contribute to cortical patterning. For instance, while TF *bhlhb5* mediates the acquisition of caudal and layer5 fates (Joshi et al., 2005), TF *Tbr1*, expressed at highest level in layer 6 of the rostral (motor) cortex, has the capacity to regulate gene expression in post-mitotic neurons and suppresses caudal/layer5 identities (Bedogni et al., 2010).

1.2 NEUROGENESIS IN MAMMALIAN NEOCORTEX

1.2.1 Cortical cell heterogeneity

The majority of the neuronal and glia cells of the neocortex arise from a proliferative zone encircling the lumen of the neural tube, the ventricular (VZ), and subventricular (SVZ) zone. The cortical cells are arranged in cyto-architecturally and functionally defined patterns exhibiting specific molecular properties. The neocortex is composed of excitatory glutamatergic projection neurons that extend axons to distant intracortical, subcortical and subcerebral targets and interneurons that are GABAergic (γ-amino butyric acid) cells making local connections and born from subpallial progenitors.

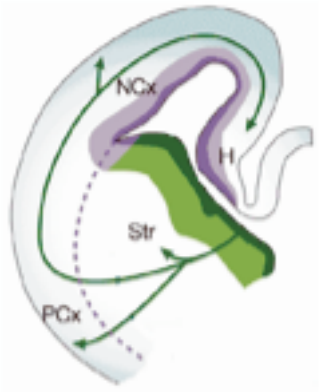

Figure 4: Origins and migrational pathways of cortical neurons. Glutamatergic projection neurons (purple) are generated in the VZ/SVZ of the neocortex (NCx) and migrate radially into the cortical plate (CP), while GABAergic interneurons (green) are generated in the VZ/SVZ of the ganglion eminences and migrate tangentially into the cortex, hippocampus (H) as well into the piriform cortex (PCx); (adopted from Marin, 2003)

While the generated in the VZ/SVZ projection neurons subsequently migrate radially along the processes of the radial glia progenitors (RGPs) to form the cortical plate, the interneurons migrate tangentially for long distances to their final locations within the

neocortex (Götz and Sommer, 2005; Marin, 2003; Nadarajah et al., 2003).
All neurons of the mouse cortex are generated during the developmental time window E9 - E18, with a peak of neurogenesis at E14.5 (Bayer and Altman, 1991). After the onset of cortical neurogenesis, the located in the VZ radial glia progenitors sequentially generate neurons, astrocytes and oligodendrocytes, according to an intrinsic program recapitulated even in primary cortical cultures *in-vitro* (Qian et al., 2000). The three cell types occur in a temporally distinct, albeit overlapping pattern (Sauvageot et al., 2002). Shortly before birth (E18.5 - E19.5), the RGPs transform into astrocytes. The oligodendrocytes are generated in two waves. During development (around E13.5), progenitors of the MGE start to generate oligodendrocytes that migrate tangentially into the cortex. In addition, beginning at postnatal stage P1, the progenitors in the SVZ produce oligodendroglial cells with a peak around P14 (Bayer and Altman, 1991; reviewed by Miyata et al., 2010).

1.2.2 Mechanisms of cortical layer formation

The huge number of neuronal and glia cells that built the mammalian cortex derive from a single pseudo-stratified layer consisting of neuroepithelial progenitors (NEPs) that line the ventricular wall of the neural tube after its closure. Before the beginning of neurogenesis (E8-E10), the NEPs undergo several rounds of symmetric cell divisions that expand the initial pool of multipotent progenitors (Götz and Huttner, 2005; Guillemot et al., 2006). The first half of the cortical histogenesis is thus marked mostly by proliferative progenitor divisions that cause a tangential expansion of the ventricular surface (Caviness and Takahashi, 1995), while the neurogenic divisions expand the cortical thickness radially (Rakic, 1972). At this early stages only a very small portion of NEPs divide asymmetrically to generate the first neurons that form the cortical preplate (PP). After the initiation of generation of CP neurons, they intercalate into the PP and subdivide it into the marginal zone (MZ), populated by the Cajal-Retzius cells, and interneurons and subplate, located below the CP (Götz and Barde, 2005; McConnell, 1995; Smart, 1973).

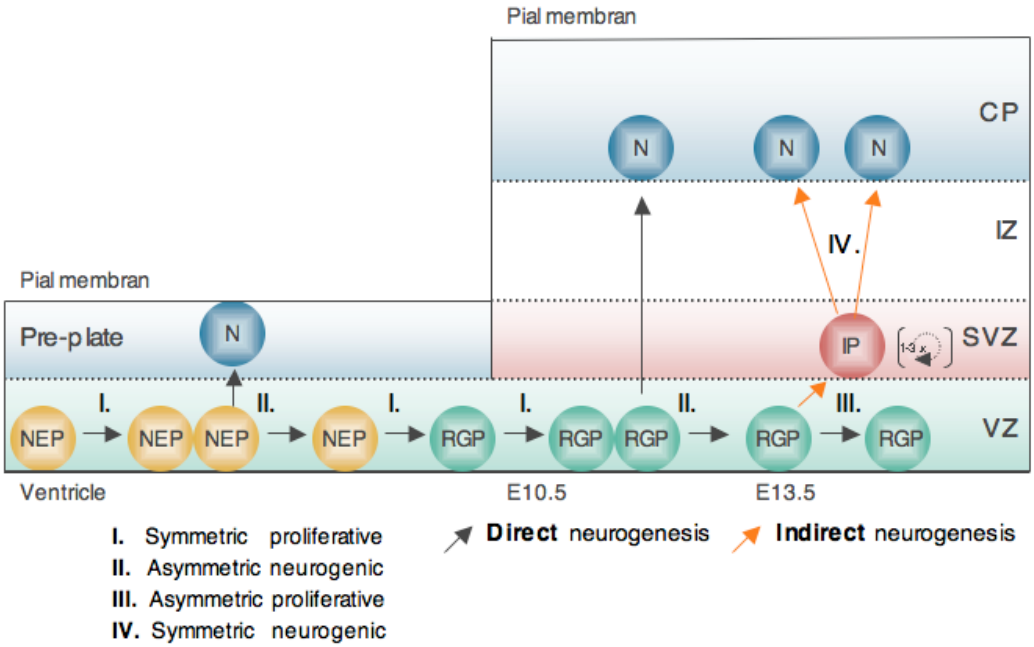

Figure 5: Progenitor cell divisions and modes of neurogenesis in the mammalian cortex. Neuroepithelial cell progenitors **(NEP)** divide symmetrically **(I.)** to expand the initial pool of multipotent progenitors. Rarely they divide asymmetrically **(II.)** to generate the first neurons in the cerebral cortex, the pre-plate cells. After the onset of cortical neurogenesis (around E9), NEPs give rise to bipolar radial glial progenitors **(RGP).** RGPs divide symmetrically **(I.)** creating two RGPs, or asymmetrically giving rise either to one RGP and one post-mitotic neuron (N) **(II**.) in the direct mode of neurogenesis, or to one RGP and one intermediate progenitor **(IP) (III).** Most of the IPs undergo directly symmetric neurogenic divisions **(IV)** to generate two neurons, while only a smaller fraction undergoes one to three more rounds of proliferative division to produce two IPs, which subsequently generate neurons (indirect mode of neurogenesis).

At the onset of cortical neurogenesis, NEPs give rise to bipolar RGPs, the second type of progenitors in the VZ. Beside their role in the generation of almost 90% of the cortical cells, the RGPs extend their long processes from the VZ to the pial surface, providing thereby a scaffold for the generated neurons to migrate to their final location in the CP (Rakic, 1972, 2003). The RGPs loose some epithelial features of NEPs, but share with NEPs some characteristics such as the interkinetic nuclear migration (INM), apico-basal polarity, apical junctions (Chenn et al., 1998), gap junctions and the expression of nestin and RC2 (Bennett and Roberts, 2003; Bittman et al., 1997; Chanas-Sacre et al., 2000; Hartfuss et al., 2001; Misson et al., 1988). During distinct phases of the mitotic cycle, the nuclei of the RGPs undergo INM: in G1 phase the nucleus is located throughout the VZ-depth, progressively moving towards the basal surface of the VZ where they enter into the S-phase (DNA duplication); in the G2 phase, the nucleus moves towards the apical (ventricular) surface of the VZ and when reaching it, the cell enters into M-phase and RGPs divide (reviewed by Götz and Huttner, 2005; Misson et al., 1988). RGPs exhibit also astroglial properties (Kriegstein and Götz, 2003) expressing markers like glial fibrillary acidic protein (GFAP), vimentin and

brain-lipid binding protein (BLBP) (Campbell and Götz, 2002; Kriegstein and Götz, 2003). Because of these glial features and the fact that they are able to transform into astrocytes around birth, it was originally proposed, that the RGPs are progenitors of the glia cell lineage only. Nowadays, however, several evidences indicated, that those cells are pluripotent progenitors, producing both neuronal and glial cells (Campbell and Götz, 2002; Kriegstein and Gotz, 2003; Malatesta et al., 2000; Noctor et al., 2001; Pinto and Götz, 2007).

To produce cortical neurons, RGPs undergo three different types (see Fig.5 I-III; Noctor et al., 2004) of divisions: 1) Symmetric divisions giving rise to two identical daughter cells which both represent RGPs (self-renewal); 2) asymmetric divisions generating one RGC and one post-mitotic neuron, (direct mode of neurogenesis) and 3) asymmetric divisions generating one RGP and an intermediate progenitor (IP), named also basal progenitors. The IPs are amplifying cells that undergo mitosis at the basal (abventricular) side of the VZ to generate neurons (via indirect mode of neurogenesis). After stage E13.5 in the mouse embryo, their histological accumulation forms a second proliferative zone - the subventricular zone (SVZ) (reviewed by Campbell and Götz, 2002; Götz and Sommer, 2005).

At molecular level, IPs can be distinguished from the RGPs by the expression of TF *Tbr2* (Englund et al., 2005), *Cux1* and *Cux2* (Nieto et al., 2004; Zimmer et al., 2004), *Svet1* (Tarabykin et al., 2001), *Ngn2* (Miyata et al., 2004) and as recently shown by *Insm1* (Farkas et al., 2008). In contrast to RGPs, the IPs express neither the TF *Pax6* nor members of the pro-proliferative *Hes* family of transcription factors (Cappello et al., 2006; Englund et al., 2005; Ohtsuka et al., 2001). The absence of apico-basal polarity is thought to restrict IPs to the symmetric mode of division and might explain why such divisions can occur with nearly random cleavage-plane (Attardo et al., 2008). Most of the IPs are exclusively neurogenic (IV in Fig.5) by generating two neuronal daughter cells, while a smaller fraction of them undergo one to three rounds of proliferative divisions in SVZ to produce two IP daughter cells, which will subsequently give rise to two neurons (Haubensak et al., 2004; Miyata et al., 2004; Noctor et al., 2004; Wu et al., 2005). Thus, the IPs actually amplify the output of distinct neuronal fates generated after the asymmetric RGP division at a given developmental stage (indirect mode of neurogenesis). Remarkably, the proportion of IPs and hence the SVZ, becomes very large in the cerebral cortex of primates. During mid-neurogenesis, it contains more than 90% of the progenitor pool (Rakic, 2002; Smart et al., 2002).

The neurons of the different neocortical layers are generated in a tightly controlled temporal order, as illustrated in Fig. 6 (Caviness and Takahashi, 1995; Nowakowski et al., 2002). The laminar structure of the neocortex is generated through proliferation, migration and differentiation of neurons in a stereotypical “inside first - outside last” pattern.

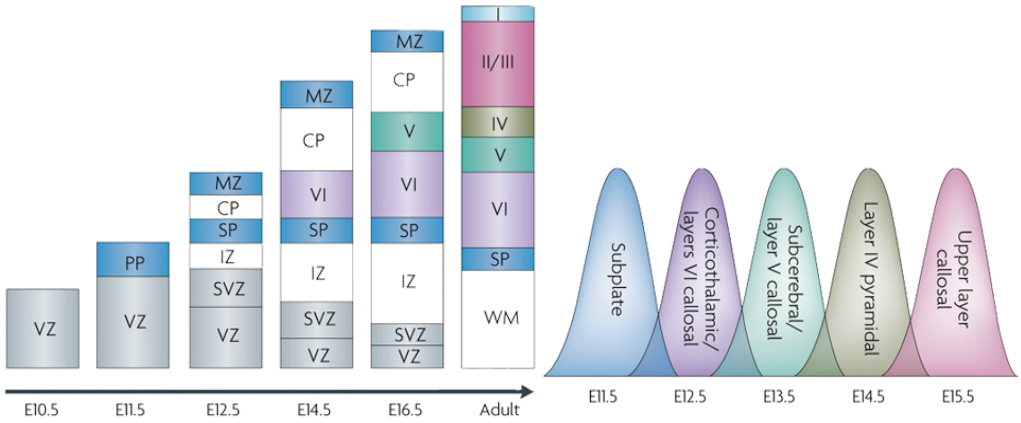

Figure 6: Generation of neocortical layers. Progenitors in the germative layers (grey) produce the neurons of the cortical layers in an "Inside-first outside-last" schedule between E10.5 and E18.5 (mouse). The peak of neurogenesis of the individual layers is indicated on the right, while their appropriate position in the postnatal / adult cortex is highlighted on the left in corresponding colour, (adopted from Molyneaux et al., 2007)

The earliest generated cortical neurons which appear at around E10.5 in mice, migrate away from the VZ to form the preplate (PP), which is subsequently split via the first cortical plate neurons into the marginal zone (MZ) and the subplate (SP) (Luskin and Shatz, 1985). Early-born neurons (during the period E10-E14 in mouse) form the lower layers 6 and 5 (L6, L5) and neurons generated by the late progenitors (E14.5-E18.5) form the upper layers (L4-2) (Rakic, 1988). The newly post-mitotic neurons are specified to adopt the laminar position characteristics of their time point of generation (McConnell, 1995) since neurons that end up in the same laminar position tend to share similar functional properties, patterns of connectivity (O'Leary and Koester, 1993) and intrinsic molecular factors (1.2.3).

1.2.3 Cortical cell fate specification and differentiation

The unique functional features of distinct neuronal populations in the cortex are also reflected by differentially expressed sets of transcription factors and regulatory molecules. Some marker genes are expressed in a certain progenitor population and subsequently, in early post-mitotic and differentiated neurons of particular layers. For example, *cut-like 2* (*Cux2*) is expressed in intermediate progenitors in the SVZ during the generation of upper-layer neurons as well as postnatal in subsets of neurons of layers 2-4, indicating that *Cux2* marks upper-layer progenitors within the SVZ (Nieto et al., 2004; Zimmer et al., 2004). TFs *Pax6*, along with *Tlx* has been shown to control the proliferation of the apical RGPs during the establishment and expansion of the VZ. In both, the *Pax6* and *Tlx* mutant mice, deep-layer neurons are generated, whereas the upper cortical layers are severely underrepresented (Estivill-Torrus et al., 2002; Haubst et al., 2004; Land and Monaghan, 2003; Schuurmans et al., 2004). Similar mechanisms were reported to underlay the cortical phenotypes of both,

Pax6-KO and *Tlx*-KO mice that include a premature exit of large portion of RGPs from mitosis, leading to a substantial limitation of the progenitor pool for late neurogenesis (Li et al., 2008; Tuoc et al., 2009).

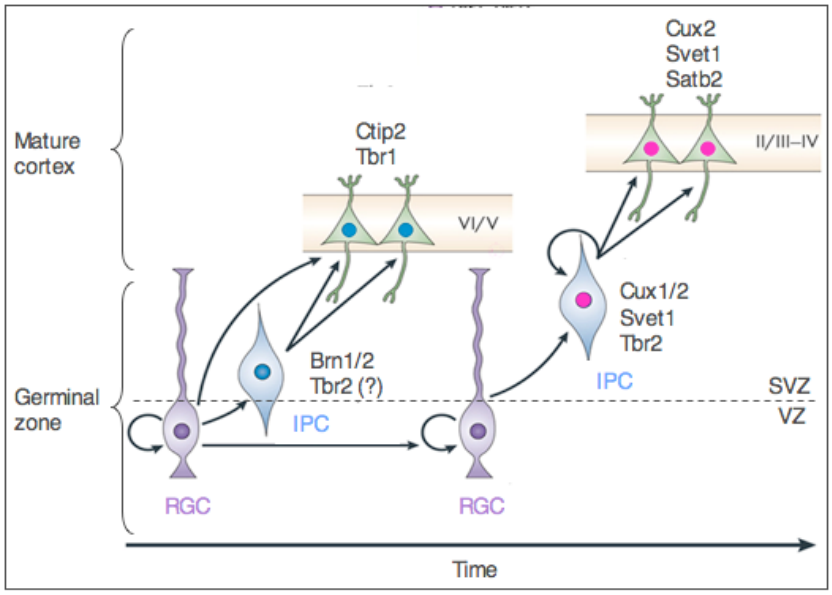

Figure 7: Lineage restricted genes in subpopulations of cortical projection neurons and their corresponding progenitors. Radial glia cells (RGC) in the ventricular zone (VZ) directly produce neurons or they produce intermediate progenitor cells (IP). The early IPs (blue nucleus) that produce neurons for the lower layers 6/5 express a different set of transcription factors than the later generated IPs (pink nucleus) that produce neurons for the upper layers 2-4. Neurons of the upper or lower layers themselves express different transcription factors that they either share with their progenitor or exclusively express after cell cycle exit (adopted from Molyneux et al., 2007; Pinto et al., 2009)

Recently, large scale *in-situ* hybridization projects (Lein et al., 2007; Visel et al., 2004), creation of transgenic mouse lines expressing GFP under the control of promoters of lineage- or layer-restricted genes (Gong et al., 2003) and micro array analysis of micro-dissected regions of the neocortex (Zhong et al., 2004), dramatically expanded the number of known layer- and subtype-specific genes (reviewed by Molyneaux et al., 2007). For instance, while the B-cell leukaemia/ lymphoma 11B (*Ctip2*) gene, is expressed at high level in neurons of layer 5 and at much lower level in neurons of layer 6 (Arlotta et al., 2005), *Satb2* is expressed only in a subgroup of the upper layer (UL) neurons. The pattern of *Satb2* expression, confined predominantly to young UL neurons, but not to SVZ progenitors, suggests that it may be involved in the control of early aspects of UL neuron specification (Britanova et al., 2008; Nieto et al., 2004; Zimmer et al., 2004). *Tbr1* is expressed in multiple types of cortical neurons and has a broad impact for neuronal differentiation (Bulfone et al., 1995; Hevner et al., 2001). In the absence of *Tbr1* there are abnormalities in projection neuron migration, and defects in axon extension (Britanova et al., 2008; Nieto et al., 2004; Zimmer et al., 2004). In addition, recent evidence indicate, that TF *Tbr1* regulates the

regional and laminar identity of post-mitotic neurons in developing cortex (Bedogni et al., 2010).

1.2.4 bHLH-TFs specify neural cell fates and regulate neuronal migration

bHLH-TFs are key regulators in the determination of precursor cells towards neural (pro-neuronal) versus other cell fates. A subset of these factors, such as the pro-neuronal bHLH proteins *Ngn1*, *Ngn2* or *Mash1* are arranged in a cascade that affects different stages of neuronal commitment and differentiation. Thereby, they act in a combinatorial code along with other transcription factors to specify neuronal identity. Pro-neuronal proteins themselves are negatively regulated by inhibitory bHLH- Id and Hes proteins (among others) that are involved in setting up a negative feedback pathway of lateral inhibition (reviewed by Justice and Jan, 2002) involving NOTCH and DELTA signalling. Thus, the pro-neuronal and inhibitory bHLH genes regulate each other in an antagonizing way, allowing only subsets of cells to undergo differentiation while keeping others to stay neural stem cells (reviewed by Bertrand et al., 2002; A. Philpott, 2010).

As a third class of bHLH factors, the differentiation proteins are regulated by the pro-neural (positively) and inhibitory (negatively) bHLH factors that act as transcriptional activators or repressors, respectively. Differentiation bHLH proteins are members of the NeuroD/ Nex family and include NeuroD, NDRF (NeuroD-related factor) and Nex (also called Math2). Like pro-neuronal bHLH factors, bHLH differentiation proteins are E-box binding transcriptional activators that, when over expressed, are sufficient to induce cell cycle arrest and neuronal differentiation in culture (Farah et al., 2000). The expression pattern of the *NeuroD/Nex* family, however hints to a distinct function *in-vivo*. Whereas pro-neural bHLH factors are expressed in progenitors that subsequently give rise to both, neurons and glia (Nieto, 2001), members of the NeuroD/Nex family, at least in the CNS, are specific to cells that are (or will become) neurons. The expression of these bHLH differentiation genes begins in the immature neuron and is maintained during neuronal differentiation (Lee et al., 2000). Accordingly, these factors are expressed in the cortical plate, but not in the ventricular zone (Schwab et al., 1998). However, the absence of a cortical phenotype for the single and double knockouts of the NeuroD / Nex family members (Miyata et al., 1999; Olson et al., 2001; Schwab et al., 2000; Schwab et al., 1998) point to the existence of yet uncharacterized molecular determinants that mediate differentiation of neurons in the neocortex. In this regard *bHLHb5*, a largely uncharacterized bHLH factor of the Olig family, has been shown to have a specific expression in post-mitotic neurons of the superficial layers of the neocortex (Xu et al., 2002), whose function in neuronal differentiation remains to be elucidated.

Pro-neuronal bHLH factors have been also shown to reinforce neuronal differentiation by inhibiting the expression of glial genes and are required *in-vivo* to prevent premature and excessive gliogenesis (Morrison, 2001). The concept of oscillating activity of bHLH proteins during the generation of neurons, astrocytes and oligodenrocytes (Ross et al., 2003) highlights the suggestion, that bHLH factors may have more than one function during development. For example, an increase in Hes proteins activity prior to the neurogenic phase may maintain cortical precursors in an undifferentiated state, whereas an increase of *Hes1* and *Hes5* expression, subsequent to the neurogenic phase support astrocyte differentiation. The maintenance of cortical precursors is thereby partially achieved through the ability of Hes factors to antagonize the action of pro-neuronal bHLH proteins. In contrast, Notch-dependent induction of astrocytes occurs in collaboration with BMPs, the interleukin-6 family of cytokines (IL-6, LIF, CT-1) and ciliary neurotrophic factor (CNTF) (Barnabe-Heider et al., 2005; He et al., 2006; Ochiai et al., 2001).

Furthermore, bHLH factors are not only key regulators in the acquisition of a generic neural fate and the specification of cell identities in a spatio-temporal order, but also in the promotion of cell migration. Mechanistically, pro-neuronal bHLH factors regulate the expression of genes critically involved in migration, including down-regulation of RhoA small GTPase and up-regulation of doublecortin and p35, which, in turn, modulate the actin and microtubule cytoskeleton assembly and enable newly generated neurons to migrate. Thus, pro-neuronal bHLH genes serve as molecular “linkers” connecting neurogenesis with migration (Ge et al., 2006).

1.3 THE TRANSCRIPTION FACTOR SCRATCH2

1.3.1 The superfamily of C_2H_2 zinc-finger transcription factors

Snail genes form the founder gene family of the Snail-like transcriptional factors. Along with the Snail family, *Scratch* genes constitute a related to, but independent subgroup of the superfamily of C_2H_2 zinc finger TFs. These families have a common origin in evolution (Fig. 9a, b), where the duplication of a single snail gene in the metazoan ancestor gave rise to two gene families, *Snail* and *Scratch*. They underwent independent duplications in the different Cnidaria and Bilateralia, and gave rise to a number of genes in each group (Barrallo-Gimeno and Nieto, 2009; Nieto, 2002). In the last years, these two founder subgroups have been augmented for further subgroups such as the Fez and Gfi factors, and Insm and Ovo proteins. Until now, more then 150 genes of 52 species have been identified that belong to this superfamily, ranging from simple placozoan to humans (Barrallo-Gimeno and Nieto, 2009; Nieto, 2002).

Common characteristic of the members of this huge superfamily is the highly conserved C-terminus of the proteins, coding for four to six zinc fingers of the C_2H_2 (cysteine/histidine) type (Fig. 8c, d), mediating DNA-binding to a site that is consisting of the six bases CANNTG. Interestingly, this so-called E-box motif is identical to the core-binding site of bHLH-transcription factors, having crucial roles in neuronal differentiation. The much more divergent N-terminus may contain a SNAG domain (Fig. 9d), that is expressed in five of the seven subgroups. This motif was initially described as a repressor domain in the zinc-finger protein Gfi1 and is important for transcriptional repression in mammalian cells, because it interacts it with co-repressors (Langer et al., 2008; Peinado et al., 2005).

The molecular mechanisms of target regulation of Snail/Scrt family are only poorly understood. Whereas *snail* genes are thought to act as transcriptional repressors, the activation mode cannot be excluded. Proven examples include the direct transcriptional repression of the *E-cadherin* gene by *Snail1,* while the direct molecular mechanisms of Scratch proteins were not yet investigated. Notably, *Snail* genes were reported to play a role in the induction of epithelial to mesenchymal transition (EMT). This is partly due to the direct repression of E-cadherin to mediate migratory properties thereby contributing to the formation of many tissues during embryonic development and development of epithelial tumours (Cano et al., 2000).

Independently of the induction of EMT, *Snail* genes protect cells from death and recent evidence shows that *Snail* genes participate in the regulation of cell adhesion and migration rather than in the determination of cell fate. Thus, EMT triggering, a feature shown so far exclusive for the members (Barrallo-Gimeno and Nieto, 2005) of the *Snail* subgroup, and regulation of cell adhesion would be mechanisms through which probably all members of the superfamily might allow cell cycle exit and cell movement.

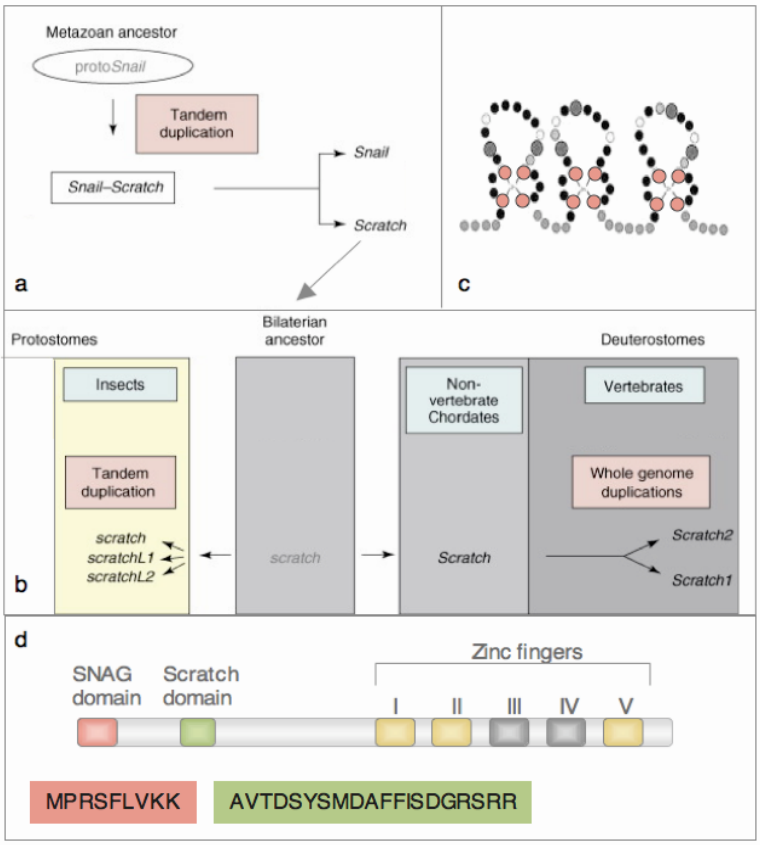

Figure 8: Evolution of C_2H_2 zinc-finger transcription factors and structural / functional domains of Scratch proteins. (a) Subdivision of the Snail- and Scratch subfamilies; **(b)** Genomic evolution of the *Scratch* genes in protostomes and deuterostomes, note the specifity of *Scratch2* in vertebrates; **(c)** schematic drawing of the C2H2-zinc fingers; cysteines / histidines are highlighted in red; **(d)** Known domains of the *Scratch* genes, the superfamily-common zinc fingers are drawn in grey, the *Scrt*-specific ones in yellow; a-c have been adopted from (Barrallo-Gimeno and Nieto, 2009).

1.3.2 Expression and functions of *Scratch* orthologs in vertebrates

In *Drosophila melanogaster,* three *Snail* and three *Scratch* (*Scratch, Scratch-like1* and Scratch-like 2) genes were found, whereas in vertebrates each of the two groups has only two representatives. The *Drosophila Scratch* is expressed in neuroblasts and was shown to be involved in promoting neuronal differentiation while inhibiting non-neuronal fates (Emery and Bier, 1995; Roark et al., 1995; Seugnet et al., 1997). Similarly, the *C. elegans* orthologue, *ces-1*, promotes acquisition of neuronal fates in gain-of-function (GOF) assays (Ellis and Horvitz, 1991) as well as neuronal cell survival (Metzstein and Horvitz, 1999). *Scrt1,* the first member of the *Scratch* family in mammals, has been identified in human and mouse, where it is expressed mostly in post-mitotic neurons in the developing brain, as well as in lung neuroendocrine cells (Nakakura et al., 2001a). Meanwhile, other vertebrate members have been identified in genomic and EST databases, including mammalian *Scratch2 (Scrt2),* chicken *Scrt2,* and three *Scrt* genes in fish (Barrallo-Gimeno and Nieto, 2005; Manzanares et

al., 2001; Nakakura et al., 2001a), but these genes have not been analyzed so far.

Results from analysis of human *Scrt1* after transfection into P19 embryonic carcinoma cells indicated that *Scrt1* might positively influence neuronal differentiation. Indeed, *Scrt1* binds to the *Snail* consensus sequence *in-vitro* and acts as a repressor by interfering with *Mash1* (Nakakura et al., 2001a). From the other hand, it was suggested that *Scrt1* is possibly functioning downstream of the pro-neuronal bHLH proteins, since forced expression of *Mash1 /NeuroD* could induce *Scrt1* expression (Nakakura et al., 2001a). This is very much in accordance with the role described for *Drosophila scratch* gene (Nakakura et al., 2001b). In the zebra fish embryo, a *Scrt* homologue is specifically expressed in primary neurons, further suggesting, that Scrt family members possibly have similar neuron-specific function in invertebrates and vertebrates.

In contrast to the *snail* genes, which are ubiquitinously expressed, the *scratch* genes are expressed almost exclusively in the nervous system of all species analysed to date (Marin and Nieto, 2006; Nakakura et al., 2001a; Roark et al., 1995). With respect to cell differentiation, Scratch proteins have been proposed to antagonize the role of Snail proteins to promote neural differentiation in *Drosophila, C. elegans* and mouse. However, functional analyses of mammalian *Scratch* genes particularly *in-vivo* have not been described so far.

1.4 SCOPE OT THE THESIS

The number of identified modulators, involved in the regulation of differentiation and maturation of neural progenitor cells during corticogenesis is still insufficient to encode the mechanisms behind the generation of the most complex tissiue of higher vertebrates.

The newly identified member of the C_2H_2 zinc-finger transcriptional factors, the vertebrate-specific factor Scratch2 (*Scrt2*) has a high potential to play a role in cortical development, due to its CNS-specific expression and the predicted ability to bind to E-box containing target proteins, like the key regulators of neural specification, the bHLH-TFs. However, no functional analysis of *Scrt2* has been reported so far.

The aim of this study is to characterize the expression of *Scrt2* in the mouse brain and to examine its role in the regulation of mammalian corticogenesis. Therefore, a gain-of-function *in-vivo* approach has been chosen to examine the effect of miss-balanced Scrt2 protein in different aspects of the embryonic and postnatal corticogenesis.

2. RESULTS

2.1 EXPRESSION OF *mSCRT2* DURING EMBRYONIC AND POSTNATAL DEVELOPMENT

2.1.1 Expression in the mouse embryo

Multiple genes with regionalized graded expression in VZ/SVZ and/or CP of the developing mouse cortex have been identified in a micro array screen, performed previously in the group (Mühlfriedel et al., 2007). Given the crucial role of TF Pax6 in cortical neurogenesis, identification of genes acting in a *Pax6*-dependent genetic pathway, is of great importance. Therefore, my work started with a study of the expression pattern of ten selected gene-candidates by *in-situ* (ISH) hybridization analysis on brain sections of wild type (WT) and homozygous *Pax6/Small eye* (*Sey/Sey* allele) mutant mice at E16.5. Among the tested candidates, the most intriguing alteration of the expression pattern (as presented below in Fig. 10 a-c) was found for the gene *Scratch2* which was chosen for further detailed expression and functional study, the subject of this PhD work.

Whole-mount ISH using *mScrt2*-specific riboprobe revealed a restricted expression of *mScrt2* in the developing central nervous system of the E11.5 embryo (Fig. 9a), which is in agreement with previously published data, using a radioactive-labelled ISH probe (Fig. 9b; BGEM - Brain Gene Expression Map). ISH on cryosections of the E12.5 embryo (Fig. 9d-e,) revealed expression of *Scrt2* in the earliest-born neurons of the preplate (arrow). At stage E15.5 (Fig. 9f), a strong *Scrt2* expression was detected in the SVZ of the cortex (pallium, filled arrow) as well as in the SVZ of the hippocampus (Hi), thus outlining a medial-high to lateral-low expression gradient. A fainter diffuse *Scrt2* expression was observed in the lower intermediate zone (IZ), as well as in the cortical plate (CP) (Fig. 9g).

For protein detection, a rabbit polyclonal anti-Scrt2-specific antibody was generated, since there was no commercial antibody available. The specifity of the antibody was proven by recognition of the two epitopes on a dot-blot (Fig. 40 in the Supplement), western-blot analysis of cortical cells (Fig. 16b, c), and cultured cells after cell transfection with CMV-*Scrt2* expression vector, shown in Fig. 29b. Using this antibody, strong Scrt2 expression could be immunohistochemically detected in the SVZ/IZ of the E15.5 cortex (Fig. 9h, white arrow) and in cells migrating along the rostral migratory stream (RMS) towards the olfactory bulb (OB). The uppermost part of the CP showed moderate labelling (filled arrow), and Scrt2-positive cells were distributed throughout the whole depth of the CP. In order to examine whether Scrt2 is expressed in proliferating cells, BrdU-labelling experiment was performed. Pregnant mice at stage E15.5 were injected with BrdU (i.p, 140μg /g body weight) and analyzed after one hour. As shown in Fig. 9c, double-immunostaining with anti-BrdU antibody (labelled in green) and Scrt2 antibody (labelled in red) revealed absence of Scrt2 protein in fast proliferating cells.

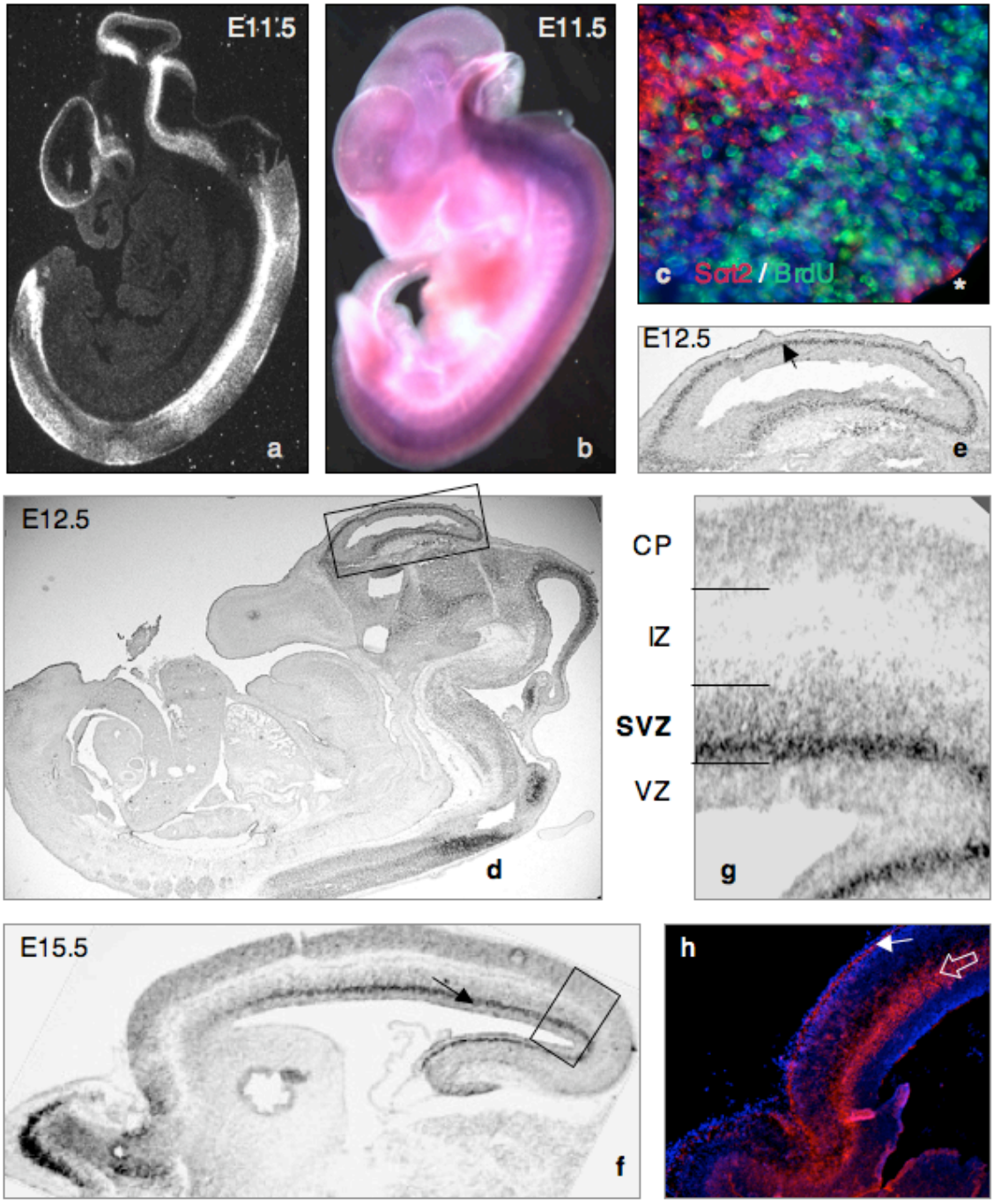

Figure 9: Scrt2 expression in the embryonic mouse brain. (**a)** Radioactive ISH with E11.5 embryo (data from BGEM); **(b)** Whole mount ISH with E11.5 embryo; **(c)** double-IHC on a coronal section of a E15.5 brain; after 1hr of *in-vivo* BrdU pulse labelling the S-phase proliferation marker BrdU (in green) is expressed in cells of the VZ and apical SVZ; Scrt2 protein (in red) is expressed in the basal SVZ and IZ and does not co localize with BrdU staining; * marks the ventricle **(d)** Scrt2-ISH on sagittal section of E12.5 embryo; **(e)** higher magnification of d showing labelled preplate neurons; **(f)** Scrt2-ISH on sagittal section of E15.5 brain; **(g)** higher magnification of f showing strongly labelled subventricular zone (SVZ) and weaker labelling of the intermediate zone (IZ) and cortical plate (CP); **(h)** Scrt2-IHC on sagittal section of E15.5 brain. Abbreviations: CP- cortical plate, IZ- intermediate zone, HB- hindbrain, Hi- hippocampus, MB- midbrain, OB- olfactory bulb, RMS- rostral migratory stream, SC- spinal cord, SVZ- subventricular zone, T- telencephalon, VZ-ventricular zone.

2.1.2 Down-regulation of *mScrt2* expression in the *Pax6*- deficient cortex

The TF Pax6 has a crucial role for the specification of both, radial glial progenitors located in the VZ and intermediate progenitors, located in the SVZ (Hevner et al., 2006). In order to study whether the *Scrt2* expression is under the control of TF *Pax6*, ISH expression analysis was done on sections from E15.5 WT and homozygous *Pax6/Small eye* mutant embryo brains. As shown in Fig. 10, in the *Pax6*-deficient cortex, the expression of *Scrt2* was almost completely abolished in the dorso-lateral cortex, but was preserved in the medial cortex.

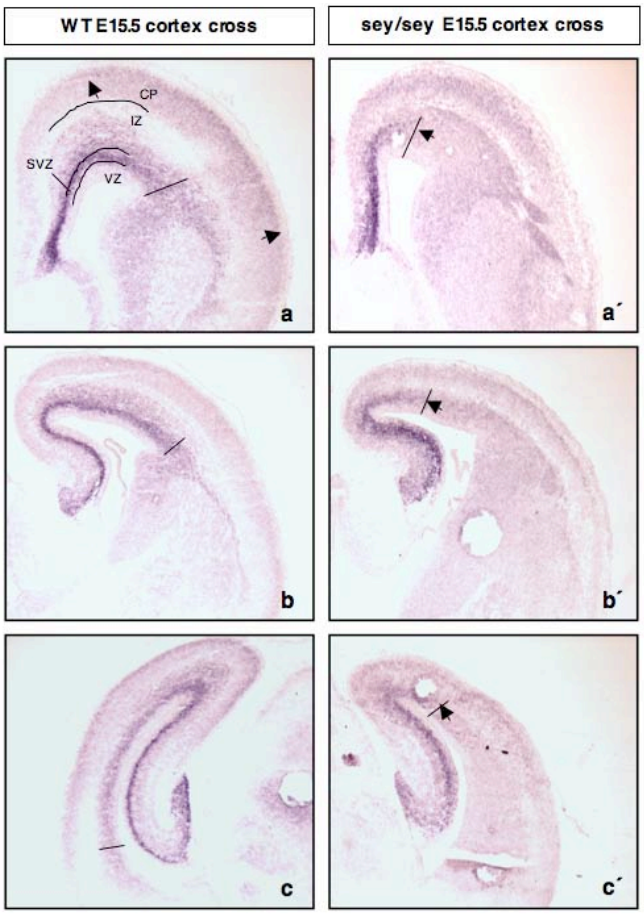

Figure 10: *Pax6*-dependent down-regulation of *mScrt2* expression in the embryonic cortex. Coronal sections at three rostro-caudal levels (a to c) of E15.5 brains from wild type (WT) and *Sey/Sey* embryos were hybridized with *Scrt2* ISH probe. Note the regionalized down-regulation of *Scrt2* expression in the ventro-lateral and dorsal pallium (up to a border pointed by the arrow).

Interestingly, a similar defect of the expression of *Ngn2*, a bHLH-TF acting as a direct Pax6 target gene was reported (Fig. 11c, d; (Scardigli et al., 2003; Stoykova et al., 2000). The *E1-Ngn2* enhancer element is activated only by high Pax6 dosages (Scardigli et al., 2003) what may explain the regionalized inhibition of the *Ngn2* expression in *Sey/Sey* embryonic cortex, confined to regions of VZ (ventral, lateral, dorsal pallium), showing high endogenous *Pax6* expression. Together, these data suggest that TF Scrt2 is involved *in Pax6*-dependent genetic pathway of cortical neurogenesis.

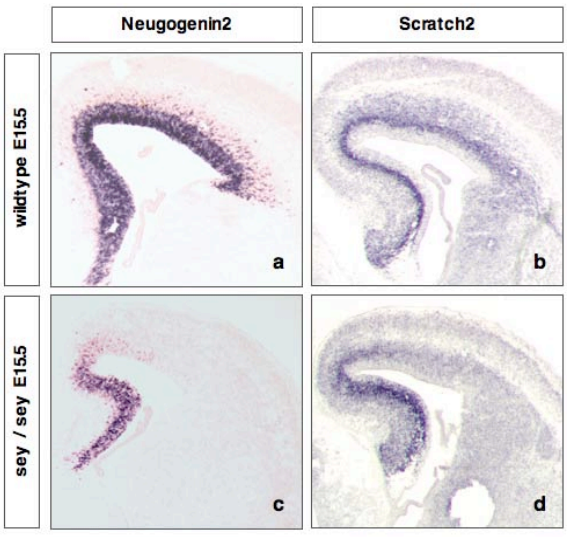

Figure 11: TFs *Scrt2* and *Ngn2* show similar regionalized pattern defects in the *Pax6* deficient cortex. Coronal sections from E15.5 WT **(a, b)** and *Sey/Sey* **(b, d)** brains were tested by *in-situ* hybridization using probes for *Ngn2* **(a, c)** and *Scrt2* **(b, d).**

2.1.3 *mScrt2* expression in the perinatal and postnatal murine brain

Although cortical neurogenesis is fully accomplished around stage E18.5, the neuronal migration towards the CP is achieved only at postnatal (P) stages, (in mouse at P10). In order to further characterize the expression of *Scrt2* in the postnatal brain, IHC analysis has been performed on brain sections at stage E18.5 and P10 (Fig. 12). Using double-IHC with antibodies against doublecortin (Dcx), a marker for immature but already post-mitotic neurons, and Scrt2 antibody at stage E18.5 an almost complete co-localization of Scrt2 and Dcx immunoassaying within the uppermost CP was observed (Fig. 12a). Different to Dcx, staining with Scrt2-antibody was detected in fibres of the IZ, possibly reflecting the cytoplasmic localization of Scrt2 protein, recognized by the generated Scrt2-antibody. Very recently, a commercial antibody against Scrt2 became available (Santa Cruz). Using this antibody, immunoassaying of cortical sections at P10 revealed co-expression of Scrt2 and NeuroD1 - a marker for differentiated neurons - in most neurons of the CP (Fig. 12b), which is in accordance with *in-situ* data of Marin and Nieto (2006).

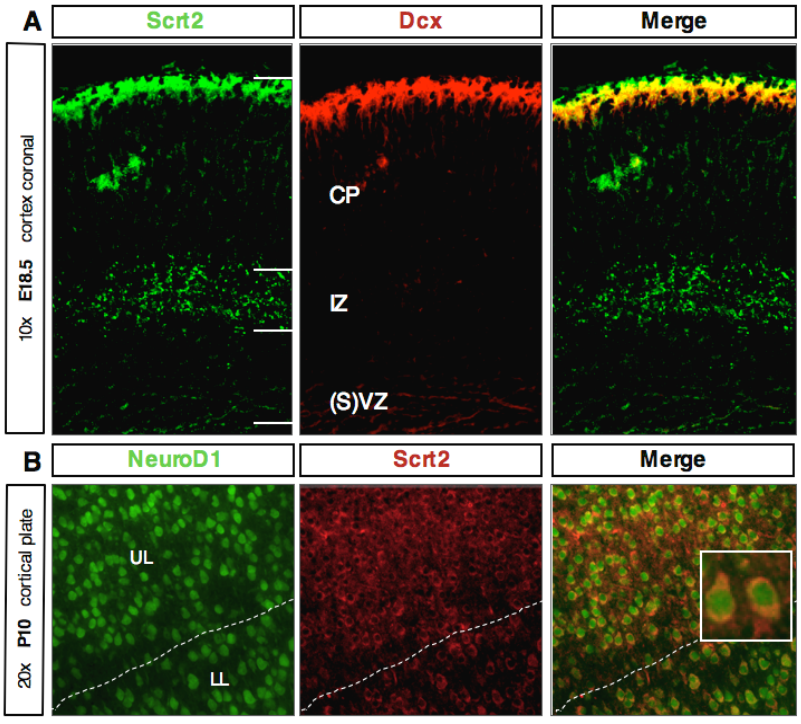

Figure 12: Scrt2 protein expression in the late embryonic and postnatal cortex. (A) Coronal section of E18.5 WT cortex, immunoassayed with α-Scrt2 antibody and α-DCX (doublecortin) antibody. Note the overlapping strong staining with the two antibodies of post-mitotic neurons of the upper layers (UL) of the cortical plate (CP), while fibres in the intermediate zone (IZ) are stained only with Scrt2 antibody **(B)** At P10, the majority of the NeuroD1-positive cortical neurons are also stained with the Scrt2-antibody, which is mainly cytoplasmic. LL- lower layers

In the adult brain, neurogenesis proceeds in two neurogenic niches. In the SVZ of the lateral ventricle, stem cells generate neuroblasts that follow the rostral migratory stream

(RMS) to migrate into the olfactory bulb where they differentiate into GABAergic and glutamatergic interneurons (Brill et al., 2009; Reynolds and Weiss, 1992). Similarly, stem cells in the subgranular zone (SGZ) of the dentate gyrus (DG) of hippocampus generate neurons replacing the dentate granule cells (Mu et al., 2010). Interestingly, expression analysis revealed preserved *Scrt2* expression at P10 in cells of the RMS (Fig. 13c), olfactory bulb (not shown), DG of the hippocampus (Fig. 13b), as well as in the superior olivary complex (Fig. 13e) and in the inner part of the external granular layer (EGL) of the cerebellum (Fig. 13d).

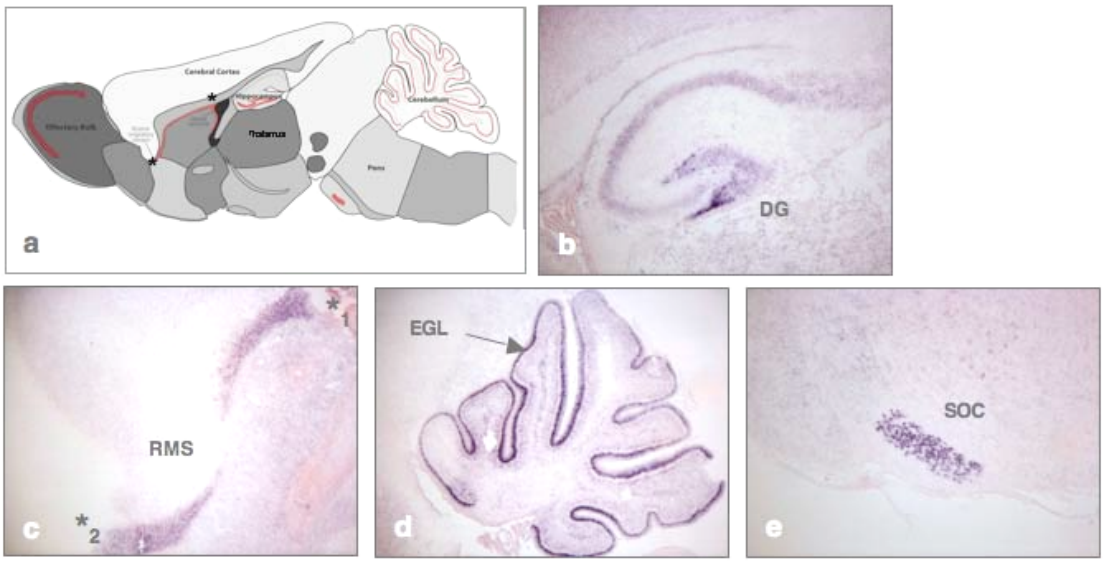

Figure 13: *mScrt2* expression in the postnatal brain. a) Schematic organisation of the postnatal / adult murine brain; **b-e)** show *Scrt2*-ISH on sagittal sections of P10 WT brain; **b)** expression of Scrt2 in the dentate gyrus (DG) and the CA1 region of the hippocampus; **c)** abundant expression of Scrt2 in cells of the rostral migratory stream (RMS) on their way towards the olfactory bulb, designated with *; **d)** strong expression of Scrt2 in the inner part of the external granular layer (EGL) of the cerebellum and in the superior olivary complex (SOC) in the pons (**e**).

Until P21, the external granular cell layer (EGL) of the cerebellum is still generating granule cells that migrate and form the internal granular layer (IGL). Previous *in-situ* analysis suggested that *Scrt2-mRNA i*s accumulated in the inner part of the cerebellar EGL (Marin and Nieto, 2006). Indeed, labelling with antibodies against TAG1 - a marker for post-mitotic granular cells (Wolfer et al., 1994) and Scrt2 indicated co-expression only in the inner EGL, which contains post-mitotic cells (Fig. 14c). Also double IHC with antibodies for Scrt2 and GABAergic interneurons (GAD67) revealed, that Scrt2-expression co localized with Gad67 (Fig. 14a, b) in the internal granular layer (IGL) of the cerebellum at P10. This result indicates that Scrt2 expression is not restricted to the glutamatergic neurons, but labels GABAergic IGL interneurons, possibly Golgi cells as well.

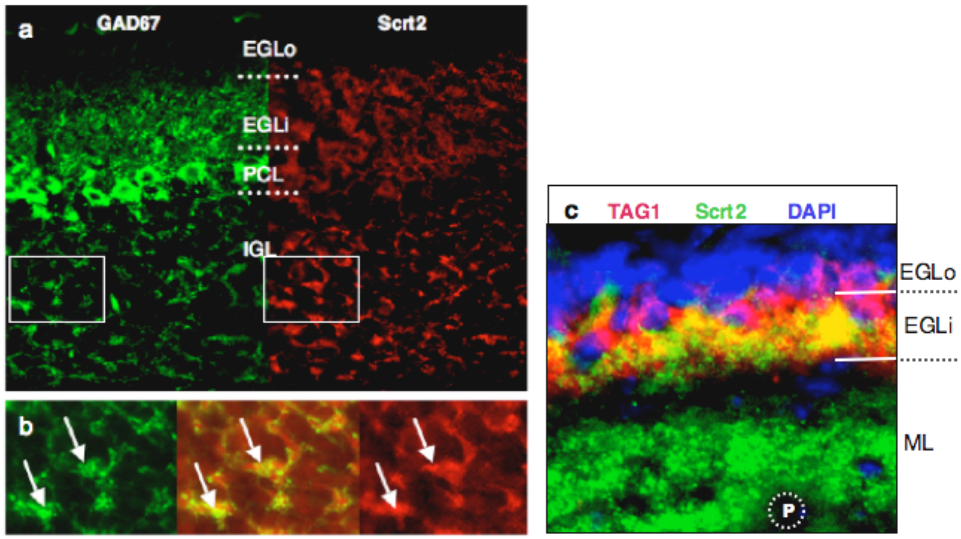

Figure 14: Scrt2 expression in GABAergic interneurons and newly post-mitotic granular cells in the IGL of the cerebellum. a) Sagittal section of P10 WT cerebellum shows IHC with α-GAD67 antibody and α-Scrt2 antibody; **b)** higher magnification and merged pictures of the IGL in a; note the overlapping strong expression of the two proteins labelling IGL interneurons (arrows); **c)** IHC with α-TAG1 and α- Scrt2 antibodies indicate a co-localization of Scrt2 and TAG1 in the inner (i) part of the EGL, containing newly post-mitotic granular cells and persistent Scrt2-expression in these cells after migration into the molecular layer (ML); note that the precursors in the outer EGL and the purkinje cells (P) are negative for both proteins.

2.1.4 *In-silco* analysis of alternative spliced mRNA isoforms of the mScrt2 gene

Most of the Snail family members of transcription factors act as repressors (Hemavathy et al., 2000). Therefore, I decided to apply an *in-vivo* gain-of-function approach to study the function of *Scrt2* after gene activation in transgenic mice. A prerequisite for generation of the necessary expression vector is knowledge for the open reading frame of the studied protein and availability of the corresponding cDNA.

In the last years several transcripts of the murine *Scrt2* gene have been predicted at NCBI (National Centre for Biotechnology Information) by in-silico analysis.

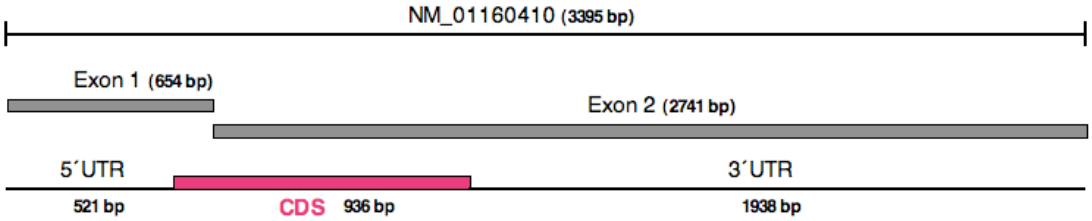

Figure 15: Structure of the provisional mouse Scratch2 transcript. Genomic Scrt2 DNA is located on chromosome 2 G3 (151.855.291-151.921.537) present in the NCBI assembly sequence NC_000068.6 (C57BL/6J). Exons are displayed in grey and the protein-coding region in pink.

The common genomic locus of the predicted three *Scratch2*-transcripts is located on chromosome 2 (G3) of the mouse genome. Because the isolation of mouse *Scrt2*-mRNA has not been successful so far, a provisional reference sequence has been announced (NCBI; NM_01160410; Fig. 15). In order to design specific PCR-primers, an alignment of the predicted isoforms was performed to identify homology regions. On the level of the amino acid sequence, a specific domain-like composition of the open reading frames in the individual mRNAs (Fig. 16a, also Fig. 46 in the Supplement) has been disclosed.

Domain A was unique for the encoded by *Scrt2.4* protein, the longest predicted spliced product of *Scrt2* (XM_619828.4), whereas domain B was only encoded by *Scrt2.3* (XM_619828.3). A nuclear localization signal (NLS), included in domain C, would be translated by two transcripts, *Scrt2.4* and *Scrt2.3*. Domain D, containing the characteristic SNAG-motif, was included in all predicted alternatively spliced *Scrt2* transcripts, as well as in a PCR product, amplified from cortical cDNA library (see section below). Whereas domain E was only present in *Scrt2.4* and *Scrt2.3*, domain F was found in all mRNAs and domain G in three predicted transcripts, but not in the PCR product. Functionally, most important is domain H, which contains all five zinc fingers that mediate DNA-binding to target genes and was encoded by all predicted *Scrt2* transcripts.

To study the existence of *Scrt2* transcripts, lysates from fibroblast (NIH 3H3) and neuronal (Neu2a) cell lines as well as E16.5 cortex were tested by western blot using the α-Scrt2 antibody for a presence of a predicted translated product (Fig. 16b). In all lysates a single band with an approximately size of 33kDa was determined. Relying on the predicted protein size (Fig. 16a) of the individual transcripts, this fragment would represent the protein translated from *Scrt2.2*-mRNA. Furthermore, the corresponding protein was detected exclusively in extracts from E12 to E18 cortices (Fig. 16c), suggesting that this encoded by *Scrt2.2* protein is specific or abundantly expressed in the developing cortex.

In order to isolate the Scrt2 cDNA, a mouse cDNA library of E15.5 cortex was screened using transcript-specific PCR primers. However, despite the applied several approaches, the amplification of the full-length Scrt2-cDNA failed. Therefore, synthetically generated DNAs, coding for the *Scrt2.2* and *Scrt2.3* predicted proteins were supplied by "GenScript" and used in all further experiments.

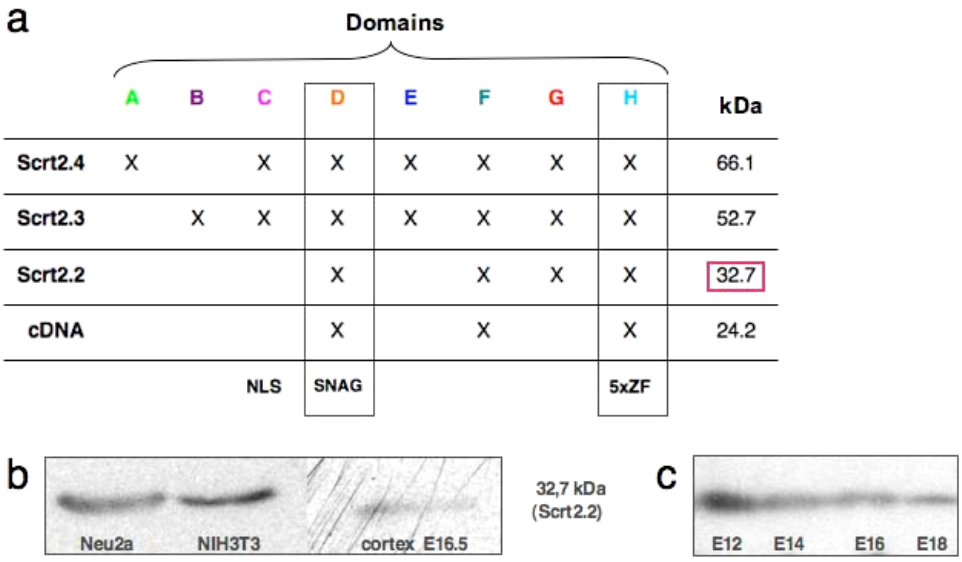

Figure 16: Predicted mScrt2 isoforms encoded by alternatively spliced *Scrt2* transcripts. (a) The presence of a certain protein domain (A - H) is indicated by X; each row is representing the composition for each predicted individual isofom and the resulting protein size (in kDa, without post-translational modifications); **(b)** Cell lysates from Neu2a, 3T3-fibroblast and E16.5 cortex have been analyzed by western-blotting and stained with anti-Scrt2 antibody (lab made, rb 1:500); **(c)** comparative protein analysis of cortical cell lysates at different developmental stages using western-blotting and staining with anti-Scrt2 antibody (lab made, rb 1:500); a and b are not quantitative blots (no internal loading standard)

In order to diminish the possibility that high GC-content could prohibit the amplification and would also complicate onward cloning procedures, the synthetic DNAs have been codon-optimizied (sequences shown in Fig. 47 in the Supplement) by replacement of some GC nucleotide pairs by AT pairs, but without changing the amino acid sequence of the resulting protein.

2.2 CONDITIONAL OVEREXPRESSION OF *mSCRATCH2* IN THE DEVELOPING CORTEX

2.2.1 Generation of a construct for conditional *mScrt2*-overexpression

In order to investigate the function of mScrt2 in cortical development, I used the developed in our group Cre-loxP based strategy for gene gain-of-function assays in transgenic mice (Berger et al., 2007). In general, two types of transgenic mouse lines are necessary for conditional over expression of a gene *in-vivo*: (a) A line, which allows a conditional activation of the gene of interest e.g. *Scrt2* and (b) a Cre-line that drives Cre-recombinase expression by a tissue-specific promoter.

In order to generate the first type *Scrt2* transgenic mouse line, I used a vector-construct (plasmid JoJo, named thereafter pJoJo; see Fig. 17) to clone the ORF of *Scrt2.2* or *Scrt2.3* followed by IRES-lacZ-reporter sequence downstream under a strong CMV/ß-actin promoter

(*CMV/βactin-loxP-GFAP-Stop-loxP-Scrt2.2/or Scrt2.3-IRES-βGal;* see Fig. 17). After crossing e.g. to the *Emx1Cre* line (Gorski et al., 2002) which promotes Cre-recombinase expression only in cortical progenitors. In the generated double transgenic mice, the Cre recombinase recognizes the loxP sequences, mediates recombination and excision of the GFP-Stop cassette and allows the CMV/ßactin promoter to drive the expression of *Scrt2*- together with the Lac-reporter. (Berger et al., 2007; Fig. 17).

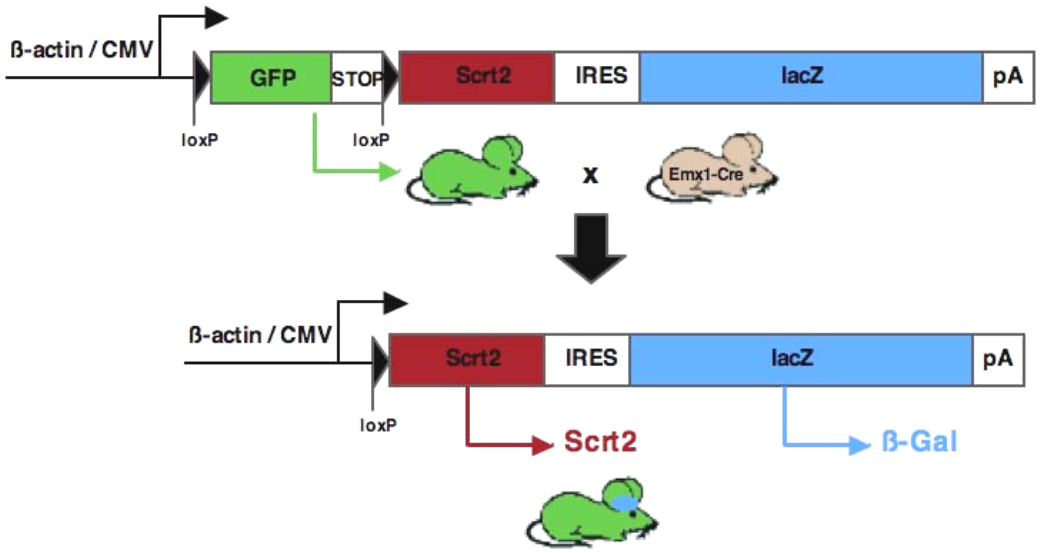

Figure 17: The principle of the Cre-loxP based strategy for conditional *mScrt2* activation in transgenic mice. Above is shown the Scrt2-pJoJo construct used to generate transgenic mice in which only expression of the GFP-cassette is allowed ("green mice"). Below is illustrated Cre-recombinase-mediated excision of GFP-Stop cassette and expression of the Scrt2-IRES-lacZ in the dorsal telencephalon (marked in blue) after crossing the "green mice" to the cortex-specific *Emx1Cre* transgenic line (Gorski et l., 2001).

In order to test the functionality of the generated constructs, *Hela* cells were transfected with the *Scrt2-pJoJo* constructs. As shown in Fig. 18a, the transfected cells with the unrecombined vector showed a bright GFP-fluorescence. Next, the *Scrt2-pJoJo* plasmid was transfected into the *E.coli* strain SW106 that had been induced to express Cre-recombinase (see also 4. 3. 2). One day thereafter, plasmid-DNA was isolated, purified and transfected into Hela-cells. One day later, the cells were fixed and stained for X-gal. As shown in Fig. 18b, cells transfected with the successfully recombined *Scrt2-pJoJo* (in the induced to express Cre-recombinase SW106 cell line) exhibited a strong ß-gal staining.

The presence or absence of the GFP-stop cassette that contains one *EcoRI*-restriction site was checked by a restriction analysis with *Eco*RI. The unrecombined *Scrt2-JoJo* plasmid, that was isolated from bacterial culture before the induction of Cre-recombinase expression, showed four DNA-fragments after agarose-gel electrophoresis (Fig. 18d left). Notably, *Scrt2-pJoJo* that has been isolated from Cre-recombinase expressing bacteria was cut only at three sites (Fig. 18 right). The size of the missing DNA-fragment in the recombined *Scrt2.2-pJoJo* corresponded to the GFP-stop-cassette (Fig. 18c, highlighted in green). Taken together, the

results from this *in-vitro* analysis revealed the functionality of the generated *Scrt2-pJoJo* construct made with both, *Scrt2.2*- and *Scrt2.3*-ORF

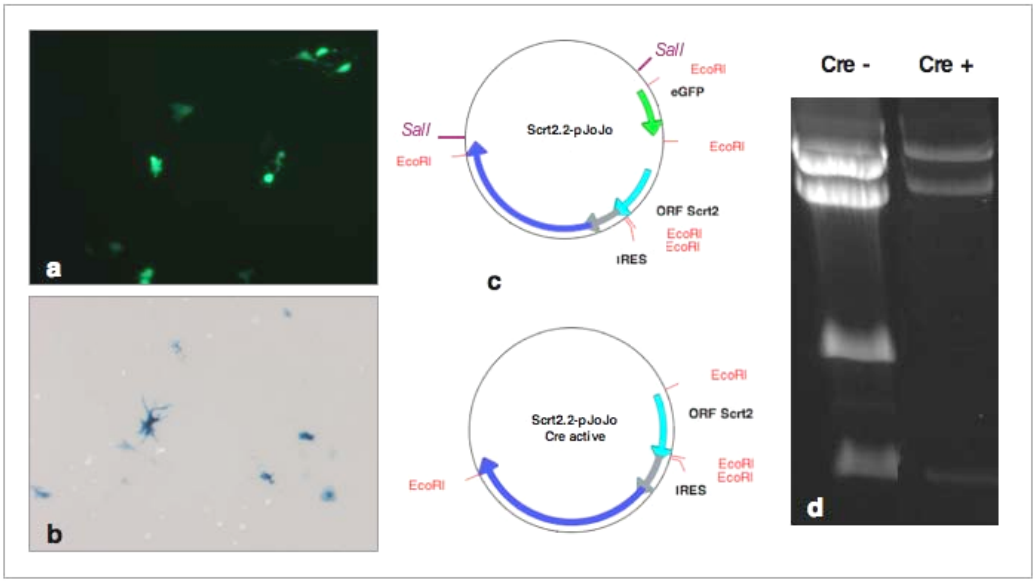

Figure 18: Functional analysis of the *Scrt2.2-pJoJo* construct. a) GFP-fluorescence of *Hela* cells transfected with *Scrt2.2-pJoJo*; **b)** ß-gal staining of Hela cells transfected with the recombined *Scrt2-pJoJo* construct after Cre-mediated recombination in SW106 cells; **c)** Schematic view of the *Scrt2.2-pJoJo* plasmid before (top) and after (bottom) Cre-recombinase mediated deletion of the GFP-Stop cassette, *SalI* sites (in pink) indicate the cassette used for microinjection; **d)** *EcoRI* restriction digest of the plasmids used for transfections in a and b.

2.2.2 Cre-recombinase mediated over expression of *mScrt2* in the developing cortex

Next, the *Scrt2.2-pJoJo* construct was used for production of a transgenic mouse line. Following the procedure as outlined below, in the last six months, work on generation of *Scrt2.3-pJoJo* transgenic mice was initiated and ended with a successful production of the line. However, analysis of the *in-vivo* cortical phenotype of *Scrt2.3-pJoJo;EmxCre* mice is still in a progress, and is not presented in the present study.

The targeting cassette shown in Fig. 17 was released from the vector backbone by *SalI* restriction digest, purified and used for microinjection into pronuclei of mouse zygotes. The generated animals were screened under the microscope for green fluorescence (Fig. 19a) and isolated genomic tail DNA was analyzed by PCR using primers for LacZ- and GFP- sequence, indicated in section 5.3. Two of five founders of *Scrt2.2-pJoJo* showed ubiquitous fluorescence of the body and the brain and transmitted the transgene to its offspring (Fig. 19a, b). Male founders were further used to generate double transgenic animals for Cre-mediated gene activation in the brain of embryos at different developmental stages.

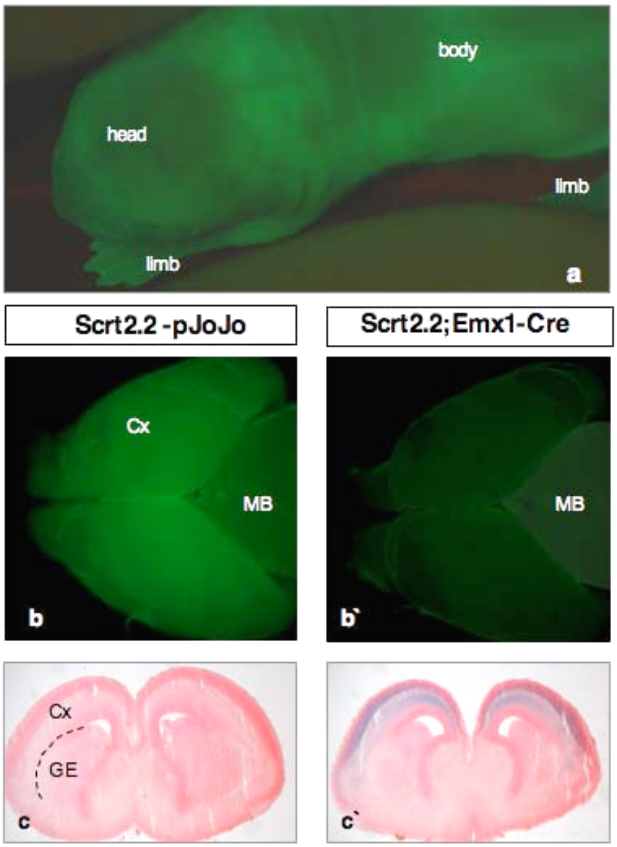

Figure 19: Cre-mediated recombination in *Scrt2.2-pJoJo;Emx1Cre* double transgenic mice. (a) *Scrt2-pJoJo* transgenic mice exhibit uniform green fluorescence in the whole body; **(b, b`)** Comparison of green fluorescence of E15.5 brains of *Scrt2.2-pJoJo* **(b)** and *Scrt2.2-pJoJo;Emx1Cre* mice **(b`)** which show a specific loss of the green fluorescence in the cortex (Cx); **(c)** Cross section of E15.5 brains after ß-Gal-staining revealed a specific lacZ expression in the cortex of *Scrt2-pJoJo;Emx1Cre* mice; GE-ganglion eminence, MB –midbrain

In order to achieve over expression of *Scrt2.2* in the developing cortex, selected male *Scrt2.2-pJoJo* founders were crossed to female mice of the *Emx1Cre* mouse line. This line drives Cre-recombinase expression selectively in the cortical progenitors and their post-mitotic progeny (Gorski et al., 2002). The recombination starts at E9.5 and reaches maximal activity at E12, affecting about 90% of the cortical glutamatergic neurons (Gorski et al., 2002; Li et al., 2003; Pinon et al., 2008). Before using the animals routinely in the experiments, the *Scrt2.2* male founders were crossed to *Emx1Cre-* females and the generated double transgenic embryos were analyzed at E15.5 to test, if the founder's offspring display a specific loss of GFP in the cortex and ß-Gal staining after Cre-expression.

The embryos were isolated at the desired stage and genotyped as the single transgenic founders (LacZ- and GFP- sequence) plus for the Cre-recombinase gene. In Cre-positive mice (*Scrt2.2-pJoJo;Emx1Cre*), the GFP-fluorescence signal in the cortex was almost completely absent (Fig. 19b´), in agreement with the efficiency of the *Emx1Cre* driver (Gorski et al., 2002). Only few cells, immigrated from the striatum or representing Cre-negative blood vessel epithelia cells showed green fluorescence, thus not over expressing *Scrt2.2*.

For more detailed lacZ-reporter expression analysis, sections of double transgenic embryonic (E18.5) and adult brains were stained for ß-gal. On a whole-mount forebrain of double transgenic animal, very strong ß-gal staining in the E15.5 neocortex was seen (Fig. 20a). Faint staining in the olfactory bulbs marked migrated neurons from the cortex, while the remaining part of the brain as well as all other tissues of the embryonic body were negative for ß-gal.

At stage E18.5, most of layer 5 neurons are located in the CP. The majority of the upper layer (UL, L4-L3) neurons is still underway towards the CP, while last sets of freshly-born UL neurons are just at the beginning of such a migration. Accordingly, at E18.5 abundant LacZ expression was seen throughout the entire CP, but also in the SVZ/IZ (Fig. 20b). The strong lacZ-staining also mirrored the *Emx1-Cre* activity in the hippocampus (see also Gorski et al., 2002).

By using the *Emx1Cre* line for conditional activation of *Scrt2.2 in-vivo*, an ectopic or over expression of *mScrt2.2* is driven in cortical RGPs and in their descendents (IPs in SVZ; and CP neurons), respectively (Gorski et al., 2002). At P10, the neurons are already located in their final layer positions in the cortex. At this stage, a fainter but still pronounced ß-gal staining was detected in all layers, more strongly in the upper layers, possibly reflecting their higher density (Fig. 20c). The expression of the LacZ- reporter was detected in sections throughout the entire rostro-caudal axis of the cortex, thus reflecting correctly the *Emx1Cre* driven recombination in the majority of the cortical progenitors and their descendents.

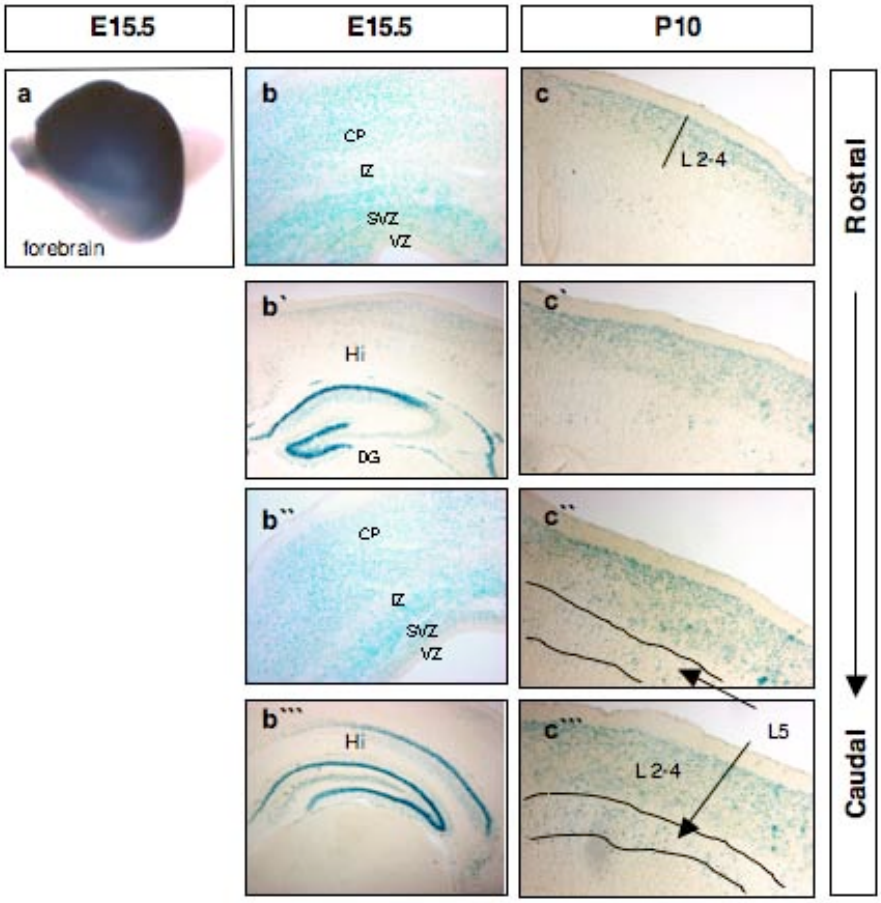

Figure 20: Cre-mediated lacZ-reporter expression in brains of *Scrt2.2-pJoJo;Emx1Cre* mice. a) On the left is shown a whole-mount ß-gal stained forebrain at E15.5; **b)** in the middle are shown stained coronal sections from E18.5 cortex and hippocampus (Hi), note that the staining spans the whole depth of the cortex, being especially strong in the SVZ/IZ; **c)** on the right are shown coronal sections from P10 brain; CP- cortical plate, DG- dentate gyrus, IZ-intermediate zone, L- layer, SVZ- subvenrticular zone, VZ- ventricular zone.

Finally, the successful *mScrt2.2* over expression *in-vivo* was proven by *in-situ* hybridization analysis using Scrt2-riboprobe on P10 brain sections from single- and double-transgenic mice. As illustrated in Fig. 21b, the *Scrt2.2-pJoJo;Emx1Cre* cortex exhibited an obvious increase of the *Scrt2* expression level in the medial, dorsal, and lateral cortex, and particularly in the piriform cortex. Noteworthy, only such "proven founders" were used for breeding with *Emx1Cre* females for the subsequent analyses.

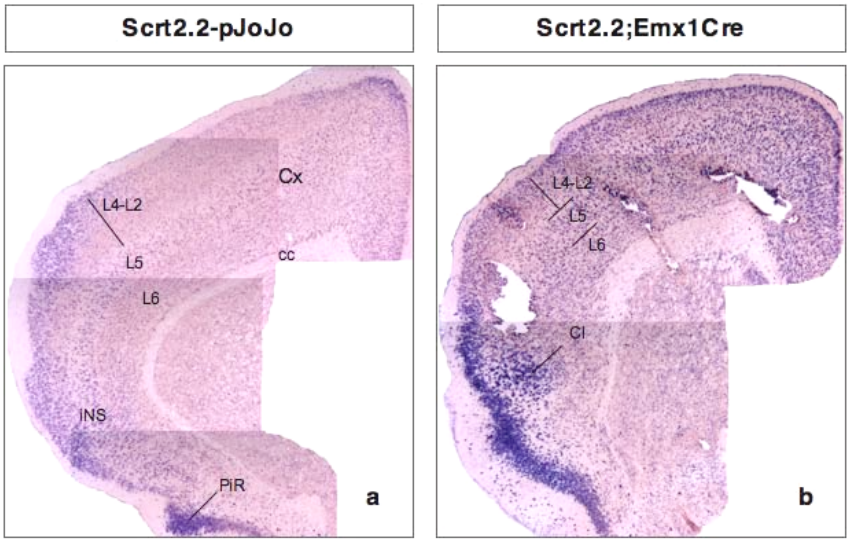

Figure 21: Over expression of *mScrt2* in the generated *Scrt2.2;Emx1Cre* transgenic mice. ISH with *Scrt2*-riboprobe has been performed on sections of single **(a)** and double **(b)** transgenic brains at P10; several pictures per slide were taken with a binocular in high magnification and assembled afterwards to achieve appropriate resolution

2.2.3 *In-vivo* analysis of corticogenesis in *mScrt2* gain-of-function condition

The most obvious postnatal phenotype at P10 of the *Scrt2.2-pJoJo;Emx1Cre* mice was the thinner cortex. Immunostaining with NeuroD antibody that marks the cortical neurons on sections from P10 brains revealed a significant reduction of the cortical thickness (by 33% of the double transgenic mice as compared to the control; Fig. 22g, h). At P10, the neurons have accomplished their migration and are located at their final layer-specific positions. To study whether the cortical layers were differentially affected upon *Scratch2.2-GOF* condition layer specific markers were applied.

Immuno-labelling with antibodies for the upper layer (L4-L2) neurons, Cux1 (Fig. 22a, b; Nieto et al., 2004) and Satb2 (Fig. 22c, d; Britanova et al., 2008; Li et al.) indicated a strong reduction of the UL neurons. Compared to controls, the density of the Satb2+ UL neurons was diminished by 25% (Fig. 22c, d). Also the staining for Cux1 showed a strong reduction of the UL neuron density (Fig. 22c, d not counted).

The zinc-finger protein Ctip2 is most pronouncedly expressed in a subpopulation of the layer 5 cortico-spinal motor neurons, projecting to the spinal cord and faintly also in

neurons of layer 6 (Arlotta et al., 2005). Labelling of the sections with Ctip2 antibody indicated an increase of the density of the L6 neurons (by 20%), while the thickness of the layer 6 seemed to be reduced. The density of the large L5 pyramidal neurons as well as the layer-thickness was not significantly affected (Fig. 22e, f).

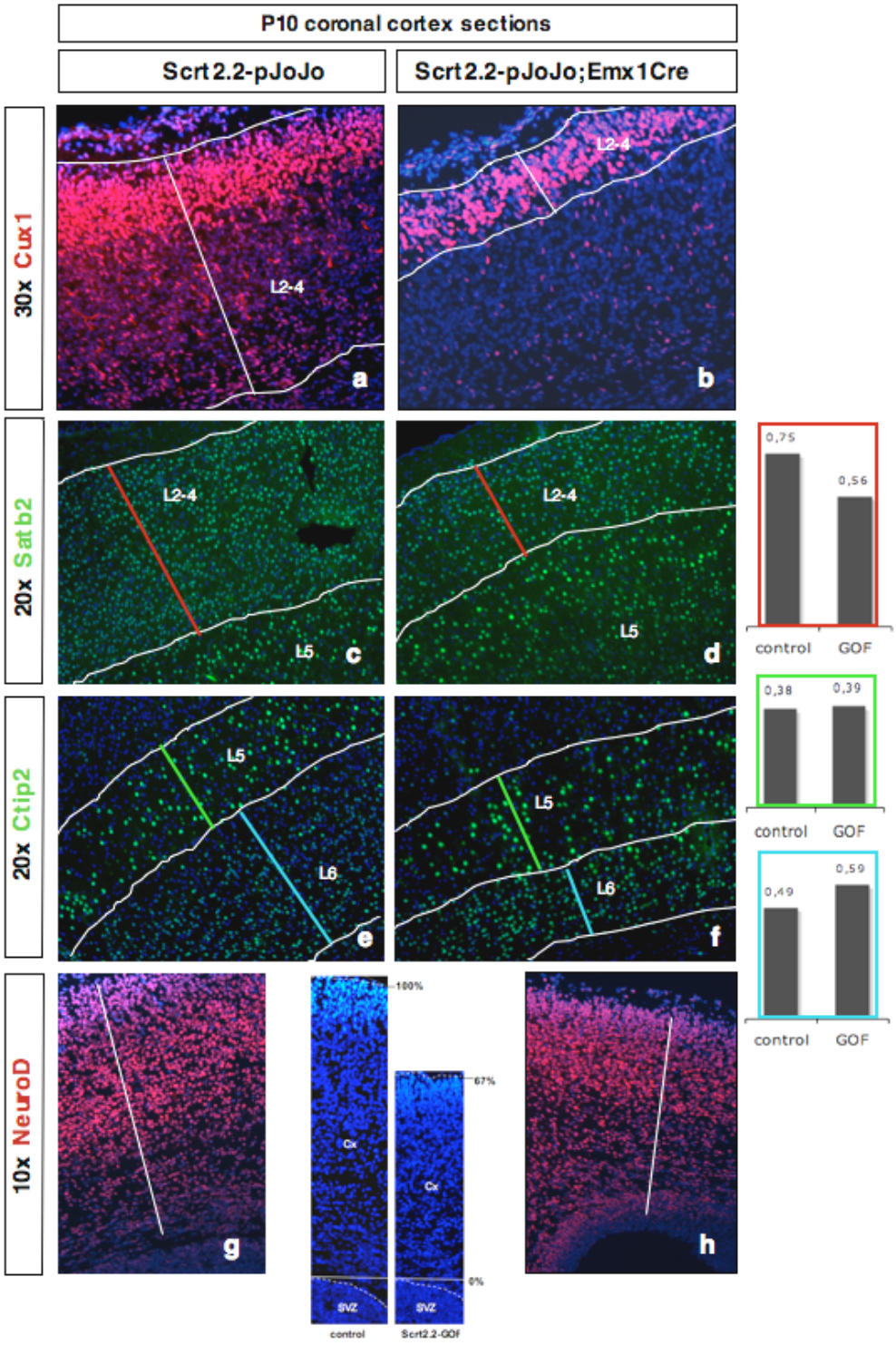

Figure 22: Decreased cortical thickness in *Scrt2.2* double transgenic brains at P10. Pictures of immunohistochemical staining for the indicated antibodies (red and green) have been compared between single (left) and double transgenic mice (right); bars indicate the radial scale of the analyzed cortical layer(s); DAPI-counterstaining in blue; lines have been drawn to visualize the borders of the neighbouring layers; (**g, h)** The

relative ratio of labelled with specific antibody neurons/versus DAPI+ total cell number was estimated. The diagrams show the results from performed counting per equal-sized cortical fields for the Satb2+ ULs (indicated by red lines), or Ctip2+L5 (indicated by green lines) and Ctip2+L6 (indicated by blue lines).

At perinatal stages the pluripotent cortical RGPs transform into astrocytes. Although the focus of the work was set on the potential role of *Scratch2* to modulate neurogenesis, it was interesting to examine the astrocyte presentation in this experimental paradigm. IHC of cortical sections at P10 with GFAP antibody clearly demonstrated, that in the *mScrt2.2*-GOF condition, the cortex contained diminished number of mature astrocytes (Fig. 23a, b). Higher magnification pictures (Fig. 23c-f) revealed an almost complete lack of GFAP+ mature astrocytes in the upper cortex of double transgenic mice as compared to control animals (Fig. 23c, d). In the lower part of the cortex (Fig. 23e, f), the control brain was full of brightly stained GFAP+ cells with multipolar, highly branched processes typical for mature astrocytes, while in the *mScrt2.2*-GOF brain only very few of these cells were observed.

Together, these findings suggest that ectopic activation of Scrt2.2 in the pluripotent cortical RGPs at the onset of neurogenesis affects both the neurogenesis and gliogenesis of the developing brain.

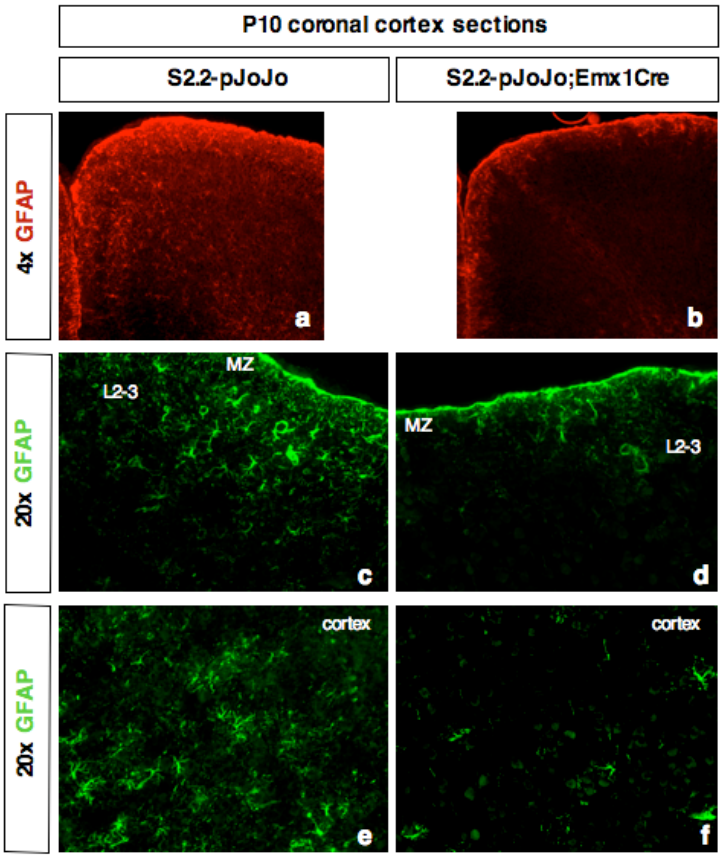

Figure 23: Decreased presentation of mature astrocytes in the postnatal cortex (P10) in *Scrt2.2-GOF* brains. The pictures represent IHC staining of brain sections single (left) and double transgenic mice (right), stained for GFAP-antibody.

To study whether Scrt2.2 exert an early effect on neurogenesis, analysis of cortical patterning at stage E12.5 on brain sections from *mScrt2.2*-GOF (*Scrt2.2-pJoJo;Emx1Cre)* and control embryos (*Scrt2.2-pJoJo*) has been performed. IHC with Pax6 antibody, which specifically labels the apical RGPs (Götz et al., 1998), revealed generally preserved expression pattern in the *Scrt2.2-pJoJo;Emx1Cre* brain at this early stage (Fig. 24a, b). The T-box TF Eomes/*Tbr2* (Bulfone et al., 1999) labels at this early stage IPs in the preplate of the ventro-lateral cortex, in which position the generation of CP neurons is advanced, as compared to dorsal and medial pallium. Notably, in the *Scrt2.2pJoJo;Emx1Cre* brain, the Tbr2 staining was enhanced suggesting an advanced neurogenesis, following the normal gradient of cortical differentiation (Fig. 24c, d). The expression of HuC/D, that marks post-mitotic but still immature neurons, was also up regulated (Fig. 24g, h) in the *mScrt2.2-GOF* cortex. At E12.5 a part of RGPs use the direct mode of neurogenesis to generate mostly neurons for future layer 6 (and to some extend layer 5, reviewed by Molyneaux et al., 2007). TF *Tbr1* is the earliest marker for mature cortical neurons (Hevner et al., 2001) and showed a slight up regulation in the *Scrt2.2; Emx1Cre* cortex, suggesting an increase of early-born layer6/5-neuronal subtypes (Fig. 24e, f).

Together, these results suggest that activation of *mScrt2.2* at the onset of cortical neurogenesis promotes the direct generation of early-born neuronal subtypes from RGPs, thus possibly diminishing the progenitor pool for neurogenesis at later stages.

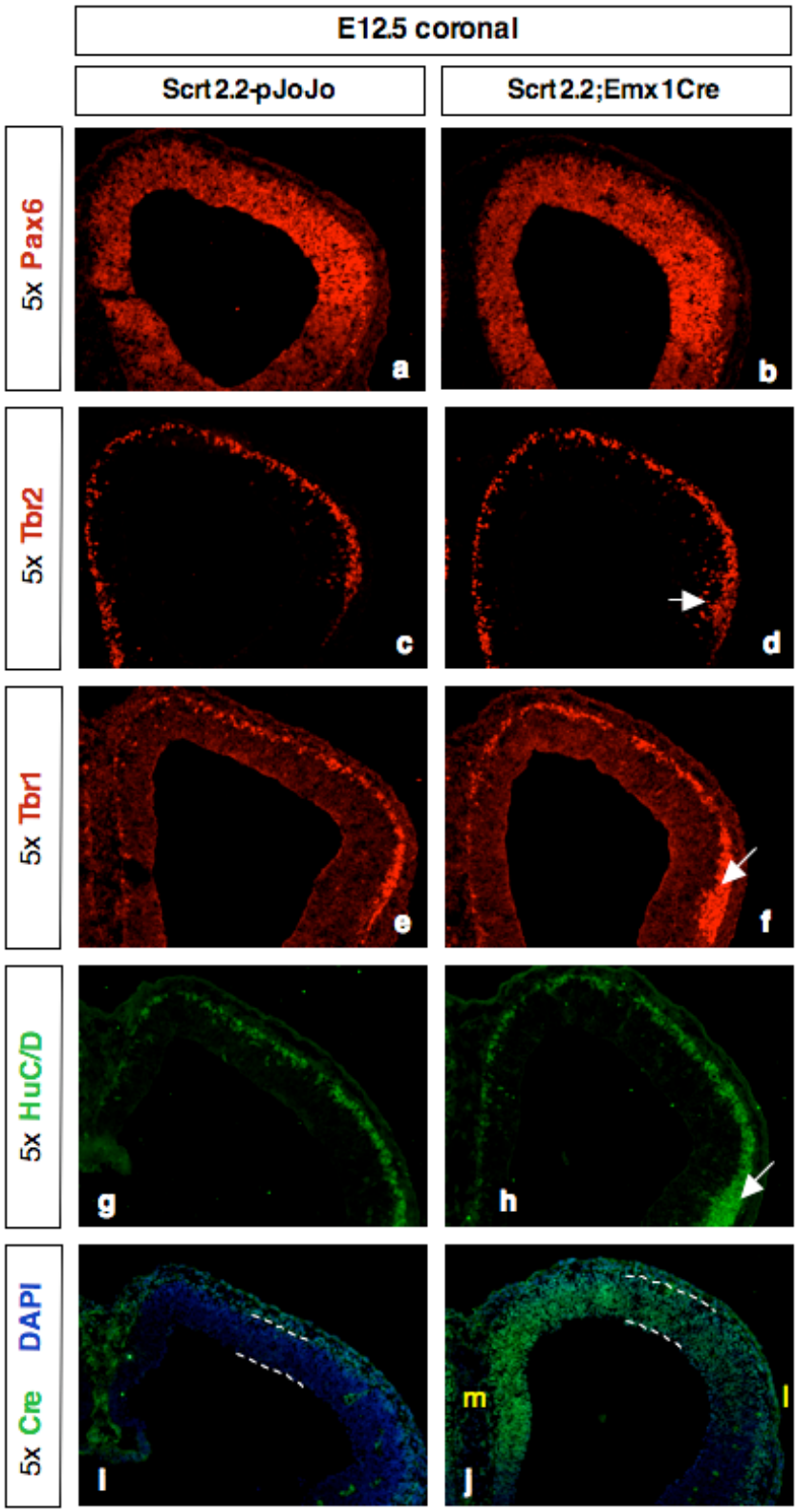

Figure 24: Early phenotype (E12.5) of the *Scrt2.2-pJoJo;Emx1Cre* cortex. IHC was performed on sections from E12.5 brains from control (left) and double transgenic embryos using antibodies as indicated. The arrows point to regions showing enhanced expression of the applied markers of neurogenesis (i, j). The graded expression of Cre-recombinase (medial-high to lateral low) is in agreement with previously reported results (Li et al., 2003).

Next, the effect of *Scrt2.2* over expression *in-vivo* at the pick of cortical neurogenesis (E15.5, E16.5) was analyzed. IHC analysis with Scrt2 antibody revealed a much wider expression in the IZ and CP of the *Scrt2.2-pJoJo;Emx1Cre* as compared to control, reflecting a successful recombination, driven by the *Emx1Cre* line (Fig. 24a, b). The wide distribution of Scrt2-positive cells in the double transgenic cortex generally paralleled the pattern of the Cre-immuno-reactivity (compare b/d in Fig. 24). However, while Cre-immunostaining was observed in the VZ/SVZ, IZ and CP, a clear Scrt2 signal in the VZ/SVZ was not visible, suggesting requirement of a long period for generation of the Scrt2 transgenic protein after the recombination.

Similarly to the registered elevation of the Tbr1 expression at E12.5, also at stage E16.5 a wider and much more densely packed band of post-mitotic early-born Tbr1+ neurons was detected in the lower CP (L6, L5) of the double transgenic mice as compared to control (Fig. 25 e, f). Furthermore, a stronger Tbr1 signal was observed in the CP of the double transgenic mice by ISH on sections from E15.5 brains (Fig. 25 g, h). Together, these findings support the idea that ectopic expression of Scrt2.2 at the onset of neurogenesis causes a larger portion of RGP daughter cells to exit from mitotic cycle and differentiate.

At stage E16.5, indirect neurogenesis via generated by RGPs intermediate Tbr2+progenitors, is promoted. Interestingly, immunostaining with Tbr2 antibody at E16.5 in the *Scrt2.2-pJoJo;Emx1Cre* mice revealed an enrichment of the Tbr2+ cells in the upper part of the SVZ and a pronounced accumulation in the IZ that normally contains post-mitotic migrating neurons (Fig. 25i, j). The increased *Tbr2*-expression at the basal SVZ and IZ could be also confirmed on mRNA-level by ISH at the same stage (E16.5; Fig. 25k, l). Moreover, the number of Mash1+ cell in the *Scrt2.2GOF*-cortex was increased as compared to control brains in which only few Mash1+ cells were detected in the corresponding region (Fig. 25m, n).

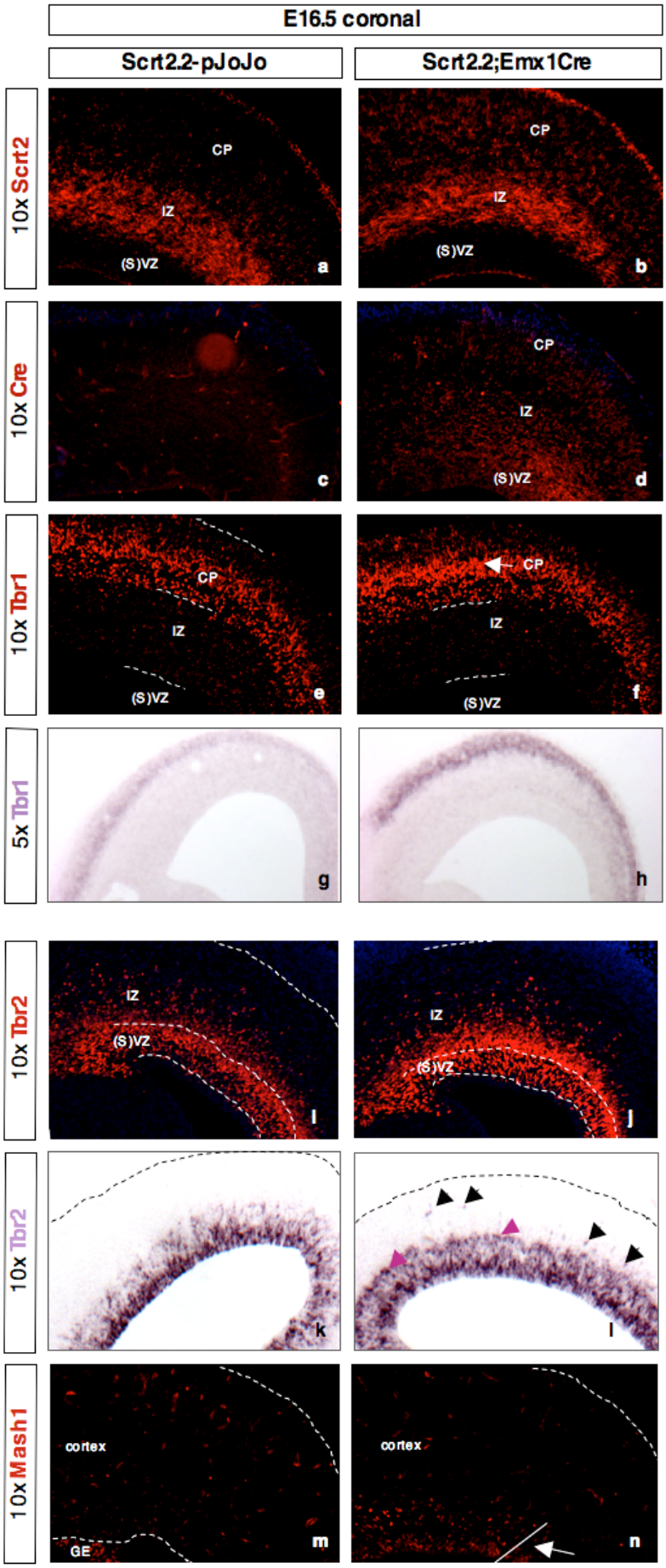
E16.5 coronal
Scrt2.2-pJoJo
Scrt2.2;Emx1Cre
10x Scrt2
10x Cre
10x Tbr1
5x Tbr1
10x Tbr2
10x Tbr2
10x Mash1
CP
IZ
(S)VZ
cortex
GE
a
b
c
d
e
f
g
h
i
j
k
l
m
n

Figure 25: Cortical phenotype of *Scrt2.2-pJoJo;Emx1Cre* mice at E16.5. Pictures of E16.5 brain sections of both genotypes after immunohistochemical staining with the indicated antibodies (red) or ISH with *in-situ* probes (**g, h** and **k, l**). The arrows indicate regions with increased expression of the corresponding markers. In **(l)** note that numerous Tbr2+ cells accumulate at the border SVZ/IZ (purple arrowheads) from where more such cells migrate into IP and CP (black arrowheads) of the double transgenic cortex as compared with the control.

During the indirect neurogenesis, neuronal differentiation is marked by a drop of the *Tbr2* expression in IPs of the SVZ and a gradual enhancement of *NeuroD* expression, that is fully replaced later by the expression of TF *Tbr1* in the post-mitotic neurons (Hevner et al., 2006). These three markers are assumed to exert a similar dynamic of expression also during the direct mode of neurogenesis (Arnold et al., 2009). Whether the increased set of brightly labelled Tbr2+ neurons in SVZ/IZ of the double transgenic mice are in the lineage of Tbr2+ IPs, or in the lineage of the direct neurogenesis (from the RGPs) was not clear at the moment and difficult to study through expression analyses. To discriminate between these possibilities, an *in-vitro* approach, presented in the next chapter of the results has been chosen.

	Developmental stage →	**E12.5**	**E16.5**	**P10**
Gene / protein:	**Marker for:**			
Pax6	RGPs	n.a.		
Ngn2	RGPs + IPs	n.a.	n.a.	
Tbr2 (strong)	IPs	n.a.	n.a.	
Tbr2 (faint)	Post-mitotic neurons	⇑	⇑	
Tbr1	Post-mitotic neurons	⇑	⇑	
HuC/D	Post-mitotic neurons	⇑		
Mash1	Differentiating neurons		⇑	
NeuroD1	Differentiating neurons			⇓
Cux1/Satb2	Upper cortical layers			⇓
Ctip2	Lower cortical layers			⇓
GFAP	Mature astrocytes			⇓

Table1: Summary of the regulatory effects in the gene expression in Scrt2.2 GOF condition.
E (embryonic day), P (postnatal day), n.a. (Not affected), ⇑ (increased), ⇓ (decreased)

2.3 INVESTIGATION OF THE MODE OF CORTICAL PROGENITOR DIVISION IN *SCRT2.2*-GOF BY CLONAL-PAIR ANALYSIS

The presented results from the phenotypic analysis of the developing and postnatal cortex after *Scrt2.2-GOF* in transgenic mice, strongly argued that the protein isoform encoded by *Scrt2.2* could act as a modifier of the number of generated neurons in developing cortex, possibly by influencing the mode of progenitors division. The majority of the cortical

glutamatergic neurons is produced from Pax6-positive pluripotent radial glia progenitors that divide at the apical surface of the VZ in one of the three types of cell division:

a) Symmetric proliferative division that predominates before the start of neurogenesis through which one RGP generates two daughter-RGP, increasing thereby the progenitor pool;

b) Asymmetric neurogenic division of RGP giving rise to one RGP (renewal) and one neuron in the direct mode of neurogenesis, predominantly acting at the onset of neurogenesis;

c) and asymmetric proliferative division of RGP generating one RG daughter cell and one IP that localizes in the second germinative zone, the SVZ and participates in the indirect mode of neurogenesis. In the SVZ the IP divides symmetrically (1-3 times) to produce either two daughter-IPs or the IP exits the cell cycle and undergoes a neurogenic division and generates two post-mitotic neurons (Noctor et al., 2004).

To investigate quantitatively the effect of both *Scrt2.2*-GOF and *Scrt2.3*-GOF condition on the cortical progenitor proliferation, clonal pair-analysis was used. This method has been established by Shen et al. (2002) and later modified by Li et al. (2003) and Sanada and Tsai (2005) allowing its application in studies after focal manipulation of gene activity though *in-utero* electroporation. Therefore, I learned to perform this sophisticated method, described in details in section 4.4.2 and in the results (part 2.4.). The generated plasmids allowing expression of either *Scrt2.2* or *Scrt2.3* together with GFP reporter under a strong CMV-promoter as indicated in Fig. 30b.

Embryo brains were electroporated with either CMV-*Scrt2.2*-GFP, CMV-*Scrt2.3*-GFP or control (CMV-GFP) empty vector at stage E13.5. At E14.5, cortices from embryos, electroporated with the same plasmid, were dissected and pooled together. The cortical material was dissociated, cultured for one day *in-vitro* (DIV1) as described in detail in the methods part (section 4.5.1 and 4.5.2) and analyzed by IHC (Fig. 26). Shortly, the dissociated cortical cells were spread in a clonal density to allow the monitoring of individual cell clone at DIV1 and the culture medium was supplemented with FGF2 to allow *in-vitro* proliferation (described in Bultje et al., 2009). Single GFP+ cells could clearly be distinguished from GFP+ clonal cell pairs and GFP-negative cells. Since the aim of this analysis was to study the influence of *Scrt2.2*-GOF condition on the division mode of progenitors, exclusively targeted (GFP+) cell pairs were analyzed.

Each experiment, including electroporations with control and GOF plasmid and IHC-analyses using antibodies for Pax6, Tbr2 and Tuj proteins, has been performed in three independent sets (data see in figure 46 in the Supplement).

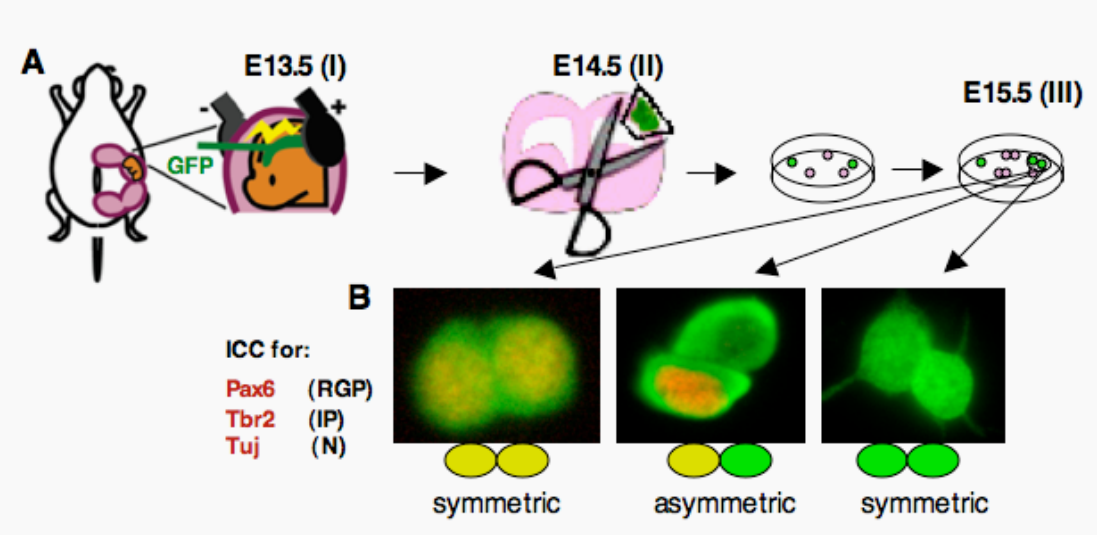

Figure 26: Principle of the clonal-pair analysis. (A) Plasmids were electroporated in the embryonic ventricle at E13.5. After one day, the cells of the targeted region of the cortex were isolated under a binocular, signalized and cultured for one day on poly-lysine coated slides under proliferative condition (Bultje et al. 2009). **(B)** Cell cultures were fixed and immuno-cytochemical (ICC) double- stained with antibodies for GFP and Pax6, Tbr2 or Tuj. Fluorescence pictures were taken in a raster to scan the slide and GFP+ pairs were examined for distribution of stained protein (in red).

As an intrinsic determinant of the RGPs (Götz et al., 1998) expression of TF **Pax6** in both cells of a clonal pair would reflect their proliferative symmetric division (Fig. 27A), while a clonal pair with only one Pax6-positive cell (Fig. 27B*)* counts for an asymmetric division, the negative one being either an IP or a neuron.

TF **Tbr2** is strongly and selectively expressed in IPs, contributing for IP cell specification (Sessa et al., 2008). Detailed recent analysis indicated that initiation of neuronal differentiation of IPs and generation of immature neurons in SVZ is marked by a diminishing of the Tbr2 expression level, concomitant with a transient expression of bHLH TF NeuroD (Englund et al., 2005). Accordingly, proliferative divisions of IPs were account only for cell pairs showing equally strong Tbr2 labelling (Fig. 27C). Cell pairs exhibiting equally faint Tbr2 expression present post-mitotic neurons produced by symmetric IP divisions. In order to prevent a misquotation of post-mitotic cells (faintly expressing Tbr2), IHC with Tuj1 antibody was included to determine post-mitotic neurons in the clonal cell pairs.

Tuj1 is the earliest marker for terminally differentiated neurons. Symmetric Tuj expression in both cells of the clonal-pair indicates a generation of two neurons through a neurogenic IP-division in the indirect mode of neurogenesis (Fig. 27E), while restricted Tuj expression to only one of the clonal partners accounts for a neuron generated by asymmetric division of RGP via a direct mode of neurogenesis (Fig. 27F).

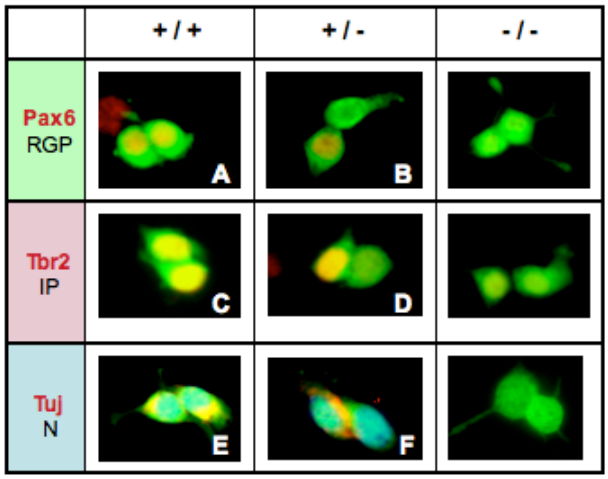

Figure 27: Clonal-pair types, analyzed by IHC-staining. The identity of a cell pair was determined using IHC-staining for Pax6, Tbr2 or Tuj, representing a radial glia progenitor (RGP), an intermediate progenitor (IP) or post-mitotic neuron (N) respectively. Clonal cell pairs have been sub-grouped according to the (a-) symmetric marker expression as A-F (same indication in figure 28).

The IPs undergo either proliferative divisions, to generate 2 IPs in SVZ, or they undergo terminal neurogenic division to generate neurons (Haubensak et al., 2004; Miyata et al., 2004; Noctor et al., 2004; Wu et al., 2005). Pairs with only one Tbr2-strongly positive cell could be therefore clearly counted as pairs composed by an IP and one RGP.

The presented below results describe the effect of *Scrt2.2*-GOF on cortical progenitor divisions, while *Scrt2.3*-GOF did not display any significant changes (data in Fig. 46 of the Supplement).

Analysis of the proliferative RGP divisions (both daughter cells are Pax6+) was not significantly altered (control: 42,0%, SEM 0,98 // *Scrt2.2*-GOF: 43,9%, SEM 0,97; p=0,79; Fig. 28A), which fits to generally unchanged expression of Pax6 in RGPs at E12.5 in *Scrt2.2-JoJo;Emx1Cre* transgenic mice (Fig. 24b). The fraction of asymmetric RGP divisions, however revealed a significant increase of Pax6 +/- expressing pairs after *Scrt2.2* over expression (control: 6,7%, SEM 0,82 // *Scrt2.2*-GOF: 23,7%, SEM 0,47; p=0.01; Fig. 27B), which might reflect enhanced direct neurogenesis, implying **a)** one RGP to generate either one neuron and one RGP, or **b)** one neuron and one IP.

The portion of clonal cell pairs with asymmetric Tbr2+ expression (+/-), counting for an IP produced by asymmetric RGP divisions, was remarkably decreased (control: 16,5%, SEM 0,58 // *Scrt2.2*-GOF: 8,7%, SEM 0,48; p=0.02; Fig. 28D), supporting the option **a)** of the discussed above options for Pax6+/- pairs. In the same line of evidence, the portion of asymmetrically labelled Tuj+ pairs (+/-), descendents of asymmetric RGP divisions producing a neuron via the direct mode, was significantly enhanced (control: 17,8%, SEM 0,29 // *Scrt2.2*-GOF: 27,3%, SEM 0,25; p=0.005; Fig. 28F). Together, these findings indicate that focal *in-vivo* activation of *Scrt2.2* in RGPs promotes neurogenesis via the direct mode at the expense of production of an adequate number of IPs. In addition, the portion of cell pairs with symmetric Tbr2 expression (+/+), reflecting proliferative IP-divisions in SVZ was clearly decreased in the GOF- cortex (control: 54,1%, SEM 1,05 // *Scrt2.2*-GOF: 25,6%, SEM 0,63; p=0.01; Fig. 28C). Thus, upon *Scrt2.2*-GOF not only asymmetric division of RGPs generates less IPs, but also these IPs are unable to multiply in the SVZ. Consequently, the IPs

prematurely undergo neurogenic terminal division in the SVZ/IZ, reflected in the generation of a higher proportion of Tuj1+/+ neurons (control: 16,9%, SEM 0,35 // *Scrt2.2*-GOF: 29,6%, SEM 0,34; p=0.007; Fig. 28E).

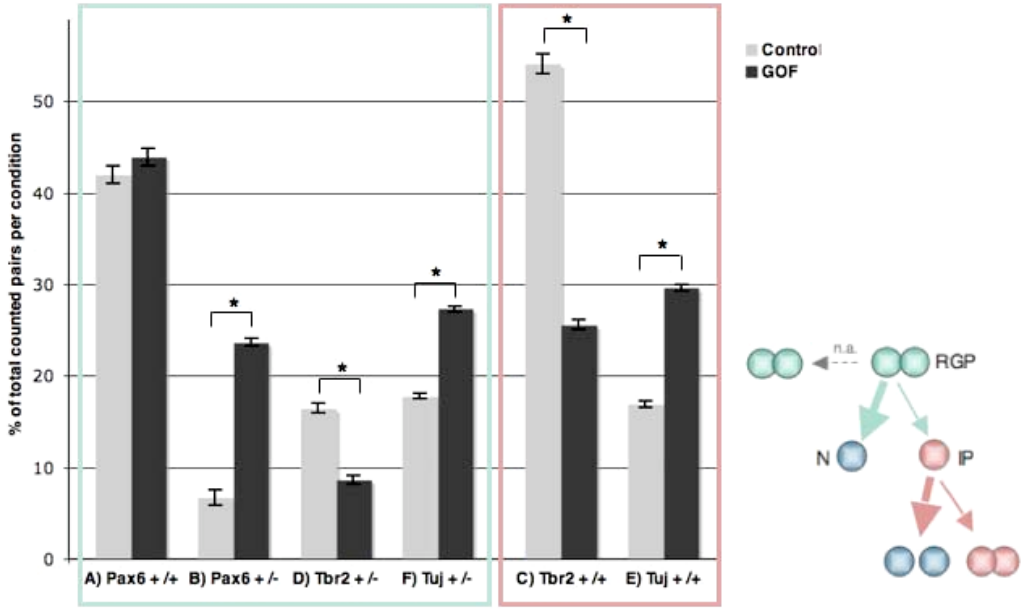

Figure 28: *In-vitro* clonal pair analysis after *in-vivo* *mScrt2.2*-GOF. The average values from three independent experimental sets are displayed. Each bar presents the percental part of 100% counted conal cell pairs per indicated ICC-marker, comparing respective subgroups between control (bright) and *Scrt2.2*-GOF (dark). Data from counting are shown in figure 46 in the Supplement. The wide arrow in the schema on the right indicates the favoured cell division after Scrt2.2-GOF. The green frame indicates changes on the level of asymmetric RGP-divisions and the red frame indicates change on the level of IP-divisions. A, B, D, F, C and E refer to the subgroups of analyzed cell pair types shown in figure 27. (n.a) not affected

Together, these findings strongly suggest that *Scrt2.2*-GOF negatively regulates the decision of RGPs to generate intermediate progenitors through asymmetric division. Instead, *Scrt2.2* appears to promote cell cycle exit and premature generation of neurons via the direct mode of neurogenesis of RGPs and via terminal neurogenesis of IPs in the SVZ.

2.4 ANALYSIS OF CORTICAL CELL MIGRATION AFTER FOCAL OVEREXPRESSION OF SCRT2.2 AND SCRT2.3 BY *IN-UTERO* ELECTROPORATION

Evidence has been presented that members of the Snail family of TFs could influence cell migration (Barrallo-Gimeno and Nieto, 2005). Since the performed IHC analysis indicated that Scrt2 is expressed in cortical plate neurons that normally undertake a radial migration along the RG processes, I was interested to examine whether mScrt2 affects the neuronal cell migration. To investigate this question, focal activation of both *Scrt2.2* and *Scrt2.3* transcripts by *in-utero* electroporation (IUE) of embryos brains has been performed. The plasmids used for electroporation (same as the ones used in the clonal pair analysis) are

indicated in Fig. 29b. The expression of the open reading frame (ORF) of *Scrt2.2 or Scrt2.3* was driven by a strong CMV (cytomegalovirus)-promoter, followed by an IRES (internal ribosome entry site) and the coding region of eGFP (enhanced green fluorescence protein). The control plasmid was devoid of *Scrt2* coding region, thus expressing eGFP only. The IUEs were performed in brains of E13.5 mouse embryos according to the method of Saito and Nakatsuji, (2001) as described in the Methods. One day after electroporation, the targeted region of the brain showed a strong GFP-fluorescence (Fig. 29c). The isolated GOF and control brains were cut in 8µm coronal sections and used in immuno-histochemical analysis.

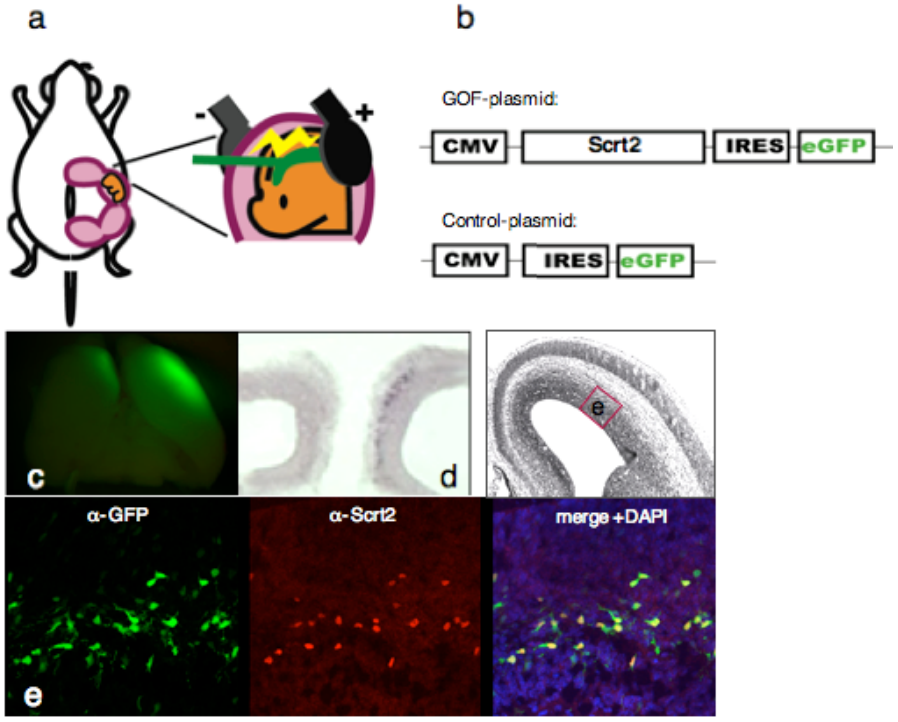

Figure 29: Focal *mScrt2.2*-overexpression in cortical progenitors using *in-utero* electroporation (IUE). (a) Schematic presentation of the electroporation procedure; **(b)** plasmid-DNA injected by IUE; **(c)** GFP-fluorescence of an E15.5 telencephalon after IUE at E13.5, **(d)** ISH on a coronal section of *mScrt2.2*-GOF brain (E15.5) with *Scrt2*-riboprobe; **(e)** GFP (green) and Scrt2 (red) expressing cells overlap to almost 100%.

As illustrated in Fig. 29e, double immunoassaying with GFP and Scrt2-antibodies revealed a strong expression of Scrt2 in almost all successfully transfected (GFP+) cells.

As shown in Fig. 30 I, three days after the electroporation at E13.5, most of the GFP+ cells in the control brains left the proliferative zones (VZ/SVZ), massively invaded the IZ and even already reached the lower CP (marked by arrowheads). Only a few cells were still located in the upper part of SVZ (white arrow). In contrast, the GFP+ cells expressing *mScrt2.2* were massively accumulated in the SVZ or in the IZ, and no GFP+/*Scrt2.2*+ cells were detected in the CP.

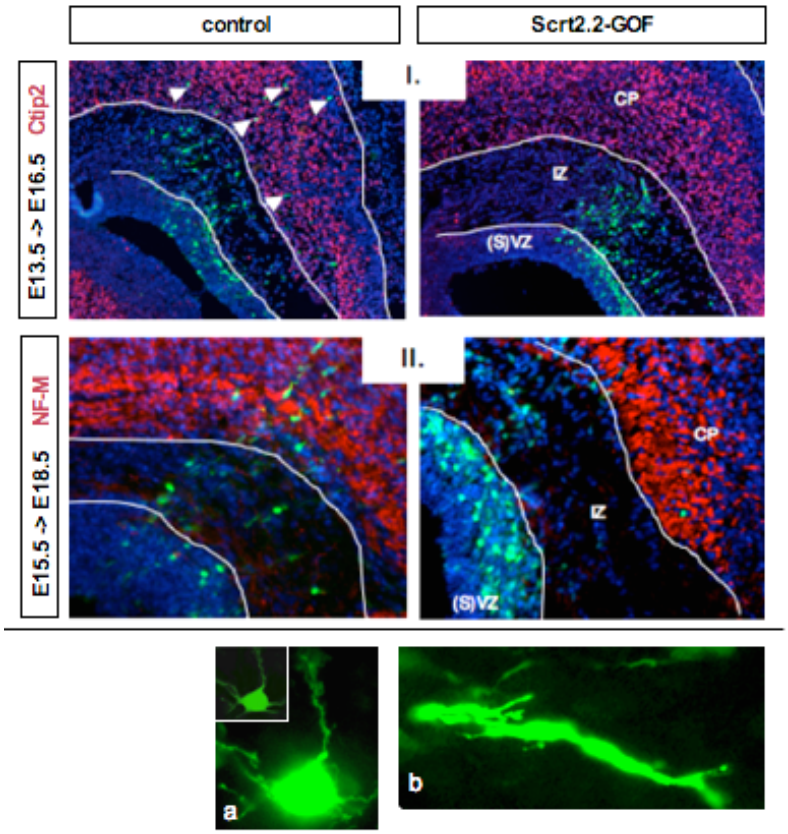

Figure 30: Accumulation of targeted cells with *mScrt2.2*/GFP+ expression vector in the SVZ of the developing cortex. Pictures after performed immuno-histochemical staining with antibodies (red) as indicated on brain sections form a brain injected with a control plasmid (left) and the *Scrt2.2* over expressing vector (right). **I.)** Ctip2 staining marks neurons in the lower cortical plate (CP); **II.)** Neurofilament M (NF-M) marks neurons and fibres above the intermediate zone (IZ); the accumulated in the SVZ cells often showed a multipolar morphology **(a)** and many of them were tangentially orientated **(b).**

Next, I studied the effect of the activation of *mScrt2.2* during late neurogenesis. Accordingly, IUE was done at E15.5 (e.g. during the peak of neurogenesis) and the analysis was performed at E18.5. The observed migrational defect in the targeted cortex with the *mScrt2.2* expression plasmid was severe, showing a clustering of GFP+/Scrt2.2+ cells in the SVZ (see Fig. 30; II).

To investigate the potentially isoform-specific effect on cell migration, IUEs have been performed to over express *Scrt2.3* according to the described above procedure. Similarly to *Scrt2.2*-GOF, three days after activation of *Scrt2.3*, the GFP+ progeny of progenitors showed a severe migrational defect. As shown in Fig. 31, almost all GFP+ cells in the cortex electroporated with the *Scrt2.3* expression plasmid were trapped in the SVZ and only few *GFP+/Scrt2.3+* cells reached the cortex. In contrast, after electroporation with the empty vector, a substantial part of the electroporated cells were located in the CP.

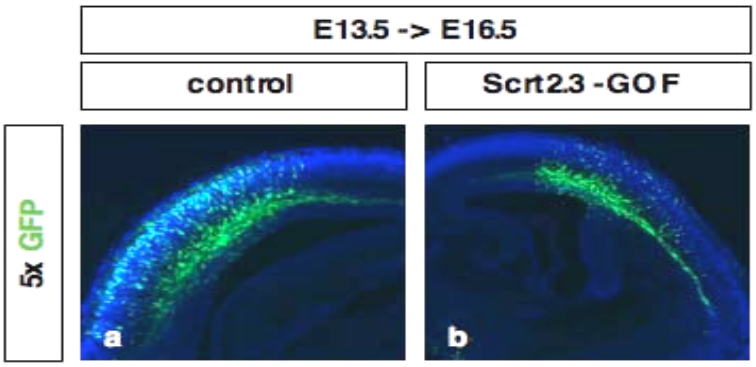

Figure 31: Impaired cell migration after *mScrt2.3* expression in cortical progenitors. Three days after IUE at E13.5, coronal E16.5 brain sections from control (a) and *Scrt2.3* injected brains (b) were stained with GFP antibody by IHC and counterstained with DAPI (in blue). Note that in the control section, the GFP+ cells massively invade the cortical plate (CP), while only few GFP+ cells expressing Scrt2.3, successfully reached the CP.

In addition, it has been attempted to study the postnatal position of the accumulated cells in the SVZ in the *Scrt2.3*-GOF experiments described above. Therefore, electroporated at E13.5 brains were analyzed at postnatal stage P3. During normal development at P3, all neurons of layer 6 and 5 and to a large extend also neurons of layer 4-2 have reached their final layer-specific locations. As illustrated in figure 32 (a, b), in the control brain almost all of the targeted GFP+ cells were located in the upper CP, while in the cortex after focal activation of *Scrt2.3* only a small portion of the GFP+/*Scrt2.3*+ cells were located in the CP. Instead, the majority of the GFP+ somata was found directly above the SVZ, or still radially migrating across the CP. Immuno-staining for Cux1, a marker for a subpopulation of the upper cortical layers, allows determination of the intra-cortical position by marking the layers 2-4 (Nieto et al., 2004; Zimmer et al., 2004). In both, control and *Scrt2.3*-GOF brains, GFP+ cells were located either in the expression domain of Cux1 in the upper CP, or across the lower CP (Fig. 32c, d). Notably however, while the majority of the neurons targeted with the GFP+/ empty vector failed to show Cux1 immuno-reactivity (Fig. 32c), most of the targeted GFP+/*Scrt2.3*+ cells were Cux1+ cells (white arrowheads in Fig. 32d). It is furthermore interesting to note that many of the accumulated GFP+/*Scrt2.3*+ cells at the SVZ/IZ border were tangentially orientated (yellow arrowhead in Fig. 32d, g) and in most cases were expressing Cux1, while such cells were missing in the control brain. In addition, examination under higher magnification of the GFP+ cells revealed different subcellular distribution of the GFP-staining. While in the electroporated controls, the GFP-staining clearly marked pyramidal-shaped neurons as well as their radially orientated axons and arborized dendrites (Fig. 32c, e, h), the GFP+/*Scrt2.3*+ targeted cells displayed mostly a round shape without extending long axonal processes (Fig. 32d, f, i). Notably, the GFP+/*Scrt2.3*+ electroporated cells showed in addition to the cytoplasmic staining also a clear nuclear GFP staining, indicating intra-cellular shuttling of the *mScrt2.3* transcript

(Fig.32 i). This is in agreement with the predicted encoded protein structure by *mScrt2.3* transcript, which contains a NLS sequence (see Fig.16).

Taken together, the experiments presented in this section indicate that a focal *in-vivo* expression of both *Scrt2.2* and *Scrt2.3* transcripts in cortical progenitors causes severe radial cell migration defects that delay the incorporation of the neuron into the CP. Additionally, upon *Scrt2.2* and *Scrt2.3* expression, a substantial portion of the cells show a tangential orientation, they have altered multipolar cell shape and changed processes outgrowth. Given the predicted presence of a NLS only in the isoform encoded by *Scrt2.3*, further experiments are necessary to address a possible role in fate specifications of the developing cortex.

Figure 32: Postnatal phenotype in the cortex after ectopic expression of *mScrt2.3* in RGPs. The brains were electroporated at E13.5 with either control (empty vector) or *mScrt2.3* expressing plasmid and migration of the targeted cells were examined by IHC for GFP expression on coronal slides of P3 brains; **A-B)** illustrate a delay in the migration of *mScrt2.3*/GFP+ cells of the GOF-cortex; **C-D)** Location of GFP+ cells in the cortical plate in the expression domain of the neuronal upper layer marker Cux1; **E-F)** subcellular GFP distribution relative to nuclear Cux1-staining; **G)** the high magnification micrograph of D illustrates, that most of the GFP+ cells in *mScrt2.3*-GOF are trapped in the IZ, express nuclear Cux1, are tangentially orientated and show cytoplasmic GFP in contrast to migrating cells. **H-I)** Subcellular localisation of GFP+ targeted cells in the cortex; **J-K)** cytoplasmic versus (peri-)nuclear GFP-staining in the control and *mScrt2.3*-GOF conditions respectively determined by DAPI and nuclear Cux1 labelling.

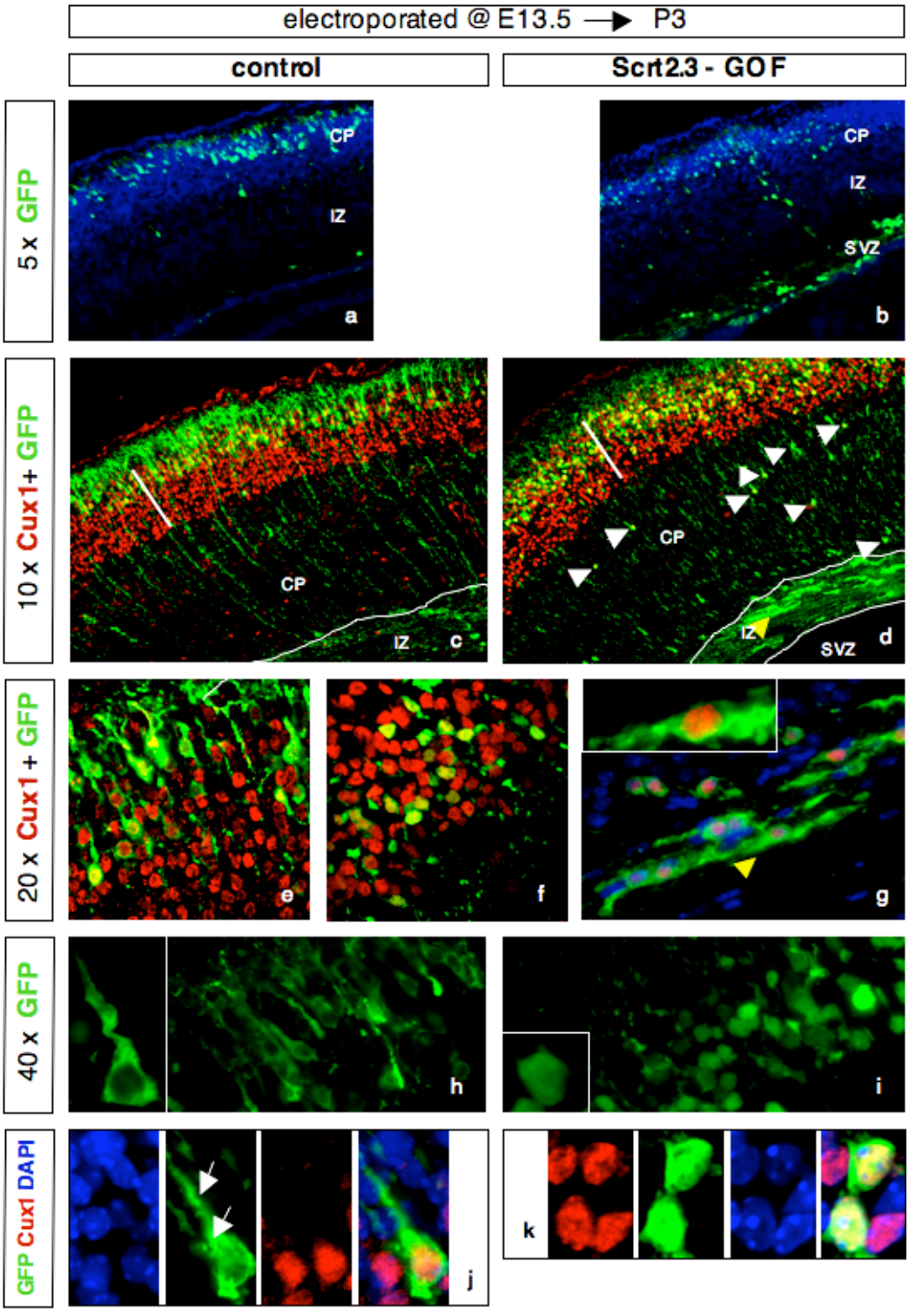
electroporated @ E13.5 → P3
control
Scrt2.3 - GOF
5 x GFP
10 x Cux1+ GFP
20 x Cux1 + GFP
40 x GFP
GFP Cux1 DAPI
CP
IZ
SVZ
a
b
c
d
e
f
g
h
i
j
k

2.5 ECTOPIC EXPRESSION OF *mSCRT2.2* IN EMBRYOS OF *XENOPUS LEAVIS*

The presented above data from the performed *in-vivo* and *in-vitro* analysis suggested that *Scratch2* modulates the neurogenesis in developing mammalian cortex. Both, *Snail* and *Scratch* subgroups of the C_2H_2 zinc-finger proteins are evolutionary conserved from simple Placozoan Trichopax to humans (reviewed in Barrallo-Gimeno and Nieto, 2009). Generally, such evolutionary conserved factors show similar control function. Therefore, in collaboration with Barbara Rust (research group of Kris Henningfeld in the department of Prof. Pieler (Developmental Biochemistry, University Göttingen)), it was attempted to gain insights into the potential role of *Scrt2* in *Xenopus leavis* neurogenesis, a well-characterized system for analysis of early vertebrate development.

In *Xenopus,* the first primary neurons are born within neural plate shortly after gastrulation in three bilateral longitudinal domains (Fig. 33). The events of neural induction lead to the expression of transcription factors that initiate a neural cell fate specification. The differentiation of the primary neurons is driven by the bHLH transcription factor neurogenin-related 1 (*Xngnr-1*) a pro-neural factor, which in turn activate the expression of the neuronal-specific type II ß-tubulin (*N-tubulin).*

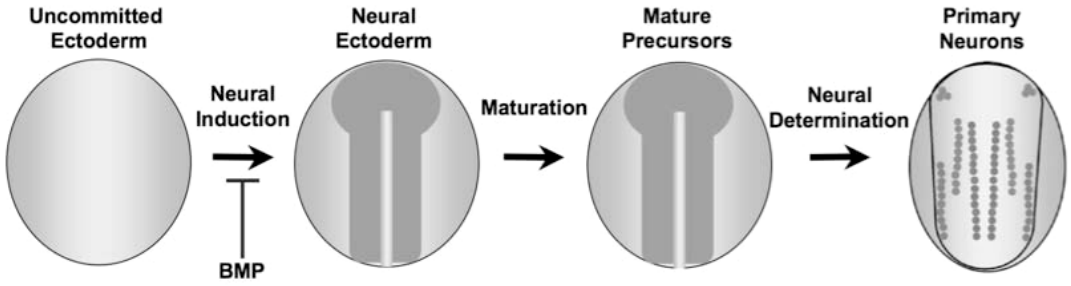

Figure 33: Schematic cascade of early events in *Xenopus* neurogenesis. At blastula stage, the animal half of the embryo consists of an uncommitted epidermal cell population. Upon BMP inhibition, the neural plate is induced (dark), demarcated by expression of pan-neural marker genes, such as *Sox3*. Maturation of the neural plate induces neural marker *Xngnr-1*. Neural determination occurs in three longitudinal stripes (circles) to both sites of the midline and in addition in the trigeminal placodes. The terminal differentiated neurons express *N-tubulin*.

The expression of these cascade genes can be visualized by whole mount *in-situ* hybridization and the relative short developmental time window allows the quick read-out of experimental manipulations.

Although it was reported that *Scrt2* is specific for vertebrates (Nieto, 2002), however only the *Scrt1* homolog could be identify in *Xenopus* so far (Barrallo-Gimeno and Nieto, 2009). The *mScrt2* coding region has been used for ectopic expression in *Xenopus* embryos performed by Barbara Rust. Injection of RNA (50 - 250pg) transcribed from *mScrt2.2* into

one blastomere of 2-cell stage *Xenopus* embryos proved to be lethal. Therefore a hormone-inducible form of Scratch2, C-terminally fused to the glucocorticoid ligand-binding domain (*mScrt2.2*-GR) was used in further experiments. mRNA encoding *mScrt2.2*-GR (100pg) was injected in one blastomere of the 2-cell stage and protein activity induced at the onset of gastrulation (stage 10).

To evaluate the influence of *mScrt2.2* on neurogenesis, injected embryos were analyzed for the expression of molecular markers that indicate distinct steps during neural development (Fig. 34). While the neural precursor cell population was increased at the open neural plate stage (marked by the enlarged neural plate, stained by *Sox2*; 75.5%, n=49), the expression of the pro-neuronal gene *Xngr-1* (homolog of mammalian Ngn2) was decreased (78.0%, n=41), indicating a decrease in neuronal commitment as further demonstrated by a strong reduction of the expression of *N-tubulin*, a marker for post-mitotic, differentiating neurons (82.4%, n=68), suggesting that also in *Xenopus, mScrt2.2*-GOF condition modulates the neurogenesis.

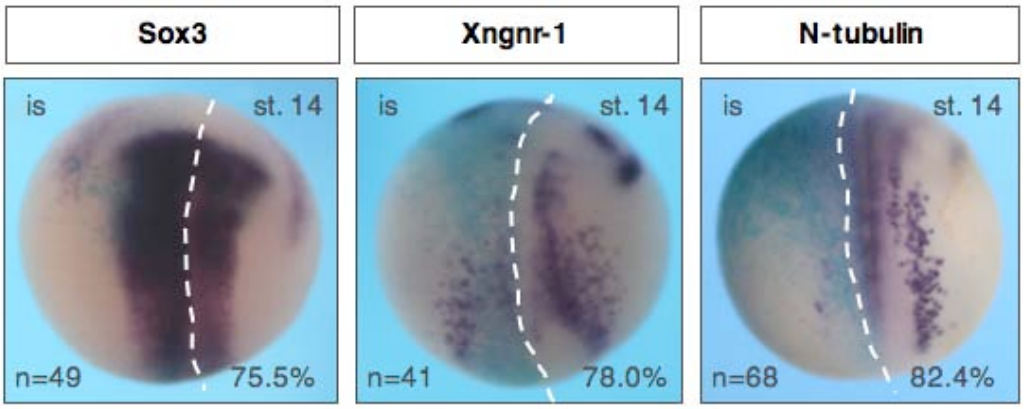

Figure 34: *mScrt2.2*-GR expands the neural plate and inhibits neuronal commitment with consequent less neuronal differentiation at the open neural plate stage. Embryos were injected with 100pg *mScrt2.2*-GR together with 50pg lacZ mRNA into one blastomere of the 2-cell stage and inducted with dexamethasone at stage 10. Embryos were collected at stage 15 and the injected site was subsequently determined by ß-Gal staining and is always oriented to the left site.

To evaluate the effect of *mScrt2.2* on neural development of the brain, *mScrt2.2*-GR was targeted to the head region by injection into one dorsal blastomere of the 8-cell stage embryo. The *mScrt2.2* expression was activated at the onset of gastrulation (stage 10) or at the end of neurulation (stage 20) and embryos were stained by ISH for *N-tubulin* expression.

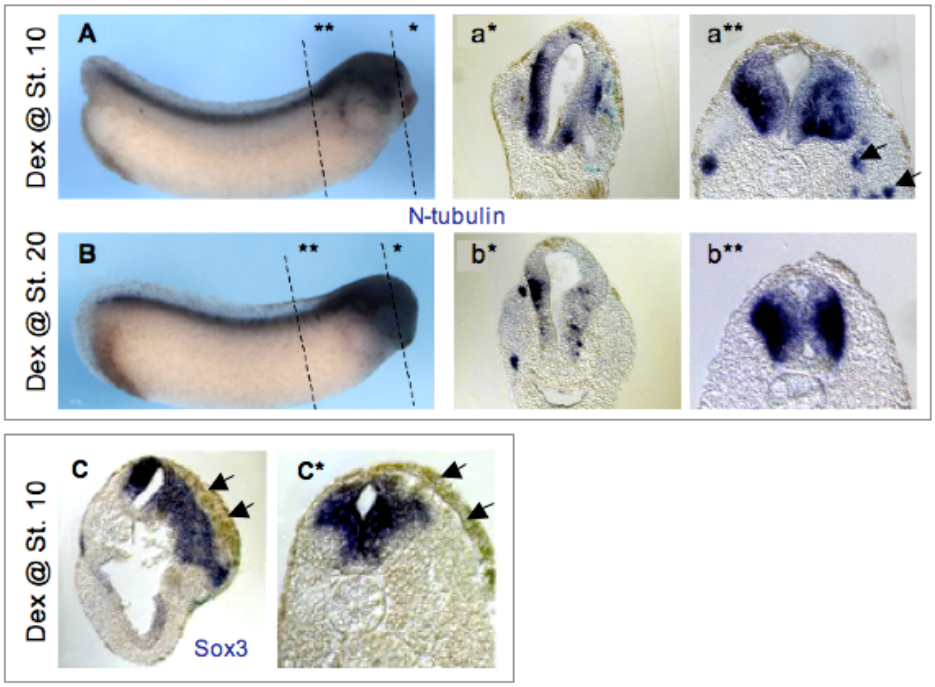

Figure 35: At the tail bud stage, *mScrt2.2*-GR reduces the number of differentiating neurons anteriorly and. 100pg *mScrt2.2*-GR together with 50pg lacZ mRNA was injected into one blastomere 8-cell stage embryo and induced with dexamethasone (dex) at stage 10 **(A, C)** or 20 **(B).** Embryos were cultured until stage 26 to 29, the injected site labelled by ß-Gal staining, and subsequently marked for *N-tubulin* (A, B) or *Sox3* (C) expression. 30 *µ*m gelatine-albumin sections were cut; the arrows in a**, point to ectopic localisation of *N-tubulin*+ neurons and the arrows in c and c*, indicate the thickening of pigmented epidermis

Induction at gastrula stage reduced *N-tubulin* expression in the brain (Fig. 35a*/**). Late induction of *mScrt2.2*-GR however resulted in a decrease of *N-tubulin* expression in its normal expression domain (Fig. 35b*), while no alteration of the *N-tubulin* expression domain could be observed within the neural tube more posterior (Fig. 35b**). Additionally, when *mScrt2.2*-GR was specifically induced in the head region, *Sox3* expression was only increased in the anterior brain region most probably outside the brain (Fig. 35c), while a thickening of the pigmented epidermis was determined anterior and posterior (Fig. 35c,c*), suggesting doe-dependent effects of mScrt2.

The animal cap consists of a special population of cells that has pluripotent stem-cell characteristics and when dissected, develops under native conditions into atypical epidermis. However, if a gene is sufficiently potent it can induce differentiation of these cells into derivates of all three germ layers. Thus, to determine whether *mScrt2.2*-GR is sufficient to direct a neuronal fate, an animal cap assay was performed. *mScrt2.2*-GR was injected alone or in combination with noggin (to neuralize the explants) into both blastomeres of the 2-cell stage, cultured until stage 9 and the animal cap dissected from the embryo. Total RNA was extracted, cDNA synthesized and subjected to qPCR to determine the expression of *Sox3 and N-tubulin*. In neuralized caps, *mScrt2.2*-GR synergistically induced *Sox3*-expression already

at the equivalent of stage 15 and even stronger at stage 26, while mScrt2.2 failed to activate *Sox3* in naïve caps (Fig. 36A).

Also the up-regulation of *N-tubulin* was only observed in neuralized caps (Fig. 36B). These data indicate that the expansion of the brain and neural tube upon *mScrt2.2*-injection, observed in the whole embryo, requires an additional signal providing competence to adopt a neural cell fate.

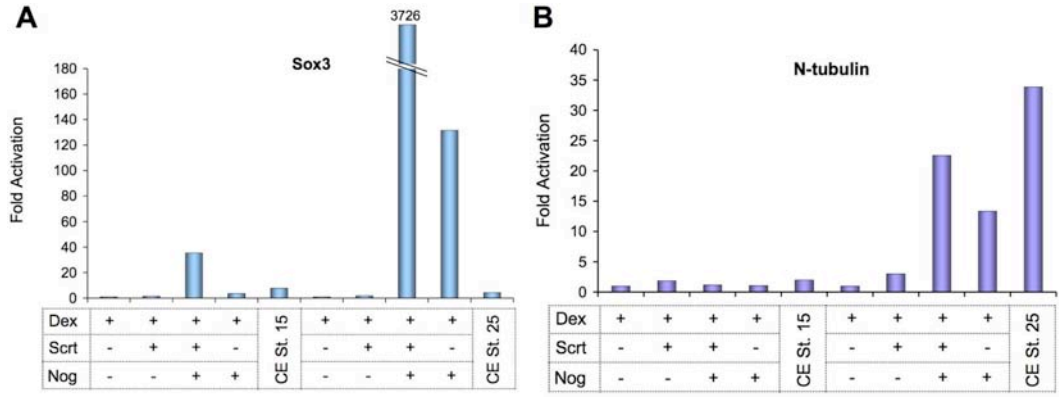

Figure 36: *mScrt2.2*-GR affects neural marker gene expression only in neuralized *Xenopus* animal caps. Embryos were injected with 75pg *mScrt2.2*-GR together with or without animally into both blastomeres of the 2-cell stage, cultured until stage 9 and the animal caps dissected. Caps were treated with dexamethasone (Dex) at stage 10 and collected at stage 15 and 26, the RNA extracted, cDNA synthesized and subjected to qPCR analysis. Runs were performed in triplicates and values normalized to ODC-expression and marker gene expression related to un-injected control caps (CC), using the ΔΔc (t) method after Pfaffl. Nog: noggin **A)** Expression of *Sox3* in the animal caps at stage 15 and 25, **B**) Expression of *N-tubulin* in the animal caps at stage 15 and 25. Nog: noggin, Dex: dexamethasone

Together, these findings indicate that the ectopic expression of *mScrt2.2* in *Xenopus* embryos has the capacity to modulate primary neurogenesis in a spatio-temporal dependent manner. The modulation of neuronal commitment and differentiation seems to require the presence of neuralizing cues /co-factors, whereas other conserved mechanisms of Snail superfamily proteins are regulated independently.

2.6 CONDITIONAL KNOCKOUT OF *SCRT2* IN THE MOUSE

2.6.1 Generation of a construct for conditional knockout of *Scrt2*

The work on my PhD thesis started actually with an attempt to generate a Scrt2 conditional knock-out mouse line to get insights in the function of this un-described gene with the commonly used loss-off function approach. Therefore, generation of a mouse line with floxed Scrt2-locus was attempted. As outlined below, the foreseen analyses were hampered by the fact that the generated mouse chimeras did not performed germline transmission. To

overcome the difficulties with the loss of function approach, I attempted to analyze the function of Scrt2 in a gain of function condition instead. This approach was promoted by the suggestion that members of the C_2H_2 superfamily of TF mainly act as transcriptional repressors (Hemavathy et al., 2000) and experiments in the past have shown, that the transgenic phenotype by gain of function is often stronger then by loss of function of a transcriptional repressor (personal communication K. A. Nave). However, using the generated by me knock-out construct, recently an alternative approach was tried to generate *Scratch2* cKO chimeric mice that are still under breeding to test germline transmission and forthcoming analyses. Therefore, I am including in this presentation, the mastered and applied by me strategy for the generation of transgenic mice for conditional targeted disruption of the *Scrt2* gene.

The design of the construct for conditional gene targeting in ES cells was based on the Cre-loxP system. The genomic region of the murine *Scrt2* gene (64,3 kb) is located on chromosome 2 at position 151855292 bp to 151921538 bp (NC_000068.6; Reference assembly (C57BL/6J)). Two *loxP* sites, each representing a 34 bp sequence recognized by a site specific Cre-recombinase, were introduced 522bp upstream of the second coding exon and 856bp downstream of it, thus flanking a genome region of 2181 bp coding for the five zinc-finger elements of the Scrt2 protein. Upon activation, the site-specific Cre recombinase recognizes the two *loxP*-sequences and catalyzes recombination between them, finally leading to excision of the DNA between these sites, and disrupting the function of the targeted gene (Sauer, 1998; Sauer and Henderson, 1989).

To minimize the probability of deleting regulatory domains, the genomic regions adjacent to the insertion sites of the *loxP*- / NEO-cassettes were analyzed for highly conserved elements between human and mouse using the databases of the National Centre for Biotechnology Information (NCBI, http://www.ncbi.nih.org) and Ensemble (http://www.ensembl.org). There were no elements to be disturbed or deleted by the targeting construct, either in the intron sequence 5´of Exon 2, nor in the 3`UTR.

To figure out the genomic region containing *mScrt2* gene, a PAC-library (RPCI-21 Female; 129S6/SvEvTac, CHORI) was hybridized with a Scrt2-specific DNA probe. Eight PAC-clones were identified and four of them were used for subsequent analysis. Two clones contained the *Scrt2* genomic region necessary for the generation of the targeting vector as identified by PCR analysis. One of the positive PAC clones (RP21-4K18) was used to subclone the targeting region (14,1kb), including 5´and 3' homology arms via gap repair into the retrieval plasmid PL253 (Fig. 37A). Subsequently, the two cassettes from the mini-targeting plasmids (modified plasmids PL452 and PL451) were inserted to the gap-repaired plasmid by homologous recombination.

The first cassette, containing a floxed NEO cassette for positive selection in bacteria and the unique restriction site *HindIII* for later analysis of ES cell clones by southern blot technique, was inserted in PAC-PL253. Furthermore, the NEO cassette was removed by induction of Cre recombinase expression in SW106 cells (PAC-PL253/NEO1), leaving a single *loxP*-site (PAC-PL253/P1). Afterwards, the second cassette containing NEO, flanked by *frt*-sites and a downstream *loxP*-site as well as a unique *BamHI* restriction site was inserted (PAC-PL253/P1/NEO2).

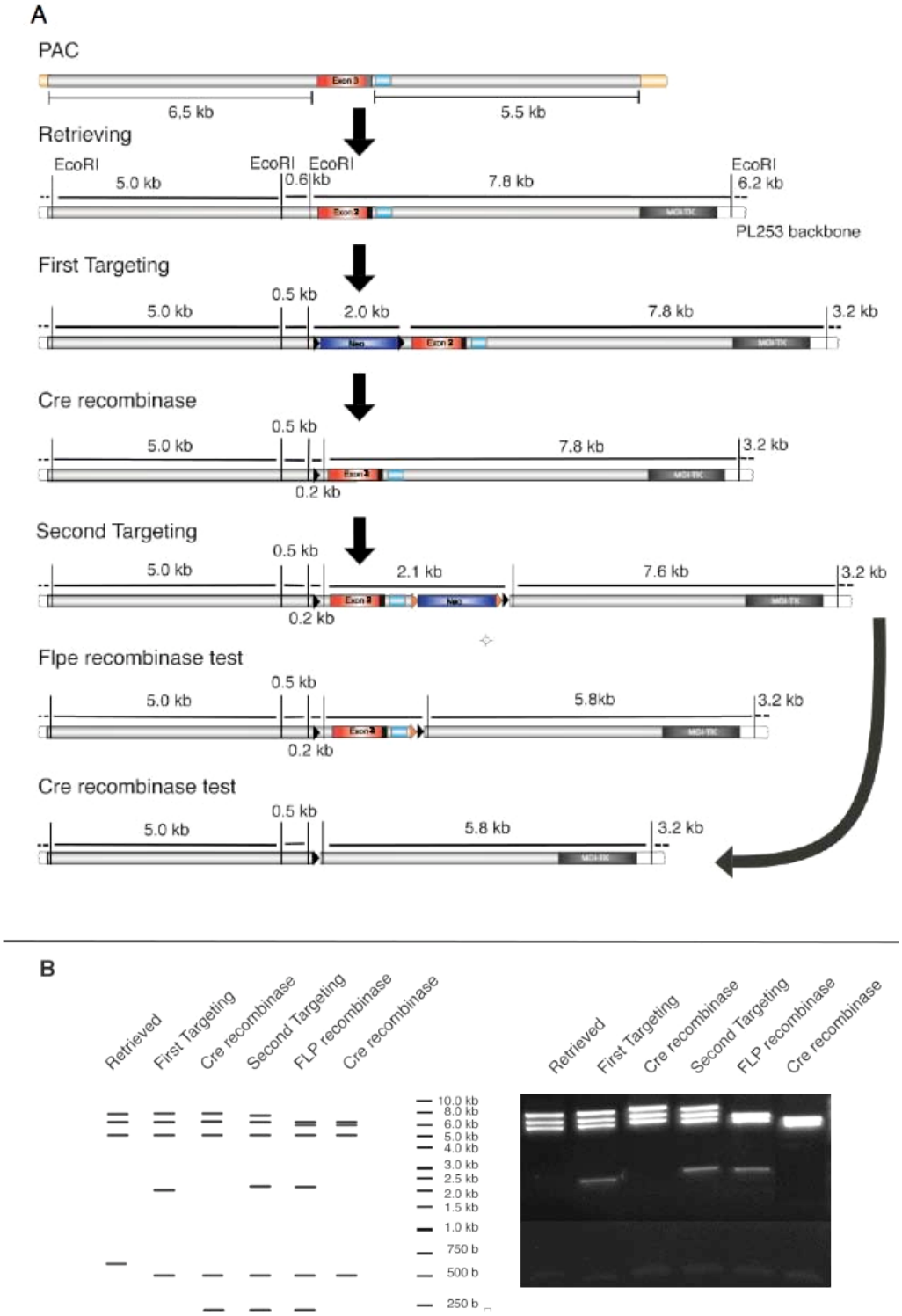

Figure 37: Construction and functional analysis of the *Scrt2* conditional knockout vector.
(A) Retrieving and targeting of the 12.2kb genomic region containing the Scrt2 coding exon 2. Targeting region is depicted in grey. Red is Scrt2 coding exon 2 and light blue display untranslated regions. Black arrowheads are *loxP*-sites and grey arrowheads are *frt*-sites. The Neo cassette is depicted in blue whereas the tk cassette is black. **(B)** *EcoRI*-digestion pattern of the plasmids at every stage of the targeting vector construction (left: expected pattern; right: actual pattern, 0.2kb -fragment not shown on gel).

Before ES cell electroporation, an *in-vitro* test to check the functionality of all intermediate plasmids had been performed (Fig. 37B). Therefore, the plasmid DNA was isolated from the appropriate *E. coli* strain that have been induced to mediate homologous recombination, Flp- or Cre- activity previously and re-transformed in DH10ß and digested with *EcoRI* to analyze the fragments sizes on an agarose gel. Additionally, the DNA was sequenced around the targeted region to ensure that no mutations were inserted.

2.6.2 Gene targeting in ES cells for generation of chimeric mice with a floxed *Scrt2* locus

The final cKO-vector (PAC-PL253/P1/NEO2) was linearizied with *ScaI* and the linear DNA-fragment was electroporated in MPI2-ES cells. Seven ES cell clones survived the positive/negative selection process and were analyzed by southern blotting for correct homologous recombination (Fig. 38a). The genomic DNA of these selected ES cell clones was isolated and digested with *HindIII* to monitor the correct insertion of the 5' *loxP*-site by using the 5´DNA probe or with *BamHI* to detect the correct insertion of the 3' *loxP*-site by using the 3´DNA probe. Since a *HindIII* restriction site was integrated upstream of the *loxP*-site, the digest resulted in a 9.1 kb band instead of the 13.0 kb band and the *BamHI* restriction site, integrated downstream of the second *NEO* resulted in a 10.7 kb band instead of the 13.9 kb band found in the wild-type (Fig. 38b). Six targeted clones (VP-1, 16, 57, 74, 86, 105) were identified with both, the 5' and 3' probe.

All positive ES cell clones were used for the production of chimeras by aggregation with CD1® morula-stage embryos and cultured to blastocyst-stage (by the animal facility team). Hence, the blastocysts were transferred into the oviduct of pseudo-pregnant female recipient mice. Chimeric offspring could easily be detected on the basis of the coat colour when the coat becomes visible at around P10. MPI-2 ES cells are derived from an agouti-pigmented sub strain of the 129 strain whereas CD1® mice are albino. To identify chimeras with germ line transmission, the chimeras were bred with CD1 mice.

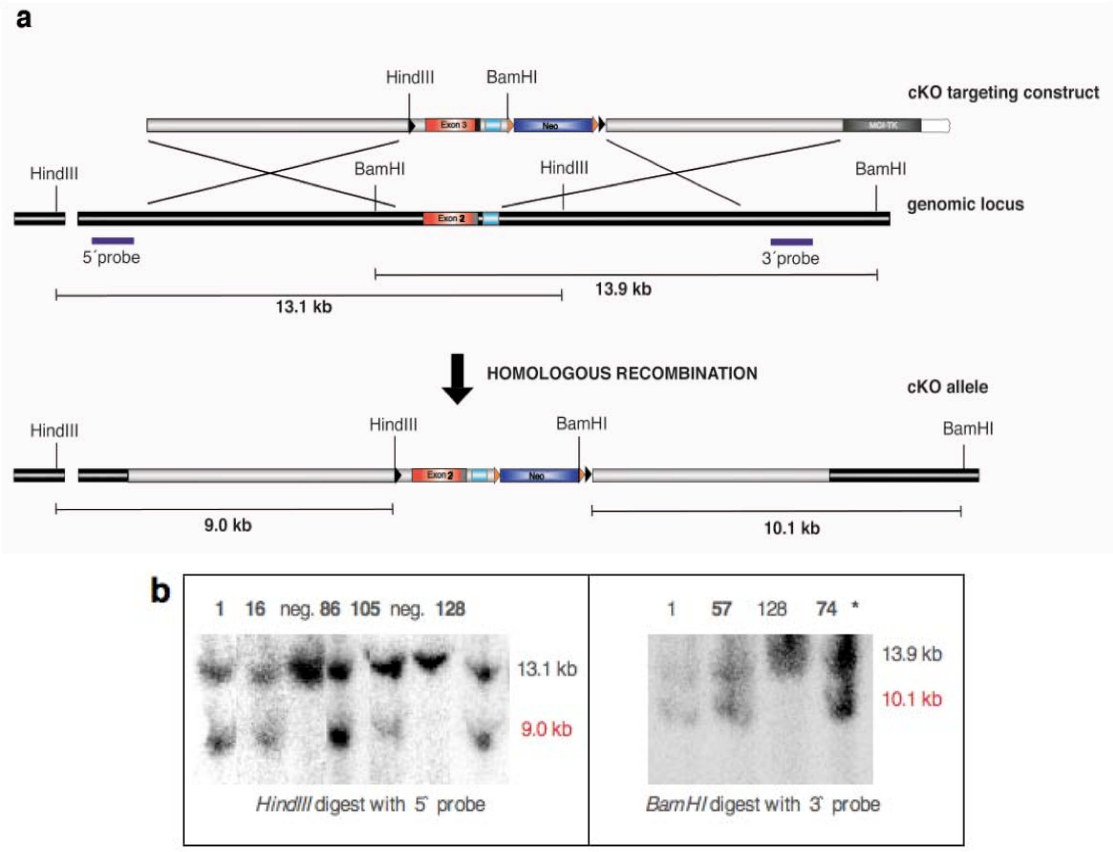

Figure 38: Targeting of the *Scrt2* genomic locus with the cKO construct in ES cells. (a) Structure of the conditional targeting construct, *Scrt2* genomic locus and targeted locus. **(b)** Confirmation of correct *Scrt2* targeting by southern blot analysis of *HindIII* (5' Probe) and *BamHI* (3' Probe) digested ES cell DNA. * The clones 16, 86 and 105 were also positive with 3´probe, but not shown here. The same holds true for correct insertion of the 5´*loxP*-site in the clones 57 and 74.

Successful transmission of the transgene would result in some offspring per litter with solely agouti-pigmented coat.

While all six correctly targeted clones have been tested by southern analysis, not all aggregations resulted in production of chimeras (although up to twenty embryos were transferred in eighteen recipient mice). Clone 74 and 86 failed to do so, the remaining aggregations led to chimeras. In detail, clone 1 resulted in one male and one female chimera, afterwards pointed out to be infertile, while the male chimera produced more than twenty-nine litters with several offspring each. Clone 16 resulted in seven male and eight female chimeras with five of them showed only very low chimerism (not tested for germ line transmission).

While six of the remaining chimeras did not give rise to offspring, the other four chimeras produced more than 140 littermates all together (11litters). Aggregation of clone 57 resulted in two male and one female chimeras, which generated more than 210 littermates (18 litters).

Despite these intensive breeding efforts, including crossing to different CD1-partner mice, none of the tested chimeras showed germ line transmission of the transgene. Consequently, it was decided to apply the Cre-LoxP strategy for generation of transgenic mice for conditional activation of Scrt2 in cortical progenitors, which was successful as presented in the proceeding part of this PhD thesis. In order to attempt another approach, ES cell clones 1, 16 and 105 were transferred into blastocytes by pronuclear DNA-injection. Using this approach, three chimeras were generated from clone 1, three from clone 16 and four from clone 105, these chimeras were not able to transmit the transgene to their offspring (e.g. the three chimeras of clone 16 generated more than 50 littermates (8 litters) in crossings with up to four mating partners per male). Finally, the potential, fertile chimeras died due to decrepitude (age higher than 1,5 years).

3. DISCUSSION

Understanding the mechanisms that regulate such complex processes as the generation of the mammalian neocortex is the ultimate task of neurobiological research. As outlined in the introduction, this ambitious intention can be only achieved by puzzling single insights together to gaining knowledge about the molecular players, involved in these processes.

The aim of this project was to get knowledge about the role of TF *mScrt2* in brain neurogenesis. The presented findings are first functional data in the literature from a mouse model, indicating that the vertebrate specific gene *mScrt2* exerts an interesting modulatory role in mammalian corticogenesis. Firstly, it was shown here that the mammalian *Scrt2* exerts a restricted expression within zones related to neurogenesis in developing and adult brain, acting in a genetic pathway controlled by TF *Pax6*. Secondly, evidences are presented that by regulating the neurogenic versus proliferative mode of cortical neurogenesis, the protein isoform encoded by *Scrt2.2* can modulate the neuronal outcome of the radial glial and intermediate progenitors and thereby the cortical architecture. Thirdly, it was shown that both predicted protein isoforms, encoded by *Scrt2.2* and *Scrt2.3,* negatively influence the migration of generated neurons towards the cortex that accumulate at the border SVZ/IZ. Fourth, ectopic expression of the *mScrt2.2* in *Xenopus leavis* embryo severely affected the primary neurogenesis depending on the spatio-temporal context along the AP axis of the embryo.

3.1 Expression of the *mScratch* gene in the developing and adult brain suggests a role in the transition from cell proliferation to differentiation

In a previously performed in our group micro-array screen, a number of molecular determinants with a graded expression across the AP and ML axis of the developing mouse cortex have been identified (Mühlfriedel et al., 2007). Because TF Pax6 plays a pivotal role in cortical neurogenesis, including arealization and layer formation (Götz et al., 1998; Pinon et al., 2008; Tuoc et al., 2009), it was attempted to identify novel molecular players that act in a *Pax6*- dependent manner in these processes. The predicted, mammalian *Scratch2* gene attracted my interest, because it showed Pax6-dependent, graded and restricted to the cortical SVZ/IZ expression pattern. Moreover, based on the affiliations of *Scrt2* to the C_2H_2 zinc finger transcription factors (Barrallo-Gimeno and Nieto, 2009), it was expected that *mScrt2* could control different developmental processes.

mScratch2 belongs to the evolutionary conserved *Snail* gene superfamily (C_2H_2 zinc finger) of TFs. During early metazoan evolution, a duplication of a unique *Snail* gene resulted in two highly related genes, *Snail* and *Scratch* (reviewed by Manzanares et al., 2001; Nieto, 2002). The Scratch domain was found in all vertebrate Scratch proteins, but also in

the *Drosophila scratch*. In *Drosophila*, intra-chromosomal duplications are assumed to cause the presence of three linked together *Snail* genes (*snail, escargot, worniu*) and three linked *Scratch* genes (*scratch*, *scratch-like1* and *scratch-like2*). In vertebrates, whole-genome duplication was proposed to be responsible for the presence of two *snail* genes (*Snail, Slug*) and two *Scratch* genes *(Scratch1* and *Scratch2)*.

The mammalian *Scrt1* gene is the first vertebrate *Snail* family specifically expressed in neural tissue (except for the lung epithelium) (Nakakura et al., 2001). As shown here, the expression of *mScrt2* was also confined to the developing CNS, which is in agreement with the previously published results from ISH experiments (Marin and Nieto, 2006). These authors reported predominant expression of both *Scrt1* and *Scrt2* in the mantle zones, confined mostly to the basal plate of the developing spinal cord and the brain, beginning at E9.5 in the midbrain and including the forebrain at E11.5. While *Scrt1* is expressed in both the dorsal and ventral telencephalon, *mScrt2* is restricted to the dorsal telencephalon, suggesting a specific function of m*Scrt2* in corticogenesis.

As shown in this work, in the pallium *Scrt2* was expressed in the earliest-born (E10.5) neurons of the preplate. Later, *Scrt2* expression was detected in the upper part of the SVZ, an interface of proliferating progenitors (IPs) and differentiating cells, with a progressive decrease in the IZ and CP. Immunohistochemical analysis with a generated Scrt2 antibody revealed a particularly strong expression in the upper cortical layers. The registered expression behaviour suggested a role of Scrt2 for the differentiation and migration of the pallial neurons. Noteworthy, very similar expression patterns have been reported for the bHLH-TF Math2 (Nex) and NeuroD, both involved in taking a decision for neuronal differentiation (Schwab et al., 1998; Lee et al., 2000). Although one hour BrdU-pulse labelling at E15.5 failed to detect a co-localization with Scrt2 protein in the SVZ cells, it can not be excluded that the expression of *Scrt2* starts during the last mitotic phase of the SVZ progenitors, just before their exit from the mitotic cycle to become post-mitotic neurons. In a further support of this idea, IHC at the peak of neurogenesis in the cerebellum (P10), showed a co-localization between the Scrt2 and TAG1 immuno-reactivity. As TAG1 marks the granular neurons (Wolfer et al., 1994) just exiting the proliferative zone of the EGL, the co-localization between TAG1- and Scrt2 immuno-staining supports the possibility that TF Scrt2 may influence the progenitor decision to exit from mitosis and initiate a differentiation program that includes also neuronal migratory ability. Since the *Scrt2* expression level in cells exiting mitosis might be too low to detect by standard IHC and the time frame to detect cells at this transition point is very narrow, more detailed birthdates-labelling experiments and /or real-time observations are required to examine this possibility.

It was highly interesting to observe, that m*Scrt2* was expressed also in niches for neurogenesis in the postnatal and adult brain, namely the subgranular zone of the dentate

gyrus and all along the RMS. Generation of new GABA- and dopaminergic interneurons from stem cells in RMS of the postnatal brain that renew the olfactory bulb interneurons throughout the life has been recently demonstrated (Brill et al., 2009; Reynolds and Weiss, 1992; Gage, 2000). Notably, during postnatal and adult cortical neurogenesis, a sequential expression program of TFs in the order, *Pax6*, *Tbr2*, *NeuroD* and *Tbr1* has been established in cortical progenitors of the VZ/SVZ (Hevner et al., 2006). The same transcription cascade participates during neurogenesis in the adult hippocampus (Hodge et al., 2008), during postnatal/adult olfactory bulb neurogenesis (Roybon et al., 2009) and in the developing cerebellum (Englund et al., 2006), suggesting that these TFs are a part of a conserved genetic program that specifies general properties of brain neurons. Notably, the expression of *mScrt2* in the *Pax6/Small* eye mutant cortex was gradually lost, implicating that *mScrt2* is involved in genetic pathway, controlled by TF *Pax6*. Taken together, the results of the performed *in-situ* and immunohistochemical expression analysis placed TF *mScrt2* into the evolutionary conserved *Pax6*-dependent transcriptional cascade that controls neurogenesis of cortical glutamatergic and cerebellar granule neurons in the developing and adult brain.

3.2 TF *Scrt2* modulates the neuronal outcome of cortical neurogenesis

The available to date functional data suggested, that promotion of neuronal differentiation might be a function associated with both the Snail and Scratch members (Nieto, 2002). All three *Drosophila Snail* genes are expressed in the nervous system, but their individual inactivation lead to very mild phenotypes requiring their simultaneous inactivation (Ashraf and Ip, 2001). Similarly, elimination of the pan-neuronal *Drosophila scratch1* results in a mild reduction of the photoreceptor cell number, but does not disrupt morphogenesis of the embryonic nervous system, unless both the *scrt1* and the pro-neuronal bHLH gene *deadpan* (*dpn*) have been eliminated (Roark et al., 1995). In contrast, ectopic expression of *scrt1* during embryonic and adult development leads to overproduction of supernumerary neurons, suggesting that *scrt1* promotes neuronal cell fates (Roark et al., 1995). Similar conclusion was made for the *scratc1h* homologue *ces-1* in *C. elegance* (Metzstein and Horvitz, 1999).

It was reasoned therefore, that application of transgenic gain-of-function approach would be more straightforward strategy in order to study the role of *mScrt2* in mammalian corticogenesis. Based on the *Cre/LoxP* strategy for conditional gene activation (Berger et al., 2007), two types of mouse transgenic lines were generated that allow studying the consequences of ectopic activation of either *mScrt2.2* or *mScrt2.3* in the developing cortex. So far, the experiments have been restricted to the use of the *Emx1Cr*e line that allows Cre-recombinase activation in the pallial RGPs and their descendents, starting at E9 and reaching full activity at E12 (Armentano et al., 2007; Gorski et al., 2002; Li et al., 2003). The gross

morphology of the brain showed similar diminishing of the cerebral cortex thickness in both, *Scrt2.2*- and *Scrt2.3*-GOF condition. However, the phenotypic analysis presented in this study, concerns only the *Scrt2.2-pJoJo;Emx1Cre* line.

Ectopic expression of the *Drosophila Scrt1* results in the formation of surplus of neurons (Roark et al., 1995), while over expression of the murine *Scrt1* was sufficient to confer neuronal morphology and *Tuj1* expression in a subset of mouse P19 embryonic carcinoma cells (Nakakura et al., 2001b). Judged by the clearly enhanced expression of the early post-mitotic neuronal markers HuC/D and Tbr1 in the *mScrt2.2-pJoJo;Emx1Cre* mice, *Scrt2.2* over expression caused an enhancement of neuronal production at the onset of neurogenesis, particularly evident in the ventro-lateral cortex (Fig. 24,h). Following the normal differentiation gradient, at stage E12.5, the ventro-lateral pallium is more advanced in the differentiation, compared to dorsal and medial pallium. One structure in ventro-lateral pallium that is almost fully differentiated at E12.5 is the piriform cortex that acts as a primary olfactory centre, integrating direct projections from the olfactory bulb (OB). Mitral cells of the OB send their axons tangentially along the lateral olfactory tract (LOT) to the piriform cortex (Hinds, 1972). LOT cells have been reported to originate from NEPs of the dorsal and medial neocortex where they undergo final mitosis between E9.0 and E11.0 (Sato et al., 1998). Thereafter, the LOT cells migrate ventrally to their final position and show a scattered distribution in the piriform cortex at E12.5 (Tomioka et al., 2000). Thus, the advanced thickening of the piriform cortex in the E12.5, *Scrt2.2-pJoJo;Emx1Cre* forebrain, likely reflects the earliest consequence of promoted neurogenesis in the *Scrt2.2*-GOF condition. Consistent with these findings, at stage E16.5 the CP of the *Scrt2.2-pJoJo;Emx1Cre* embryos contained a much denser band of early born (L6-L5) Tbr1-positive neurons as compared to the control brains, evident after *in-situ* and immunohistochemical analysis.

During the late (E13.5- E18.5) cortical neurogenesis, the indirect mode of neurogenesis predominates, in which the RGPs divide asymmetrically to generate a RGP daughter cell and an IP that moves into the SVZ. Immunostaining for Tbr2 antibody or ISH on brain sections at E16.5 revealed an accumulation of strongly labelled Tbr2+ cells at the interface of the SVZ / IZ in the *Scrt2.2-pJoJo;Emx1Cre* embryos. The IP-marker *Tbr2* is differentially expressed in IPs and their differentiating daughter neurons at high and at low levels, respectively (Englund et al., 2006). However, the massive cell accumulation of Tbr2 + cells on brain sections from the double transgenic cortex hampered to distinguish between the two options: migrational problems of post-mitotic neurons or enhanced production of IPs after *in-vivo* activation of *mScrt2.2*. This issue was successfully addressed through the application of a clonal-pair analysis, as discussed.

It should be noticed here that *mScrt2.2*-GOF appeared to cause an enhancement of the expression of bHLH TF *Mash1* in the pallial VZ/SVZ as well as in IZ in the double transgenic cortex. The pro-neuronal gene *Mash1* is expressed in the telencephalic progenitors and is involved in establishment of the pallial/subpallial border (Fode et al., 2000; Scardigli et al., 2001; Schuurmans et al., 2004). Although further experiments are necessary to clarify the effect of *mScrt2.2*-GOF on the expression of *Mash1* at early and late neurogenesis, it is worthy to notice, that over expression of *Mash1* in pallial progenitors has the capacity to promote progenitor maturation, instructing the VZ-progenitors to produce prematurely cells that exit from the VZ into the SVZ and accumulate at the VZ/SVZ border, instead of rapidly migrating into the IZ and CP (Britz et al., 2006). Premature cell cycle exit of progenitors from mitosis at the onset of neurogenesis would predict decreased overall number of neurons after accomplishment of the corticogenesis. Indeed, at P10, the cortex in the *Scrt2.2-pJoJo;Emx1Cre* mice was hypo-cellular with severely affected thickness of the upper cortical layers. Thus, *in-vivo* activation (E9.5 - E12) of *mScrt2.2* in cortical progenitors lead to enhanced production of early-born neuronal sets, whereas the final neuronal number in the adult cortex was significantly depleted.

Scrt2.2-GOF affected not only the production of neurons during embryogenesis, but also this experimental condition inhibited also the generation of cortical astrocytes, the majority of which are produced postnatal. In addition, the piriform cortex in the *Scrt2.2-pJoJo;Emx1Cre* mice at P10 was augmented. Recent genetic fate-mapping analysis provided evidence for postnatal de novo formation of glutamatergic pyramidal neurons from oligodendroglial progenitor cells (OPC) within the normal murine piriform cortex (Guo et al., 2010). Given the restricted postnatal expression of *mScrt2* in the cortical SVZ, it will be interesting to study in future whether *TF Scrt2* could positively influence the OPCs to acquire neuronal fate in the adult brain.

3.3 *mScrt2.2* promotes neurogenic versus proliferative division of cortical progenitors

Data discussed above suggested that *mScrt2.2* expression in RGPs and IPs might promote neurogenesis by influencing the mode of progenitor division. A definitive support of this idea was obtained after performance of clonal-pair analysis that allow quantitative estimations of the proliferative versus neurogenic mode of cell division, as described in details in results (Bultje et al., 2009; Li et al., 2003; Sanada and Tsai, 2005).

The most prominent effect of *mScrt2.2* miss-expression in the cortical progenitors at E13.5 (analyzed after DIV1) was a general increase in neurogenic cell divisions, at both levels, RGPs and IPs. The symmetric division of RGPs was not significantly changed in cell-pairs generated from *mScrt2.2*-GOF, thus keeping the RGP-pool unaffected, which was consistent with an unaltered *Pax6* expression *in-vivo*, on sections from E12.5 cortex. However, RGPs

undergoing asymmetric division in culture generated directly a significantly increased portion of post-mitotic neurons and diminished set of IPs. The promoted direct mode of neurogenesis at the onset of neurogenesis under *mScrt2.2*-GOF was consistent with detected thicker CP in the ventro-lateral cortex in brain sections of E12.5 *Scrt2.2-pJoJo;EmxCre1* embryos and enhanced *Tbr1* expression in the CP at E16.5. Thus, in a general agreement with what has been reported upon over expression of the *Drosophila scratch1* and the *C. elegance ces-1* gene, the ectopic expression of *mScrt2.2* in RGPs at the beginning of neurogenesis also results in enhanced production of early-born neuronal subtypes.

The results from the clonal pair analysis further suggested that upon *Scrt2.2*-GOF not only the pool of IPs is depleted, but instead of re-entering into the cell cycle to multiply through proliferative symmetric divisions, also the smaller pool of IPs undergoes neurogenic terminal divisions and directly produce neurons. Such an effect of *mScrt2.2* is fully consistent with the predicted function based on expression pattern, as discussed above. The IPs are viewed nowadays as general multipliers of diverse neuronal fates, produced during a specific developmental window, with a more profound effect for the late neurogenesis. Together with the premature neurogenic division of RGPs that cause a diminishing of the IP- pool available for the later neurogenesis in *mScrt2.2*-GOF, one would expect diminished neuronal number in the matured cortex, which was indeed the phenotype already discussed above.

All together, the presented findings from the phenotypic analysis of cortical neurogenesis in transgenic mice and from clonal-pair analysis *in-vitro* indicate, that by influencing progenitor decision to undergo neurogenic asymmetric (RGPs) or neurogenic terminal (IPs) division, the mammalian *Scrt2.2* regulate the production of the final number of neurons, that built distinct cortical layers of the mature brain.

We are far ways from understanding the molecular mechanisms behind the presented phenotype under ectopic *Scrt2.2* expression. Interestingly, Snail family members have been implicated in the regulation of mitosis in imaginal discs *in Drosophila*, mouse throphoblasts and human karyocytes (reviewed by Nieto, 2002). The *Drosophila Escargot* and the mouse *Snail* induce progression of cell cycle to mitosis. This effect in *Drosophila* was related to activation of *String*, a protein involved in mitotic control, coupled with the asymmetric cell division (Ashraf and Ip, 2001). In this aspect, it is also important to notice a similarity in several aspects of the cortical phenotype in the conditional Pax6-LOF (Tuoc et al., 2009), and *mScrt2*.2-GOF (this study) transgenic mice, in which assays one and the same Cre-driver mouse line (*Emx1Cre*-line, Gorski et al., 2001) has been used. The conditional depletion of *Pax6* (Tuoc et al., 2009) or conditional ectopic expression of *mScrt2.2* (this study) in RGPs of VZ at the onset of neurogenesis caused a premature differentiation of early-born neuronal fates via the direct mode of neurogenesis, which diminishes the progenitor pool for neuronal production late in development (also Estivill-Torrus et al., 2002). Consequently, the adult

cortex in both experimental conditions was hypo-cellular with more profoundly affected number of the upper layer neurons (Quinn et al., 2007). Together with the already discussed loss of *mScrt2.2* expression in the *Pax6*-deficient cortex, these findings further suggest a genetic interplay between TF *Pax6* and *mScrt2.2* in the regulation of cell cycle progression and neuronal differentiation at early developmental stages.

3.4 mScrt2 influences cell migration in the developing cortex

Cell migration is an important aspect of cortical differentiation. Born in VZ, the neurons undertake long journeys toward the CP using two well known migrational modes, locomotion and somal translocation (Miyata et al., 2001; Nadarajah et al., 2003; Rakic, 1972). During locomotion, neurons with a bipolar morphology migrate along the RG cell processes that transverses the entire thickness of the cerebral wall. In somal translocation, neurons with a monopolar morphology extend radially oriented leading process that terminate at the pial surface; as the migration of the soma advance, the leading process becomes progressively shortened. In a number of studies have been shown, that when passing through SVZ and IZ, the neurons slow down their migration, and many cells in these zones assume a multipolar shape (Bayer and Altman, 1991; Nowakowski and Rakic, 1979).

A general feature of all Snail family members is the ability to control the epithelial-mesenchymale transition (EMT) through which epithelial cells in a given embryo region can dissociate from the epithelium and migrate to reach different location or EMT-related processes in aspects of regulation of migration.

The presented in this study results indicate that both, *mScrt2.2* and *mScrt2.3* influence the neuronal migration. Focal expression of both *mScrt2* isoforms by IUE in cortical progenitors lead to an accumulation of Tuj1+ neurons at the border SVZ/IZ. These cells extended multipolar processes and many of them appeared to take tangential instead of radial orientation. Intriguingly, by using similar to the applied in this thesis IUE approach, Tabata and Nakajima (2003) presented evidence for existence of a third mode of cell migration in the developing cortex, named “multipolar migration”, characteristic for the post-mitotic neurons accumulated in SVZ/IZ. Such multipolar cells do not move straight towards the CP, but instead they change migrational direction, possibly searching for an appropriate direction of axonal growth for migration towards the CP (Sasaki et al., 2008). According to the proposed by Tabata et al. (2009) model, if a subset of e.g. UL neurons joins the zone of the multipolar cells (SVZ/IZ border), they will be hampered to initiate immediately a radial migration and consequently such cells will be delayed in their arrival in the CP. In other words, depending on the options to pass through the zone of multipolar cell accumulation or not, two neuronal subsets that are born at the same developmental stage (thus devoted to join a specific layer) will reach the CP at different time. Intriguingly, after a focal expression

of *mScrt2.2* through *in-utero* electroporation at E13.5, an accumulation of cells with multipolar appearance at the SVZ/IZ border was detected. Furthermore, focal expression of *mScrt2.3* in the embryo brain at E14.5 and IHC analysis at P3, revealed that a substantial part of the Cux1+ UL neurons have been still kept in the SVZ/IZ and most of the cells showed multipolar shape, being tangentially oriented (Fig. 32). These findings arise the possibility that both type of Scrt2 proteins might contribute to the acquisition of the "multipolar cell fate" at the SVZ/IZ zone. It should be noticed here that in contrast to *mScrt2.2,* the encoded by *mScrt2.3* isoform contains a NLS signal (RRRRRRRRRRRAR), indicating that the function of the two Scrt2 isoforms as transcription factors might be differentially regulated via cell mechanisms for nuclear shuttling.

The molecular mechanism regulating the multipolar mode of neuronal migration is fully unknown. The *Svet1* /UNC5D is a widely accepted marker for SVZ progenitors and UL neuronal fate (Tarabykin et al., 2001). As recently reported by Sasaki et al. (2008), *Svet1*/UNC5D is actually expressed only in post-mitotic multipolar cells at E16.5 that extend pulsing tangential processes. Since UNC5 proteins constitute an axon-repulsive subfamily of chemotropic netrin ligands, the specific expression of *Svet1*/UNC5D in multipolar cells with UL fate could mediate their arrest in the SVZ/IZ until withdraw of netrins occurs or receiving further unknown signals. The expression of *Svet1*/UNC5D in the SVZ and in UL neurons is abolished in the *Sey/Sey* cortex (Tarabykin et al., 2001). If indeed Scrt2 contributes to the acquisition of multiple cell fate at the border SVZ/IZ and given the loss of expression in the *Pax6*-LOF cortex of both, *Svet1* and *mScrt2* (this study), it is possible that these two TFs may act downstream of *Pax6* in the molecular control of "multipolar cell migration" in the developing mammalian cortex.

Different signalling transduction pathways have been implicated eventually to lead to expression of the Snail family of transcription factors in various developmental processes and in carcinogenesis (reviewed by Nieto, 2002). During gastrulation, Snail converts the epithelial into mesenchymal cells in a process that involves down regulation of the expression of *E-cadherin,* the only so far identified Snail direct target gene (Batlle et al., 2000; Cano et al., 2000). E-cadherin can sequester ß-catenin, which plays an important role for the activation of the canonical Wnt signalling pathway with multiple important consequences for neural development. By lowering the level of E-cadherin via maintenance of the transcriptional repressor snail1, the FGF signalling promotes the canonical Wnt signalling and the stabilized ß-catenin can translocate into the nucleus to act as transcriptional regulator. Such a mechanism could be likely another conserved mechanism used by Snail and Scratch proteins for regulation of the migrational behaviour of the multipolar cells as well as in the promotion of neuronal differentiation by repressing mitosis, as already discussed. An interesting question for future examinations would be therefore to study, whether the *mScrt2*

expression depends on Wnt-signalling to promote neuronal differentiation. It is worthy to note, that similar cortical phenotypes were found in *mScrt2.2*-GOF (this study) and after stabilization of ß-catenin, both of which were shown to promote the direct mode of neurogenesis and to impair generation of IPs at mid-corticogenesis (Hirabayashi et al., 2004; Wrobel et al., 2007).

The role of Snail family members in mesoderm delamination and neural crest migration has been well documented. In *Xenopus*, *Slug* antisence treatment or expression of dominant-negative *Slug* constructs caused defects in neural crest migration (Carl et al., 1999; LaBonne and Bronner-Fraser, 2000). Furthermore, *Slug*-GOF leads to an increase in neural-crest production in the chick embryo (del Barrio and Nieto, 2002). Moreover, ectopic expression of the mammalian mScrt2.2 in *Xenopus* embryos led to an impaired neurogenesis. Differential onset of *mScrt2.2* expression as well as regional and temporal specific targeting in *Xenopus* embryos furthermore revealed that *mScrt2.2* could accomplish its pro-neuronal function only in neural-induced cells (possibly allowing interaction with other molecular determinants), while additional functions might be independent from this context.

3.5 Putative Scrt2-dependent mechanisms that could modulate the cortical neurogenesis and gliogenesis

The balanced activity of functionally antagonistic factors from the bHLH family is crucial for important processes in neural development from differentiation of primary neurons in the induced neuroectoderm to acquisition of distinct cell fates in the developing CNS, reflected in the sequential generation of neurons, astrocytes and oligodendrocytes (reviewed by Ross et al., 2003).

All *scratch* proteins (human, murine, *Drosophila, C. elegans*) have the capacity like other Snail-like family members of the C_2H_2 zinc fingers to recognize the E-box enhancer motif (CANNTG), a common target also for the bHLH TFs. As demonstrated by Nakakura et al. (2001a), human *Scrt1 (hScrt1)* is able to repress the activation of E-box containing reporter by bHLH TF *Mash1* plus its dimerization partner E12 in cell culture. It has been suggested therefore, that competition between Snail/Scratch and bHLH family of TFs for common target genes may account for modulation of the activity of bHLH factors and thereby for neuronal differentiation. It is worthy to note, that upon *mScrt2.2* over expression in RGPs, the expression of *Mash1* in E16.5 cortex was enhanced as compared to the controls. Since the expression of *Mash1* in pallial VZ is negatively controlled by bHLH TF Ngn2, it seems possible that *mScrt2* could antagonize the repressive control of the Ngn2 activity on the *Mash1* promoter (Britz et al., 2006). In order to maintain a progenitor status, the inhibitory bHLH factors Hes1 and Hes5 repress the transcription of *Mash1* (Chen et al., 1997; Ishibashi

et al., 1995). Accordingly, *mScrt2* might promote neuronal differentiation by antagonizing the activity of Hes proteins. Similar mechanisms but involving bHLH TFs important for glial differentiation could be envisioned to explain the preliminary data about involvement of Scrt2 in acquisition of glial cell fate.

The presented here results strongly suggest that evolutionary conserved and vertebrate specific TF mScrt2 play an important modulatory function on mammalian corticogenesis. At cellular level, the involved mechanism includes a regulation of the neurogenic mode of progenitor division (RGP; IPs), thus contributing to establishment of a normal cyto-architecture of the adult cortex. *mScrt2* might be also important for acquisition of glial cell fate in developing cortex, although further evidence are necessary to be elaborated. The accumulated so far findings indicate, that mScrt2.2 likely regulate neuronal differentiation and transition to gliogenesis by modulating the temporal coordinated activity of bHLH-factors. Accordingly, the investigation of how the mammalian TF Scrt2 interacts with bHLH proteins in the temporal differentiation of neurons and glia with distinct identities will be an important issue for future examinations.

4. METHODS

4.1 ANIMALS

The GOF-founder mice (*Scrt2.2-pJoJo* and *Scrt2.3-pJoJo*) have a C57/B6N background. *Emx1Cre* knock-in mice (Gorski et al., 2002) were maintained in a C57/B6J background. For *in-utero* injection and primary cell culture, CD1 wild type mice were used. The day of vaginal plug was considered as embryonic day (E) 0, the day of birth as postnatal day (P0).

4.2 HISTOLOGY

4.2.1 Cryo-conservation and sectioning of mouse brains

Murine embryos were removed by caesarean section from time-pregnant mice and killed by cervical dislocation. For extraction of genomic DNA and genotyping, a sample was taken from yolk sack or tail. The brains were dissected in ice-cold PBS and the tissue was fixed in 4% PFA (in PBS) on ice with the following fixation times:

- E12 whole embryo 2.0 hrs
- E13.5 / E14.5 brains 1.5 hrs
- E15 / 16 brains 2.0 hrs
- E18 / P0 brains 2.5 hrs
- P4 brains 3.5 hrs
- P10 brains 5.0 hrs

After three times washing with 1xPBS, the tissue was placed in 20% sucrose/PBS for cryo-protection at 4°C until it sank and afterwards embedded in Tissue Tek. Frozen blocks were stored at –20°C until sectioning with a cryostat (CM 3050 S, Leica). Sections were collected on SuperFrost microscope slides and allowed to dry on a 30°C-heating plate for 30 min. Afterwards the slides were stored at –80°C until use.

4.2.2 Cresylviolet (CV) staining

For a morphological overview cryosections were stained with cresylviolet after the following protocol at RT:

- 4% PFA 5 min
- 1x PBS 2x5 min
- H_2O 2 min
- K_2SO_3 15 min
- H_2O 2x1 min
- CV 10 min
- Acetate-buffer 3x1 min
- Acetic Acid (0.14%) 30 sec
- H_2O 1 min up & down
- 70% EtOH 30 sec
- 100% EtOH 2x2 min
- Histoclear 10 min or more

- Coverslipping with Eukitt®.

Cresylviolet:	1.5% cresylviolet dissolved in acetate buffer and filtered
Acetate buffer:	10mM sodium-acetate, 10mM acetic acid in H2O
K_2SO_3:	50% potassium (meta-) bisulfite in water, heat for solubilize

4.2.3 ß-galactosidase staining (whole mount)

The murine forebrains of E15/16 embryos were isolated in ice-cold PBS and fixed in solution B for two times 30 minutes on ice. After two times washing for 20min with 1xPBS, the brains were stained in the dark at 30°C over night. After washing with 1xPBS, photos were taken with a binocular (Olympus SZX12).

FixB (in 1x PBS):	1.0 % formaldehyde; 0.2 % glutaraldehyde; 0.2 % NP-40; 0,1% sodium-desoxycholate
Staining solution:	2.5 % X-Gal (40mg/ml in dimetyl formamide); 5mM $K_3Fe(CN)_6$ (in 1x PBS); 5mM $K_4Fe(CN)_6$; 2mM MgCl2

4.2.4 ß-galactosidase staining (cryoslides)

The cryosections were fixed for 10 minutes with 0.2% glutaraldehyde (in PBS) on ice followed by incubation in lacZ buffer (3x 5min at RT), before staining over night or up to 3 days at 37°C (dark). The reaction was stopped by washes with PBS (2x 5min RT) and the slides were mounted with mowiol.

LacZ buffer:	2mM MgCl2; 0.02% NP-40; 0.01% sodium-DOC in PBS
Staining solution:	1.03% X-Gal (40mg/ml in dimetyl formamide); 5mM $K_3Fe(CN)6$; 5mM $K_4Fe(CN)_6$ in lacZ buffer

4.2.5 Generation of DIG-labelled anti-sense RNA probes

For preparation of a DNA-template, 15µg of cDNA containing plasmid were linearized by restriction enzyme digestion. The sample was purified with phenol-chloroform and the DNA was precipitated with 7.5M NH_4Ac and 100% ethanol. Finally the DNA was dissolved in 10µl DEPC-H_2O. 1µl was loaded on a 1% agarose gel to control the linearization efficiency and to estimate the amount of template, needed for DIG-probe synthesis. For generating the antisense RNA the following reaction was used:

- 5x transcription buffer (Roche) 4.0µl
- 0.1M DTT 2.0µl
- DIG-labelled nucleotide mix (Boehringer) 2.0µl
- Template-DNA 1.0µl
- RNasin (Promega) 0.5µl
- RNA-polymerase (T_3, T_7 or SP_6) (Roche) 1.0µl
- H_2O fill up to 20µl

The reaction was incubated for two hours at 37°C, spun down and digested with 2µl DNase I (1U/µl) for 10 min at 37°C. Afterwards the RNA was precipitated and purified as following:

- Add 2.0µl 0.2M EDTA
- Add 2.5µl 4M LiCl
- Add 75µl 100% ethanol (-20°C pre-cooled)
- 2 hrs incubation at -80°C
- Spin 15 min at 13000rpm (4°C), remove supernatant
- Add 100µl 70% ethanol to pellet
- Spin 5 min at 13000rpm (4°C), remove supernatant
- Dry pellet and dissolve in 50µl DEPC-H_2O for 10min at 65°C
- Load 1µl on a 1% agarose gel

4.2.6 *In-situ* hybridization on cryosections

In situ hybridization was performed on 16µm-cryosections with digoxigenin (DIG)-labelled rib probes. The sections on the glass slides were encircled with a fat pen to prevent leakage of solutions. The tissiue slides were treated like following in cuvettes:

- 4% PFA in PBS 15min RT
- 1x PBS 5 min RT
- 1x PBS 5 min RT
- Proteinase K 4 min 37°C
- 0.2% glycine in PBS 5 min RT
- 1x PBS 5 min RT
- 1x PBS 5 min RT
- Postfixation 20min RT
- 1x PBS 5 min RT
- 1x PBS 5 min RT

The pre-hybridisation was performed in a sealed, humidified chamber (50% formamide in 5x SSC pH4.5) at 70°C for 2 hours by applying smallest volume of hybridization-buffer on the sections. The DIG-probes were diluted in hybridization-buffer regarding to their estimated concentration, denaturated at 80°C for 3 min and applied on the slides over night at 70°C (humidified chamber). On the next day the following steps were performed in cuvettes:

- 2x SSC pH4.5 5 min RT
- 2x SSC pH4.5 / 50% formamide 30 min 65°C
- 2x SSC pH4.5 / 50% formamide 30 min 65°C
- 2x SSC pH4.5 / 50% formamide 30 min 65°C
- KTBT 10 min RT
- KTBT 10 min RT

The glass slides were placed in a chamber with H_2O-soaked paper and incubated for 2 hours in blocking buffer (RT). Afterwards the anti-DIG antibody coupled to alkaline phosphatase was applied 1:2000 in blocking buffer over night at 4°C. On the third day subsequently steps were performed in cuvettes:

• KTBT	5 min	RT
• KTBT	5 min	RT
• KTBT	5 min	RT
• KTBT	30 min	RT
• KTBT	30 min	RT
• KTBT	30 min	RT
• NTMT	5 min	RT
• NTMT	5 min	RT
• NTMT	5 min	RT

For staining, 2% NBT/BCIP (Roche) solution in NTMT was applied on the slides (dark, wet chamber) until an adequate blue staining was observed under the binocular. The reaction was stopped by three washes at 5 min in PBT. The slides were mounted with mowiol and sealed with clear nail polish.

Proteinase K:	50ml of 1M Tris-Cl pH 8.0; 10ml of 0.5 EDTA; add to 1l Millipore water; freshly add 0.5ml proteinase K (10mg/ml)
Postfixation:	4% PFA / 0.2% glutaraldehyde in PBS
Hybridisation buffer:	50ml of formamide; 25ml of 20 x SSC pH4.5; 1g of blocking powder (Boehringer); 1ml of 0.5M EDTA; 1ml of 100 mg/ml total RNA; 0.1ml of 100 mg/ml Heparin; 0.1ml of Tween-20; 1ml of 10% CHAPS; add DEPC-water to 100ml
KTBT:	100ml of 1M Tris-Cl pH7.5; 60ml of 5M NaCl; 20ml of 1M KCl; 20ml of Tween-20; add water to 2L autoclave all components and mix before
Blocking Reagent:	10% normal sheep serum in KTBT
NTMT:	100ml of 1M Tris pH 9.5; 20ml of 5M NaCl; 50ml of 1M MgCl2, 1ml of Tween-20; add water to 1L; add freshly 0.24 g levamisole

4.2.7 Immunohistochemical staining (IHC)

Cryosections were encircled with a fat pen and the cryomatrix was removed by 15 minutes washing in PBS. The sections were then blocked in PBT (PBS + 0.1% Triton 100) and 10% NGS for one hour at RT. Diluted primary antibodies were incubated on the slides for overnight at 4°C in blocking solution. After washing in PBS (2x15 min), the sections were incubated with the secondary antibodies (in blocking solution) for 2 hours at room temperature. Before mounting, the sections were washed in PBT (2x30min) and sealed with Vectashield mounting-medium (Vector), containing DAPI as nuclear counter stain. The mounted sections were kept at 4°C, protected from light and pictures were taken at the Olympus BX60 fluorescence microscope.

4.2.8 Immunohistochemical staining (IHC) for goat-antibodies

Cryosections were encircled with a fat pen and the cryomatrix was removed by 2x5 minutes washing in PBS. The slides were put in a plastic cuvette with 1x target retrieval solution (S2369 Dako) and boiled for 4 min in a microwave followed by a cool down on ice for 20 min. This procedure was repeated two more times. After 2x5 min washing in PBS, the encircled sections were covered with permeabilization solution (0.3% Triton X-100 in PBS) for 15 min and afterwards for 30 min with quenching solution (0.1M glycine, pH7.4) and 3x5 min PBS washing. The blocking solution (0.3% Triton X-100, 0.2% gelantine in PBS) was applied for 1 hour at RT. The sections were incubated with the primary antibody diluted in blocking solution over night at 4°C. On the next day, the material was washed 2x15 min in PBS and the secondary antibody (diluted 1:400 in blocking solution) was applied for 2 hours at RT. Before mounting, the sections were washed in PBS (2x30min) and sealed with Vectashield mounting-medium (Vector), containing DAPI as nuclear counter stain. The mounted sections were kept at 4°C, protected from light and pictures were taken at the Olympus BX60 fluorescence microscope.

4.2.9 Immuno-cytochemical staining (ICC)

Primary cortex cells or differentiated NS were used for subsequent ICC. The media was removed and the cells were washed with PBS. After fixation for 20 min in 4% PFA on ice and 3x5 min washing in PBS, the cells were permeabilized (0.5% Triton X-100 in PBS) for 5 min at RT and washed 2x5 min in PBT (0.1% Tween in PBS). The blocking solution (10% FCS in PBT) was applied for two hours at RT. Cells were then incubated overnight at 4°C with primary antibodies (in blocking solution), washed 4x5 min with PBT on the next day, before incubation with the secondary antibody followed (45min at RT). After 4x5 min washing in PBT (in the dark) the cover slips were mounted onto glass slides by using the Vectashield mounting medium with DAPI (Vector laboratories). Images were taken using a BX60 fluorescence microscope (Olympus).

4.3 GENERATION OF SCRT2 CKO-VECTOR BY RECOMBINEERING

In order to produce Scrt2 deficient mice via ES cell targeting (genomic integration), a conditional knock out (cko) targeting construct was designed. The vector was created using a method described as recombineering (recombination-mediated genetic engineering; Liu et al., 2003; Muyrers et al., 2001; Warming et al., 2005). It is based on homologous recombination via the gap repair mechanism. The method makes use of *E.coli* strains containing a defective λ-prophage in the bacterial genome. This defective prophage expresses the recombination genes *exo, bet* and *gam* from the λ PL promoter, which is under the

control of the temperature-sensitive repressor λ cI857. *Exo* encodes a 5'→3' exonuclease (Exo) that creates single-stranded overhangs on introduced linear DNA, *bet* encodes a pairing protein (Beta) which protects these overhangs and promotes the subsequent recombination process and *gam* encodes for the gam protein that prevents degradation of linear DNA by inhibiting E. coli RecBCD protein. The proteins are not expressed, when bacteria are cultured at 32°C and is only active at 42°C to allow the expression of *exo, bet* and *gam*.
For homologous recombination between the target DNA (here the retrieval plasmid, containing the genomic sequence of interest from a PAC - and a linear DNA with 300-500 bp of homology in the 5' and 3' ends), the cassettes were cut out from the mini-targeting vectors, that have been generated and electroporated before into the SW102 bacteria already containing the target -DNA (Liu et al., 2003; Warming et al., 2005). The overall size of the targeting region was 14143bp and the *loxP*-sites were introduced 522bp upstream of the second coding exon and 856bp downstream of it, deleting finally a region of 2181bp. The 5' homology arm was 6490bp and the 3' homology arm was 5473bp long. For gene targeting in ES cells, the final targeting construct (19681bp) was linearized with *ScaI* and electroporated into ES cells. The different steps in the recombineering process are described in figure 38 and 39 and below.

4.3.1 Hybridisation of high-density filters (PAC library)

To obtain genomic DNA of mScrt2, a mouse PAC library was screened (RPCI-21 Female (129S6/SvEvTac, CHORI), where mouse genomic DNA has been partially digested with *MboI* and cloned between the *BamHI* sites of the pPAC4 vector (Osoegawa et al., 2000). Among other features it has a kanamycin resistance and flanking *T7*- and *SP6* promoter sequences. The ligation products have been transformed into DH10ß electro-competent cells and the library has been arrayed and gridded onto 22x22cm nylon high-density hybridization filters for screening by probe hybridization.
For hybridization of the PAC library, a Scrt2-specific DNA probe was used in order to identify a whole gene containing clone for mScrt2. For this purpose a RIKEN-clone (G630034H08) containing 2178bps of Scrt2-cDNA (AK090280) was cloned 5´to 3´ between the *SalI* and *BamHI* sites of the pFLCI vector. The plasmid was linearized with *SpeI* and transcribed by the T3 DNA polymerase generating 997bps antisense-probe homologue to the 3´UTR of mScrt2. The hybridization with the radioactively labelled and purified DNA-fragment on the high-density filters was performed according to the instructions of the producer (http://bacpac.chori.org/highdensity.htm). By autoradiography the positive clones were determined and identified by their positional grid data. The clones were ordered from ImaGenes as bacterial LB agar stab cultures. To isolate the large PAC-DNA (clone RP21-4

K18) with more than 10Kb, a procedure with rapid alkaline lysis miniprep, but without organic extractions or columns, suggested by the producer was used (HTTP://BACPAC.CHORI.ORG/BACPACMINI.HTM). The DNA was tested by PCR with primer pairs A/B and Y/Z for the presence of the required part of the *Scrt2*-genomic region for targeting.

4.3.2 Generation of a conditional knock-out construct via recombineering

The cKO-construct was created using a method described as recombineering or recombinogenic engineering (Liu et al., 2003; Muyrers et al., 2001; Warming et al., 2005). This method is based on homologous recombination via the gap repair mechanism mediated by the λ phage Red proteins in E. coli. The entire cloning procedure is described in detail in the results section and here in figure 39.

Construction of retrieval- and mini-targeting-vectors

The genomic regions for retrieval of the genomic sequence of *Scrt2* flanking Exon 3 (14,1 kbp) were amplified from the PAC-template with primer pairs P100/P101 (downstream, product A/B) and P102/P103 (upstream, product Y/Z) using a proofreading polymerase (*Pfu*-Polymerase, Fermentas) to avoid mutagenic events. The PCR product A/B (429 bps) was digested with *NotI* and *HindIII* and the product Y/Z (413 bps) with *HindIII* and *SpeI* to subclone by triple-ligation into the retrieval-vector PL253 (*NotI, SpeI*). This vector is based on *pBluscript* and contains a TK (thymidine-kinase) cassette, driven by the MC1 promoter to allow negative selection in ES cells. The plasmid had a size of 6386 bps after inserting the retrieval arms.

The first mini-targeting vector serves to introduce a removable (*floxed)* NEO-cassette into the retrieval vector for positive selection by recombineering using small homologous arms amplified with primer P104/P105 (downstream, product C/D) and P106/P107 (upstream, product E/F). The PCR product C/D was digested with *SaII* and *EcoRI* and (465 bps) and the product E/F (410 bps) with *BamHI* and *NotI* to subclone sequentially by ligation into the appropriate sites of the PL452-vector. For identification of correctly cloned construct via restriction digest, a unique *HindIII*-site was introduced upstream of the first *loxP*-site with primer P105. Deletion of the NEO-cassette after selection will leave the 5´-*loxP*-site and the additional *HindIII*-site in the retrieval vector and later in the genomic locus of Sctr2.

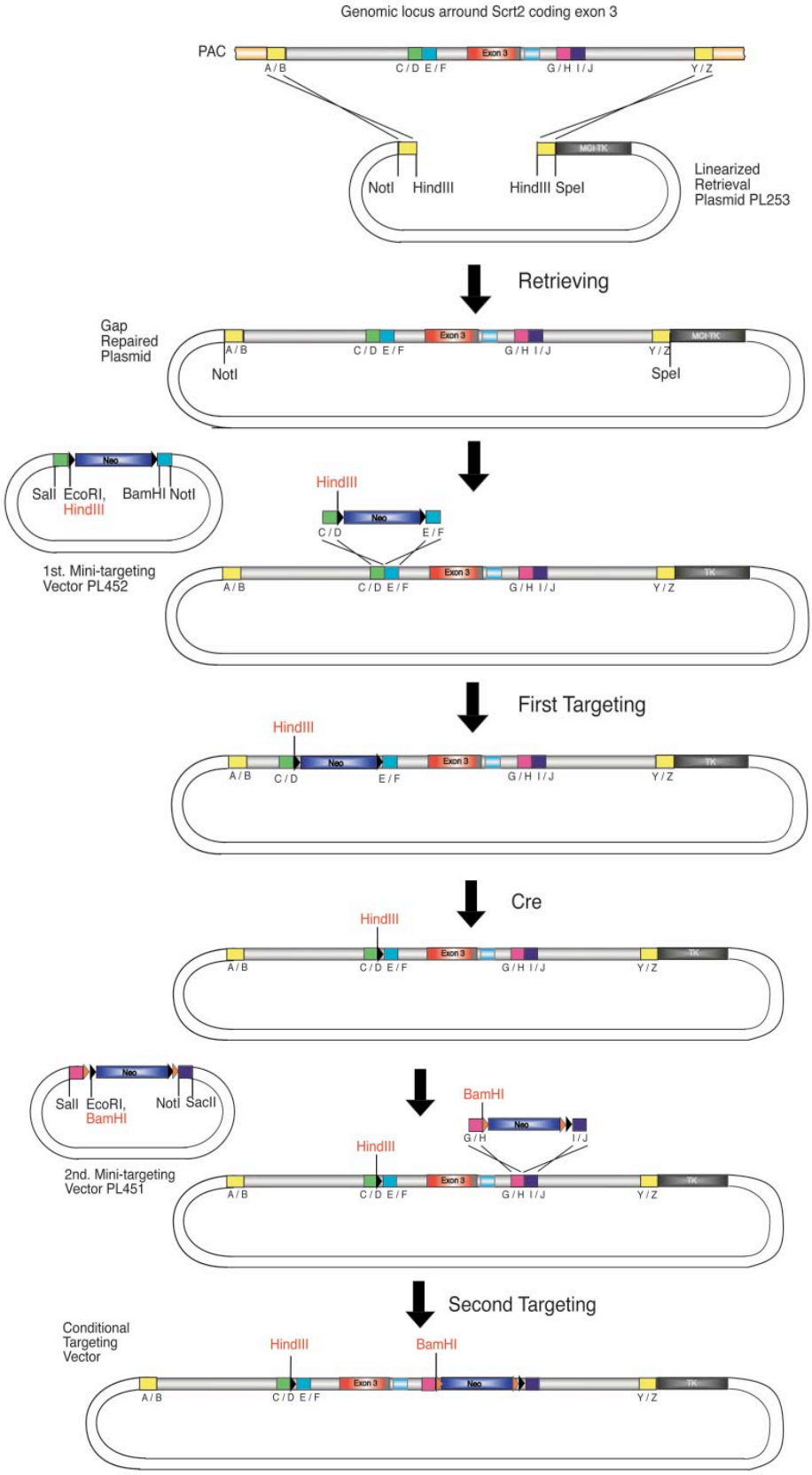

Figure 39: Generation of the Scrt2 conditional knockout vector via recombineering. Targeting region is depicted in grey, the Scrt2 coding exon 2 in red and the 3´untranslated region is displayed in light blue. Black arrowheads indicate *loxP*-sites and orangey arrowheads indicate *frt*-sites. The Neo cassette is depicted in blue whereas the tk cassette is drawn in black.

The second mini-targeting vector also contains a NEO-cassette, but flanked by frt-sites (Flpe recognition targets) for later recognition of *Flp*-recombinase for deletion after *in-vivo* targeting. Downstream of this cassette is a further l*oxP*-site, that will be the 3´-*loxP*-site in the retrieval vector and later after targeting upstream of Exon 2 in the genomic locus of *Scrt2*. The homologous arms for recombineering were amplified with primer P108/P109 (downstream, product G/H) and P110/P111 (upstream, product I/J). The PCR product G/H (491 bps) was digested with *SaII* and *EcoRI* and the product I/J (418 bps) with *NotI* and *SacII* to subclone sequentially by ligation into the appropriate sites of the PL451-vector. For identification of correctly cloned construct via restriction digest, a unique *BamHI*-site was introduced upstream of the first *loxP*-site with primer P109.

Transformation of PAC- and plasmid-DNA into *E. coli* strain *SW102*

The generated plasmids had to be transformed into a special *E.coli* strain (SW102) with the ability to express all required components for homologous recombination after thermal induction. A single colony of SW102 was inoculated as a 5ml-culture over night at 32°C and diluted 1:50 in LB-medium for further 3-5 hours incubation at 32°C until the cultures reached an OD_{600} of 0.6 at the next day. All further steps were performed at 4°C afterwards. First the cultures were pelleted in 50ml-falcons (5min at 5000rpm) and further proceed to make bacteria electro-competent as described in 5.6.10. The plasmid-DNA of interest was transformed as described in 5.6.11 and plated on LB-agar-plates over night at 32°C with the appropriate antibiotic for selection.

Retrieving and targeting of plasmids in heat-activated *SW102* cells

To activate the expression of the defect λ-prophage, the cells have to receive a heat-shock induction (42°C). Therefore the SW102 cells already containing the PAC-clone were cultivated as described. 10ml of a diluted culture were incubated for 15 min at 42°C (water bath) with smooth shaking. The remaining part of the initial culture serves as control and was meanwhile further incubated at 32°C. Both cultures were afterwards cooled down by shaking for a few minutes in ice water and made electro-competent for transformation. For retrieving, the modified vector PL253 was linearized with *ScaI* before transformation and for the first and second targeting, the cassettes of the modified vectors PL452 and PL451 were cut out with *SalI* and *NotI* or *SacII* and purified with gel extraction. In single or co-electroporation, 1-10ng plasmid-DNA or 100ng of purified cassette were used. Several colonies were inoculated and the DNA isolated in mini-preps for subsequent restriction analysis. For retrieving, the selection was done with ampicillin and for targeting with kanamycin due to the resistance of the NEO-gene. Due to enhanced appearance of “rolling circle replications” in SW102 cells repressing the RecBCP proteins, the retrieving- and

targeting vectors containing SW102 clones were re-transformed (1ng) in DH10ß. DH10ß strain was used to prevent plasmid multimers, since re-transformation favours monomers.

Deletion of the NEO-cassette

To delete the first floxed NEO-cassette that has been inserted with the first mini-targeting vector the targeting construct was transformed into *SW105* cells. Furthermore the functionality of the l*oxP*- and *frt*-sides were tested in *SW105* and *SW106* cells respectively. The strain SW106 comprise the gene for *Cre*-recombinase, the *SW105* strain the gene for the *Flp*-recombinase. Both genes are under the control of the arabinose-inducible *AraC* /P_{BAD} promoter to allow the expression of the recombinase-genes in the presence of arabinose in the culture medium.

First a 10ml- culture of *SW105* or *SW106* was incubated over night at 32°C in LB-medium, diluted 1:50 and further grown for 2-3 hours until OD_{600} reached 0.4-0.5. 10ml of this culture were supplemented with 10% L (+) arabinose (Sigma A-3256) to a final concentration of 0.1%. The induced culture was grown for one more hour at 32°C in a shaking water bath. The cells of the un-induced culture (10ml) as well as the induced culture (10ml) have been made electro-competent and used for transformation.

4.3.3 Gene targeting in mouse ES cells to produce chimeric mice

The final *Scratch2* cKO-vector (PAC-PL253/P1-Neo/P2) was linerazied with *ScaI* and purified with phenol-chloroform extraction. 30µg of the purified DNA-fragment were electroporated in MPI2-ES cells. The positive selection of the ES cells was carried out in the first 2-4 days by addition of 2mM ganciclovir, the negative selection by addition of 250µg/ml geneticin (G418, *Neomycin*-gene mediated resistance) to the ES-culture medium for 10 days. The NEO-cassette conduces therefore to selection of cells with positive recombination. Because of the *frt*-sites flanking the NEO-cassette, it can be removed after targeting in the ES cells via expression of *Flp*-recombinase, either in the ES cells or by crossing the chimeras to *Flp*-expressing mice. Surviving ES clones were trypsinated in 96-well plates and cultivated for 9 days in 24-well plates on feeder cells (mouse fibroblast cells). Finally, the ES cells were transferred onto gelantine-coated plates, digested with proteinaseK in SDS-lysis buffer and the genomic DNA isolated by isopropanol-percipitation in 80µl TE to be analyzed with southern blot for correct recombination.

4.3.4 Southern blot

Radioactively labelling and purification of the DNA-probes

The DNA probes for southern blot analysis were prepared using the Amersham Rediprime II

Random Prime Labelling System (GE Healthcare) and [α-32P]-dCTP (Amersham Biosciences). The labelling reaction was performed as recommended by the manufacturer. ProbeQuant G-50 Sephadex Micro Columns (GE Healthcare) were used to purify labelled nucleic acids. The Micro Columns were used according to the instruction of the manufacturer. The specific activity of radioactive labelled DNA was measured using the LS 1701 scintillation counter (BeckMan). Probes were used if they had more than 800.000 cpm/µl.

Restriction digest of the genomic DNA

The restriction digestion of genomic DNA was set up in a total volume of 40µl. 5-10µg genomic DNA was digested with the appropriate restriction enzyme (10U / µg of DNA) and 0.2µl RNaseA (10 mg/ml stock) was added. The reaction was incubated at 37°C overnight.

Agarose-gel electrophoresis

To separate the digested DNA, the reaction was occupied with 5µl of 6x DNA-loading buffer, denaturated for 3 min at 56°C and load on a 0,7% agarose gel (in 0.5x TBE, 10µg/ml ethidium bromide). The gel was run at < 1 V/cm at approximately 30 V overnight. Afterwards the upper part of the gel above the wells and all unnecessary parts were removed. On edge of the gel was marked by cutting off a piece, and a photo with a ruler adjacent to the gel was taken under UV-light. The gel was incubated under shaking for 15 min in 0.25M HCl and for 40 min in Blot buffer I (1.5 M NaCl, 0.5 M NaOH), with dH_2O washes in between. Then it was incubated for 40min in Blot buffer II (1 M Tris, pH 7.2, 1.5 M NaCl) and for 20min in 20x SSC (3 M NaCl, 300 mM Na-Citrate).

The capillary blot system

An equally large piece of nylon membrane (GeneScreenTM Hybridization Transfer Membrane, PerkinElmer) was soaked in dH_2O and afterwards in 20x SSC until the colour changed totally from white to light grey. The blotting system was set up as shown below and run for 48 hours in 20x SSC. The wells of the gel were marked on the membrane with a pencil before the gel was removed and the DNA on the membrane was cross linked by UV irradiation (0.5 J/cm2).

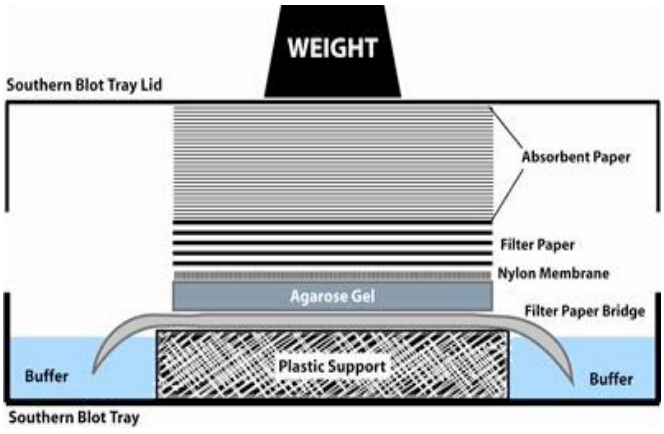

Hybridisation

The membranes (up to 4) were transferred in roller bottles and washed with 1 volume (50-100ml) pre-warmed 2x SSC containing 0.5% SDS for 30 minutes at 65°C. Blots were prehybridized in 100ml pre-warmed hybridization-buffer (5x Denhardt's solution, 5x SSPE, 0.5% SDS and 5 mg/ml Salmon sperm DNA; 50xDenhardt's (10 g Ficoll 400, 10 g polyvinylpyrrolidone, 10g BSA in 1 litre dH_2O); 20x SSPE (174 g NaCl, 27.4 g $NaH_2PO_4xH_2O$, 7.4 g EDTA, pH 7.4 in 1 litre dH_2O) for 2 hours at 65°C. the prehybridization solution was poured off and replaced with fresh hybridization solution (prehybridization solution containing the probe ($1x10^6$cpm/ml)). Hybridization took place overnight while gently rotating at 65°C. The next day the hybridization solution was removed and the membranes were washed twice with pre-warmed (65°C) 2× SSC containing 0.5% SDS for 30min. Afterwards they were washed once with pre-warmed (65°C) 0.1× SSC containing 0.5% SDS for half an hour and air-dried for 30min on a whatman-paper.

Autoradiography

The corners of the blots were stuck to a whatman-paper and everything was wrapped in plastic foil before fixing on an imager plate (BAS-IP MS, Fuiju photo film) into a film cassette. Exposure took place at least 2 hours until over night. The image plate was transferred from the cassette to the reading plate in the dark. The image plate was read out with the following parameters: Sensitivity S10.000, pixel size 25μm, latitude L4 and mode 20 x 25.

4.4 ANIMAL TREATMENTS

4.4.1 BrdU injections

For pulse labelling, pregnant mice were injected intraperitoneal at a defined embryonic day with BrdU (100μl of 0.014 g BrdU (Sigma-Alderich) in 1 ml PBS /10 g body weight). The embryonic brains were then dissected after a certain period of time before cryo-sectioning followed by IHC.

4.4.2 *In-utero* electroporation

Timed pregnant mice (CD1 strain) with embryos at a gestational age of embryonic day 13 or 14 received painkiller in the drinking water from one day before the operation until 3 days after. The mouse was anaesthetized by intraperitoneal injection with a mixture of ketamine (2mg/30g), xyclazin (0.4mg/30g) and acepromazin (0.06mg/30g) in 0.9% NaCl. Injection capillaries were made from glass micropipettes pulled to produce a long taper and broken under a dissection microscope at an inner diameter of 10–20μm. The mouse was fixed on its

back on a warming plate and deep anaesthesia was verified by the absence of pain reflexes. The abdomen was cleaned with 70% ethanol and the uterine horns were exposed after caesarean with a 2cm vertical incision along the abdominal midline and arranged on a sterile gaze pad.

During the whole procedure the uterus was kept wet with warmed 0.9% NaCl. Per embryo 2µl of plasmid DNA (2-3µg/µl) was mixed with 1µl Fast Green (0.1% in PBS, Sigma) and suck in the injection capillary with a mouth pipette. With the help of Fast Green the injection into the lateral ventricle (one hemisphere of the embryo) could be optically controlled through the darkening of the ventricle. Tweezer electrodes were placed laterally to the head with the plus pole next to the injected hemisphere. 5 electric pulses (50msec power on, 950msec power off) with 30C (E13.5 embryo) or 34V (E14.5 embryo) were given to direct the DNA to the dorso-lateral wall of the cortex. Maximum two embryos per uterus horn were electroporated with minimum one embryo in between. The uterine horns were replaced back in the abdominal cavity with O-ringed forceps and the abdominal wall was closed after applying 500µl of Trammel® with 4 to 6 stitches (Ethicon 5-0 surgical suture). The abdominal skin was closed with 3 to 4 clips. The mouse was put in a cage with clean papers standing on a warming plate (37°C) under surveillance until it wake up approximately 30 to 45 minutes later. The injected embryos were sacrificed 1 to 9 days after injection. These experiments run under the license number 33.11.42502-04-033/08.

4.5 CELL CULTURE

4.5.1 Cortex dissection and dissociation

Embryos were removed by caesarean section from time-pregnant mice killed by cervical dislocation. The brains were dissected in ice-cold Hanks balanced salt solution (HBSS, GIBCO). The meninges were removed, the telencephalic hemispheres separated, the hippocampus and the olfactory bulbs were removed and the cortex was separated from the ganglion eminence and collected in a 2ml-tube with HBSS+ (containing 10 mM HEPES). The excessive liquid was carefully removed and the tissiue was digested for 10 min with 500µl of 0.25% Trypsin/EDTA in DMEM in a water bath. The reaction was stopped with 500µl Ovomucoid and the tissiue was mechanically dissociated by titurating 10-25x with a fire-polished glass pipette. After two washes with DMEM (centrifuged for 5 min at 1000 rpm in between), the singularized cells were either used for differentiation on coated cover slips for up to four days or to perform clonal pair analysis.

4.5.2 Clonal pair analysis and immuno-cytochemistry

Clonal pair analysis was performed in order to estimate the effect of ectopic *Scrt2* expression in the radial glia cells of the developing neocortex regarding the mode of cell division of neural progenitor cells. Primary cortical cells at E14.5 were dissociated, after the embryonic brains have been either electroporated with GFP-control plasmid, Scrt2.2-IRES-GFP or Scrt2.3-IRES-GFP at E13.5. The brains were isolated in cold HBSS+ and the roughly the GFP-positive region of the cortex was dissected under a fluorescence binocular. The material was pooled from 2-3 brains per condition and collected with HBSS+ in a 2ml eppendorf tube. The tissiue was allowed to sink down and the supernatant was removed for digestion with 500µl 0.25% trypsin/EDTA for 10min at 37°C-waterbath. The reaction was stopped with 500µl Ovomucoid and the tissiue was titurated 10-15x with a fire-polished glass pipette until no cell clumps were visible anymore. 9ml DMEM were added and the cells spun for 5 min at 1000rpm to resuspend them in 1ml C-medium (DMEM with 1% glutamine supplemented with 1% penicillin-streptomycin, N2, B27). 2x 10^5 cells were plated per ½ chamber on poly-D-lysine coated chamber slides in 1ml C-medium, freshly supplied with FGF-2 (10 ng/ml). The cells were incubated for 22hrs with 5% CO_2 at 37°C. Then the medium was removed, the cells were washed once with PBS and fixed for 20min in 4% PFA. After three times washing in PBS for 5min, the cells were blocked at RT for 30min in blocking-solution (PBS with 10% FCS and 0.3% triton). Antibodies against GFP (chicken 1:500, abcam), together with Pax6 (rabbit, 1:300, Covance), anti-Tbr2-antibody (rabbit, 1:200, abcam) or Tuj1 (mouse, 1:500, Covance) were applied over night at 4°C in blocking solution. On the next day the slides were washed three times for 5min in PBST (PBS with 0.1% triton) and incubated with secondary antibodies for 2hrs at RT to the exclusion of light. Finally the slides were again washed three times 5min in PBST and once for 5min in PBS, before they were covered with Vectashield® mounting medium with DAPI (vector). Pictures were taken at the Olympus BX60 fluorescence microscope. The mean number of clones was obtained from three independent experimental batches. The composition of the clonal pairs per experiment was determined by the percentage values of antibody-positive cells of total counted pairs (GFP+) per condition.

4.5.3 Over expression *in-vitro* by transient cell transfection

NIH-3T3, Hela and Neuro2A cells were maintained and cultured in DMEM medium plus 10% FCS. Cells were transfected with plasmid by using Lipofectamine 2000 (Invitrogen) according to supplier ´s instruction.

4.6 MOLECULAR BIOLOGY

4.6.1 Extraction from genomic DNA from mouse cut-tails

Tissue from cut-tails was digested in 500µl tissue lysis buffer (100 mM Tris, pH 8.5, 200 mM NaCl, 5 mM EDTA, 0.2% SDS, freshly added 250 µg/ml Proteinase K) at 55°C overnight with shaking. For unproblematic and urgent genotyping the DNA was precipitated by hand with 0.8 volume isopropanol and 15 min centrifugation at 13000rpm. The precipitated pellet was washed with 500µl 70% ethanol, spun 5min at 13.000rpm; air dried, and dissolved in 50 µl Millipore 1xTE. For standard and sensitive genotyping, the DNA was extracted and purified using the DNeasy 96 Blood & Tissue Kit.

4.6.2 Genotyping of mice

For genotyping of GOF-mice, the Kit-prepared DNA was used and PCRs with primers for the lacZ gene, Cre-recombinase and GFP gene were performed. 1µl of genomic DNA was mixed with 29µl master mix, containing 1xGoTaq® Reaction Buffer with 1.5mM $MgCl_2$, 0.2mM dNTPs, and 0.3 µM of each primer and 0.8U GoTaq®DNA polymerase in water.

4.6.3 PCR

For cloning of DNA fragments, the DNA sequences were amplified from genomic E15.5 DNA or from E15.5 cortex cDNA or plasmids. Typically, 10ng of plasmid DNA or 200ng genomic DNA were used as template and the reaction was performed in a total volume of 50µl with the following components: 1x *Pfu*-buffer with 2 mM $MgCl_2$, 0.2 mM dNTPs, 0.3 µM forward primer, 0.25 µM reverse primer, (optional 5% DMSO at GC-rich template) and 2.5 U *Pfu*-DNA Polymerase (Fermentas) under following conditions, depending on the Tm value (52-62°C) and product size. The thermo cycling program was carried out using PTC-200 thermal cycle (Perkin Elmer). The reactions were either subsequent digested or directly load on a 0.8-1.5% agarose gel to isolate the correct band(s) for extraction / purification of the DNA.

Step	Temperature	Duration
• Initial denaturation	95 °C	3 minutes
• Denaturation	95 °C	10-30 seconds
• Annealing	50-55 °C	30 seconds
• Elongation	72 °C	~ 2 min/kb (25-35 x)
• Final elongation	72 °C	10 minutes
• Hold	4 °C	

4.6.4 DNA electrophoresis and isolation from agarose gel

0.8-2% agarose gel was prepared by melting agarose (Invitrogen) in 0.5x TBE buffer (45 mM Tris-borate, 1 mM EDTA, pH 8.0) and subsequently adding ethidium bromide to a final concentration of 0.3 μg/ml. DNA sample was mixed with 5x DNA loading buffer (25% Ficoll, 100 mM EDTA, 0.05% Bromophenol Blue), and electrophoresis was performed under approximately 1-6 v/cm in 0.5xTBE buffer. For fragment purification, the band was excised from the gel and purified with the Qiagen Gel Extraction Kit as recommended by the supplier.

4.6.5 Isolation and -purification of plasmid-DNA from *E.coli*

For subsequent sequencing, cell transfection or *in-utero* injections, plasmid-DNA was isolated from E.coli using Qiagen Mini, Midi or Maxi-Prep Kits. All steps were performed as recommended by the supplier.

4.6.6 Restriction enzyme digest of DNA

Analytical digests were performed in 50μL total volume with 5μg DNA and 25-50 U of the appropriate restriction enzyme(s) at 37°C for 2 hours or over night. For end-cutting of PCR products, the PCR product was purified with a PCR Purification Kit (Qiagen) first.

4.6.7 De-phosphorylation / blunting of linear DNA fragments

To decrease unwanted re-ligation of digested vectors, de-phosphorylation of the DNA 5'-end was performed by directly adding 1μl Alkaline Phosphatase (1U/μl, Roche) and 1x AP-buffer into the restriction mixture. After an incubation period of 30 minutes at 37°C, the mixture was incubated at 65°C for 5 minutes to inactivate the enzyme. For blund-end ligations, DNA polymerase I large fragment (Klenow fragment) (5U/μl, NEB) was used to fill-in the ends of overhang-5' DNA fragment. DNA in restriction enzyme NEB buffer supplemented with 33 μM dNTPs was incubated with Klenow at a concentration of 1U per μg DNA at 25 °C for 30 minutes. The treated DNA samples were load on agarose gel, the fragments isolated and purified with the Qiagen Gel Extraction Kit in 30μl EB-buffer.

4.6.8 Measurement of nucleotide concentrations

1.5μl of the nucleic acid was used for OD_{260} measurement with a spectrophotometer (Nanodrop 1000, Peclab) to determine the concentrations of DNA and RNA with the dilute reagent as blank reference.

4.6.9 Ligation

Ligations were usually performed with a 3:1 molar ratio insert / vector. 50-100ng of the purified vector fragment was mixed with purified insert fragment, 1x T4-DNA ligase buffer (MBI Fermentas) and 1µl T4 DNA ligase (3U/µl) (MBI Fermentas). The reaction was filled up with H_2O to a total volume of 10µl and incubated at 4°C overnight and transformed the next day.

4.6.10 Preparation of electro-competent cells

A 10ml starter culture was inoculated from a single colony of *E. coli* (*DH5α* or *DH10β*) in LB medium and cultured at 37°C shaking overnight (250 rpm). 2x5ml of the overnight culture were put in 2x1l of pre-warmed LB medium and incubated at 37°C shaking until the OD_{600} reached 0.6-0.8 (about 3 hours). The cells were chilled on ice for 10-30 minutes and all following steps were done on ice or at 4°C. After centrifugation at 5000 rpm for 20 minutes, the supernatant was discard and the cell pellet from each 1l- culture was washed with 1 later pre-chilled water and again centrifuged at 5000 rpm for 20 minutes. The pellets were resuspend each in 100 ml pre-chilled 10% glycerol, centrifuged for 10min at 6000 rpm and again resuspend with 20 ml pre-chilled 10%glycerol. After another centrifugation for 10min at 6000rpm, each pellet was washed with 2 ml pre-chilled 10%glycerol and centrifuged at 6000 rpm for 5 minutes. The pellet was finally solved in 2 ml 10% glycerol and 50µl-aliquots were frozen in liquid nitrogen and stored at –80°C.

4.6.11 Transformation of *E. coli* by electroporation

50µl electro-competent cells were thawed on ice, mixed with 1µl plasmid DNA (10ng) or 1-2µl of ligation reaction and transferred in a pre-chilled 0.1cm electrode Gene Pulser Cuvette (Bio-Rad). The electroporation was performed using a Gene Pulser (Bio-Rad) with 1.8 kV voltages, 200Ω resistances and 25µF capacitance. Afterwards, 1ml pre-warmed LB medium was immediately supplied to the electroporated *E. coli* for recovery. The cells were incubated for 45 min on a rotor at 37°C, followed by plating 100 µl on appropriate antibiotic containing agar-plate. Colonies were selected and inoculated in 5ml LB medium with antibiotic at 37°C overnight. To confirm the correct insertion of the insert into the vector, plasmid DNAs were isolated from 1.5 ml bacterial cultures by using the alkaline lysis method (Sambrook and Russell, 2001; Molecular cloning) and isopropanol precipitation. Digestion was performed at 37°C for > 3hours and the resulting products were analyzed on a 1% agarose gel.

4.6.12 Total RNA isolation

To isolate total RNA from cultured cells or mouse tissues, I used the RNeasy Mini Kit (Qiagen) including DNase treatment, as described by the manufacturer. The disruption and homogenization of the sample was done by the use of a Cell Disruptor B15 and 3 mm tip. The NA concentration (in RNAse-free water) was measure with a spectrophotometer (NanoDrop). The total RNA was stored at –80°C.

4.6.13 cDNA synthesis

The reverse transcription (cDNA synthesis) was performed in two steps, using the QuantiTect Rev. Transcription Kit (Qiagen) to produce cDNA .

4.6.14 Total protein extraction and Bradford-measurement

To extract total protein from cultured cells, the material was harvested, washed in PBS and the cell pellet resolved in RIPA+ buffer (50 mM Tris-HCl pH 7.4, 1% NP-40, 0.25% Na-deoxycholate1, 150mM NaCl, 1mM EDTA; 10ml were freshly supplemented with 1 tablet "complete mini" protease inhibitor (Roche)). After lysis at RT, the samples were spun down and the supernatant stored at -80°C. The crude protein concentration was determined with the Coomassie-Bradford Assay (Pierce) and BSA standards.

4.6.15 Western blotting

Protein extracts of mouse cortex, cultured cells or TnT reactions (*in-vitro* transcribed and translated protein) were collected as described in 5.6.14. Aliquots of the frozen supernatants were heated for 3min at 95°C in 2x sample buffer (6%SDS, 0.6% bromphenolblue, 20% glycerol, 6% ß-mercaptoEtOH) for denaturation. Afterwards 20 to 50µg protein per sample and a pre-stained marker (Fermentas) were separated by SDS-PAGE using the BioRad Mini PROTEAN system. A PVDF-membrane (Immobilion-P transfer membrane, Millipore) was activated in MeOH, rinsed with water and incubated for a few minutes in transfer-buffer as well as the gel. The sandwich, composing of paper-pad–gel-membrane-paper-pad was soaked with transfer-buffer and placed in a semi-dry transfer cell (Trans- Blot SD; BioRad) and run for 1hr with 70mA per gel (3.5mA/cm²). Afterwards the membrane was washed for 10 min in PBS and blocked for 1 hour in 5% milk powder (in PBS) at RT.
The first antibody was applied over night at 4°C in blocking solution. On the next day the membrane was washed 3 times for 20min in PBST (0.2% Tween in PBS) and the secondary antibody was applied for 2 hours at RT in blocking. After three more washing steps and 20min in PBST the immuno-specific signal was detected by chemiluminescence kit (Pierce). Quantifications were normalized to the level of actin or α- tubulin.

Running buffer (10x) → use 1x with water		**Transfer- buffer**
Glycine	144.2g	2.9g
TRIS	30.3g	5.8g
SDS	10.0g	3.7ml (10% in H2O)
Water	to 1l	to 1l
		200ml Methanol

Separation-gel (for two gels)			**Collection**-gel (for two gels)
	10.0%	**12.5%**	
Acrylamid (Roth)	3.3ml	4.2ml	660µl
1.5M Tris, pH8.8	2.5ml	2.5ml	1244µl (5.5M Tris, pH6.8)
10% SDS	100µl	100µl	50µl
Water	4ml	3.2ml	3.04ml
10% APS (Sigma)	50µl	50µl	25µl
TEMED (sigma)	3.4µl	3.4µl	2.6µl

4.7 EXPERIMENTS IN XENOPUS LEAVIS

4.7.1 Animals

The African clawed frog Xenopus laevis was used as experimental organism. Albino and pigmented frogs were purchased from NASCO (Ft. Atkinson, USA). Staging of the embryos was according to Nieuwkoop and Faber (1967).

4.7.2 Constructs

Scrt2.2/pCS2+/GR harbours the full coding sequence of the codon-optimizied ORF of Scrt2.2. The fragment was generated by PCR amplification using Scrt2.2-pCIG2 as template, and restriction sites containing primers to insert the ORF into the EcoRI/XhoI sites of pCS2+. For sense RNA, the construct was linearized with NotI and RNA transcribed with SP6 RNA polymerase.

4.7.3 Embryo isolation

Embryos were obtained from female adult Xenopus laevis by HCG induced egg- laying using 800 U HCG. Spawn was in vitro fertilized and embryos staged according to Nieuwkoop and Faber, 1956. Embryos were removed and injected in one blastomere of the two-cell stage or one dorsal of the four-cell stage as described. As lineage tracer, 75pg nuclear lacZ mRNA was co-injected. For ectodermal explants and western blotting experiments, both blastomeres were injected omitting nuclear lacZ mRNA.

4.7.4 mRNA injection

Stage 2 embryos were injected with 100pg of oScrt2.2 mRNA together with 50 pg LacZ

mRNA into a one cell of a 2-cell blastomere. Embryos were cultured over night at 18°C. Two batches of 15 embryos were collected and analyzed as described above. For synthesis of capped mRNA used for microinjection, the mMessage- mMachineTM Kit (Ambion) was used according to the manufacturer's protocol and purified with the RNeasyTM Mini Kit (Qiagen), eluted in 30 µl of RNase-free H_2O.

4.7.5 Dexamethasone treatment

Embryos were injected with inducible mRNA constructs. Animal caps and embryos were treated with fresh 1X DEX (500x Dexamethasone (Dex): 20 mM dexamethasone in ethanol) at various stages and continuously kept in solution until fixation.

4.7.6 X-Gal staining

Embryos were grown to the desired stage, fixed in MEMFA (0.1 M MOPS, pH7.4, 2 mM EGTA; 1 mM MgSO4; 3.7% formaldehyde) and stained with X-gal for 10 to 20 min. After washing and postfixation in MEMFA, the embryos were dehydrated with absolute ethanol and stored at -20°C for whole mount-ISH.

4.7.7 (Whole mount) – *in-situ* hybridisation

WM-ISH was performed as described in Harland, (1991) and Hollemann et al. (1999) using antisense RNA labelled with digoxigenin-11-UTP. (For further details, see PhD thesis of B. Rust, 2008).

5. MATERIAL

5.1 KITS

Kit	Source
Mouse NSC Kit	Amaxa
Dual-Luciferase Reporter Assay System	Promega
DNeasy 96 Blood & Tissue Kit	Qiagen
Mini, Midi or Maxi-DNA Prep Kits	Qiagen
PCR Purification Kit	Qiagen
Gel Extraction Kit	Qiagen
RNeasy Mini Kit	Qiagen
QuantiTect Rev. Transcription Kit	Qiagen
QuantiTect SYBR Green PCR Kit	Qiagen
Coomassie-Bradford Assay	Pierce
TNT Coupled Reticulocyte Lysate System	Promega
Rediprime II Random Prime Labelling System	Amersham

5.2 BACTERIAL STRAINS

Strain	Feature(s)	Source
DH5α	Amplification of plasmid-DNA	Invitrogen
DH10B	Amplification of plasmid-DNA	E. Herzog
SW102	Recombineering	(Warming et al., 2005)
SW105	Recombineering (Arabinose- inducible Flp gene	(Warming et al., 2005)
SW106	Recombineering (Arabinose- inducible Cre gene	(Warming et al., 2005)

5.3 OLIGONUCLEOTIDES

Primer for the generation of the *Scrt2*-cKO construct:

Name	5´to 3´sequence	Purpose
P100	ataagcggccgctggctcagcagttaagagca	sense for A/B
P101	gtcaagcttctctgcattggtcccagatt	a-sense for A/B
P102	gtcaagctttggttgagctacacccatca	sense for Y/Z
P103	ggactagtgcttcatcgggagttctctg	a-sense for Y/Z
P104	gggtcgacaaggggagaggcagacaatta	sense for C/D
P105	gtcgaattcaagcttcttatctgcgaaatggagcttatag	a-sense for C/D
P106	cgggatccaaaatgcaacgaaggcaaag	sense for E/F
P107	ataagcggccgcctgggtggacttctgttggt	a-sense for E/F
P108	gggtcgacctattggagccctcaatcca	sense for G/H
P109	gtcgaattcggatccgcagaggcgaacctgtagtc	a-sense for G/H
P110	ataagcggccgcctttgctagagaacagcctggag	sense for I/J
P111	tccccgcggaaagggagaggctccagaag	a-sense for I/J
P112	tgctctgctgggactctaca	sense for 5´-probe
P113	ggtcccagaatcttgagctg	a-sense for 5´-probe
P114	gcttccagacggcatatctc	sense for 3´-probe
P115	ggacaatcagccacccttta	a-sense for 3´-probe
P116	ctgacctcaaatgatactcctgctgc	seq. primer for 5´loxP-site
P117	gatggattgcacgcaggttctc	seq. primer for NEO-cassette
P118	acagtccctgggtgaagcc	seq. primer for 3´loxP-site
T7	taatacgactcactataggg	seq. primer for 5´-arms in PL253/PL451
T3	attaaccctcactaaag	seq. primer for 5´-arms in PL452

Primer for PCR amplification:

Name	5´to 3´sequence	Purpose
F-S2.2	gaagtcctacctgcacaagcac	sense Scrt2.2 cDNA (start)
R-S2.2	ggtggtaggtgggagcgg	a-sense Scrt2.2 cDNA (end)

Primer for genotyping:

Name	5´to 3´sequence	Purpose
F-Cre	ccgctcccacctaccacc	sense for Cre
R-Cre	gtgcttgtgcaggtaggacttc	a-sense for Cre
F-GFP	accctgaagttcatctgcacca	sense for GFP
R-GFP	tgggtgctcaggtagtggttgt	a-sense for GFP
F-lacZ	cgtcacactacgtctgaacgtcg	sense for lacZ

R-lacZ	cagacgattcattggcaccatgc	a-sense for lacZ

5.4 PLASMIDS AND VECTORS

5.4.1 Vectors

Name	Purpose	Source / Supplier
pCS2+	RNA expression (Xenopus)	D. Turner http://sitemaker.umich.edu/dlturner.vectors
pCIG2	*in-vivo* expression (CMV)	F. Guillemot Lab
pJojo	Targeting for GOF mice	J. Berger
pBS+	Cloning	Promega
PL253	Recombineering / Retrieving	Liu et al., 2003
PL451	Recombineering / Targeting	Liu et al., 2003
PL452	Recombineering / Targeting	Liu et al., 2003

5.4.2 Anti-sense plasmids for ISH

Gene	RE	Polymerase	Source
Mash1	*XbaI*	SP6	F. Guillemot
Ngn2	*BamHI*	T7	Lab Stock
N-tubulin			Chitnis *et al.*, 1995
Pax6	*EcoRI*	T3	C.Walther
Scrt2	*SpeI*	T3	RIKEN clone G630034H08 (AK090280)
Sox3			B. Rust, Pieler Lab
Tbr1	*HindIII*	T3	J. Rubenstein
Tbr2	*EcoRI*	T3	Labstock
X-ngnr-1			Ma *et al.*, 1996

5.5 ANTIBODIES

5.5.1 Primary Antibodies

Name	Host	Supplier	IHC/ICC	WB
BrdU	Rat	Accurate	1:50	
Cre	Mouse IgG1	Sigma-Alderich	1:200	

Ctip2	Rat	Abcam	1:100	
Cux1	Rabbit	Santa Cruz	1:250	
Dcx	Goat	Santa Cruz	1:100	
GFAP	Rabbit	DAKO	1:300	
GFP	Chicken	Abcam	1:500	
HuC/D	Mouse IgG2b	Invitrogen	1:50	
Mash1	Mouse IgG1	B & D	1:200	
Nestin	Mouse	Chemicon	1:300	
NeuroD	Goat	Santa Cruz		
Ngn2	Mouse IgG2a	D. Anderson	1:50	
Pax6	Mouse	DSHB	1:300	
Pax6	Rabbit	Covance	1:300	
Satb2	Mouse	Abcam	1:200	
Scrt2 (SM)	Rabbit			1:500
Scrt P20	Rabbit	Santa Cruz	1:20	1:500
ß-actin	Rabbit	Sigma		1:1000
Tbr1	Rabbit	Abcam	1:300	
Tbr2	Rabbit	Abcam	1:200	
Tuj	Mouse	Chemicon	1:200	

5.5.2 Secondary antibodies (peroxidase-conjugated)

Name	**Species**	**Host**	**Supplier**	**WB**
IgG	Rabbit	Goat	Covance	1:10000
IgG	Mouse	Goat	Covance	1:5000
IgG	Rat	Goat	Covance	1:10000
IgG	Mouse	Goat	Bio-Rad	1:5000

Fluor dye-coupled secondary antibodies

As fluor dye-coupled secondary antibodies Alexa Fluor® series antibodies (Molecular Probes) were used 1:500 to 1:200 diluted in appropriate blocking solution. Antibodies were coupled to fluors 488, 568 and 594 and produced in mouse, rabbit, chicken, guinea pig, goat and rat.

II. REFERENCES

Arlotta, P., Molyneaux, B.J., Chen, J., Inoue, J., Kominami, R., and Macklis, J.D. (2005). Neuronal subtype-specific genes that control corticospinal motor neuron development in vivo. Neuron *45*, 207-221.

Armentano, M., Chou, S.J., Tomassy, G.S., Leingartner, A., O'Leary, D.D., and Studer, M. (2007). COUP-TFI regulates the balance of cortical patterning between frontal/motor and sensory areas. Nat Neurosci *10*, 1277-1286.

Arnold, S.J., Sugnaseelan, J., Groszer, M., Srinivas, S., and Robertson, E.J. (2009). Generation and analysis of a mouse line harboring GFP in the Eomes/Tbr2 locus. Genesis *47*, 775-781.

Ashraf, S.I., and Ip, Y.T. (2001). The Snail protein family regulates neuroblast expression of inscuteable and string, genes involved in asymmetry and cell division in Drosophila. Development *128*, 4757-4767.

Attardo, A., Calegari, F., Haubensak, W., Wilsch-Brauninger, M., and Huttner, W.B. (2008). Live imaging at the onset of cortical neurogenesis reveals differential appearance of the neuronal phenotype in apical versus basal progenitor progeny. PLoS One *3*, e2388.

Barnabe-Heider, F., Wasylnka, J.A., Fernandes, K.J., Porsche, C., Sendtner, M., Kaplan, D.R., and Miller, F.D. (2005). Evidence that embryonic neurons regulate the onset of cortical gliogenesis via cardiotrophin-1. Neuron *48*, 253-265.

Barrallo-Gimeno, A., and Nieto, M.A. (2005). The Snail genes as inducers of cell movement and survival: implications in development and cancer. Development *132*, 3151-3161.

Barrallo-Gimeno, A., and Nieto, M.A. (2009). Evolutionary history of the Snail/Scratch superfamily. Trends Genet *25*, 248-252.

Batlle, E., Sancho, E., Franci, C., Dominguez, D., Monfar, M., Baulida, J., and Garcia De Herreros, A. (2000). The transcription factor snail is a repressor of E-cadherin gene expression in epithelial tumour cells. Nat Cell Biol *2*, 84-89.

Bayer, S.A., and Altman, J. (1991). Development of the endopiriform nucleus and the claustrum in the rat brain. Neuroscience *45*, 391-412.

Bedogni, F., Hodge, R.D., Elsen, G.E., Nelson, B.R., Daza, R.A., Beyer, R.P., Bammler, T.K., Rubenstein, J.L., and Hevner, R.F. (2010). Tbr1 regulates regional and laminar identity of postmitotic neurons in developing neocortex. Proc Natl Acad Sci U S A *107*, 13129-13134.

Bennett, S.A., and Roberts, D.C. (2003). Analysis of protein expression in brain tissue by ELISA. Methods Mol Med *79*, 283-295.

Berger, J., Berger, S., Tuoc, T.C., D'Amelio, M., Cecconi, F., Gorski, J.A., Jones, K.R., Gruss, P., and Stoykova, A. (2007). Conditional activation of Pax6 in the developing cortex of transgenic mice causes progenitor apoptosis. Development *134*, 1311-1322.

Bertrand, N., Castro, D.S., and Guillemot, F. (2002). Proneural genes and the specification of neural cell types. Nat Rev Neurosci *3*, 517-530.

Bishop, K.M., Goudreau, G., and O'Leary, D.D. (2000). Regulation of area identity in the mammalian neocortex by Emx2 and Pax6. Science *288*, 344-349.

Bittman, K., Owens, D.F., Kriegstein, A.R., and LoTurco, J.J. (1997). Cell coupling and uncoupling in the ventricular zone of developing neocortex. J Neurosci *17*, 7037-7044.

Borello, U., and Pierani, A. (2010). Patterning the cerebral cortex: traveling with morphogens. Curr Opin Genet Dev *20*, 408-415.

Brill, M.S., Ninkovic, J., Winpenny, E., Hodge, R.D., Ozen, I., Yang, R., Lepier, A., Gascon, S., Erdelyi, F., Szabo, G.*, et al.* (2009). Adult generation of glutamatergic olfactory bulb interneurons. Nat Neurosci *12*, 1524-1533.

Britanova, O., de Juan Romero, C., Cheung, A., Kwan, K.Y., Schwark, M., Gyorgy, A., Vogel, T., Akopov, S., Mitkovski, M., Agoston, D.*, et al.* (2008). Satb2 is a postmitotic determinant for upper-layer neuron specification in the neocortex. Neuron *57*, 378-392.

Britz, O., Mattar, P., Nguyen, L., Langevin, L.M., Zimmer, C., Alam, S., Guillemot, F., and Schuurmans, C. (2006). A role for proneural genes in the maturation of cortical progenitor cells. Cereb Cortex *16 Suppl 1*, i138-151.

Bulfone, A., Martinez, S., Marigo, V., Campanella, M., Basile, A., Quaderi, N., Gattuso, C., Rubenstein, J.L., and Ballabio, A. (1999). Expression pattern of the Tbr2 (Eomesodermin) gene during mouse and chick brain development. Mech Dev *84*, 133-138.

Bulfone, A., Smiga, S.M., Shimamura, K., Peterson, A., Puelles, L., and Rubenstein, J.L. (1995). T-brain-1: a homolog of Brachyury whose expression defines molecularly distinct domains within the cerebral cortex. Neuron *15*, 63-78.

Bultje, R.S., Castaneda-Castellanos, D.R., Jan, L.Y., Jan, Y.N., Kriegstein, A.R., and Shi, S.H. (2009). Mammalian Par3 regulates progenitor cell asymmetric division via notch signaling in the developing neocortex. Neuron *63*, 189-202.

Campbell, K., and Gotz, M. (2002). Radial glia: multi-purpose cells for vertebrate brain development. Trends Neurosci *25*, 235-238.

Cano, A., Perez-Moreno, M.A., Rodrigo, I., Locascio, A., Blanco, M.J., del Barrio, M.G., Portillo, F., and Nieto, M.A. (2000). The transcription factor snail controls epithelial-mesenchymal transitions by repressing E-cadherin expression. Nat Cell Biol *2*, 76-83.

Cappello, S., Attardo, A., Wu, X., Iwasato, T., Itohara, S., Wilsch-Brauninger, M., Eilken, H.M., Rieger, M.A., Schroeder, T.T., Huttner, W.B., *et al.* (2006). The Rho-GTPase cdc42 regulates neural progenitor fate at the apical surface. Nat Neurosci *9*, 1099-1107.

Carl, T.F., Dufton, C., Hanken, J., and Klymkowsky, M.W. (1999). Inhibition of neural crest migration in Xenopus using antisense slug RNA. Dev Biol *213*, 101-115.

Caviness, V.S., Jr., and Takahashi, T. (1995). Proliferative events in the cerebral ventricular zone. Brain Dev *17*, 159-163.

Chanas-Sacre, G., Rogister, B., Moonen, G., and Leprince, P. (2000). Radial glia phenotype: origin, regulation, and transdifferentiation. J Neurosci Res *61*, 357-363.

Chen, H., Thiagalingam, A., Chopra, H., Borges, M.W., Feder, J.N., Nelkin, B.D., Baylin, S.B., and Ball, D.W. (1997). Conservation of the Drosophila lateral inhibition pathway in human lung cancer: a hairy-related protein (HES-1) directly represses achaete-scute homolog-1 expression. Proc Natl Acad Sci U S A *94*, 5355-5360.

Chenn, A., Zhang, Y.A., Chang, B.T., and McConnell, S.K. (1998). Intrinsic polarity of mammalian neuroepithelial cells. Mol Cell Neurosci *11*, 183-193.

Dehay, C., and Kennedy, H. (2007). Cell-cycle control and cortical development. Nat Rev Neurosci *8*, 438-450.

del Barrio, M.G., and Nieto, M.A. (2002). Overexpression of Snail family members highlights their ability to promote chick neural crest formation. Development *129*, 1583-1593.

Ellis, R.E., and Horvitz, H.R. (1991). Two C. elegans genes control the programmed deaths of specific cells in the pharynx. Development *112*, 591-603.

Emery, J.F., and Bier, E. (1995). Specificity of CNS and PNS regulatory subelements comprising pan-neural enhancers of the deadpan and scratch genes is achieved by repression. Development *121*, 3549-3560.

Englund, C., Fink, A., Lau, C., Pham, D., Daza, R.A., Bulfone, A., Kowalczyk, T., and Hevner, R.F. (2005). Pax6, Tbr2, and Tbr1 are expressed sequentially by radial glia, intermediate progenitor cells, and postmitotic neurons in developing neocortex. J Neurosci *25*, 247-251.

Englund, C., Kowalczyk, T., Daza, R.A., Dagan, A., Lau, C., Rose, M.F., and Hevner, R.F. (2006). Unipolar brush cells of the cerebellum are produced in the rhombic lip and migrate through developing white matter. J Neurosci *26*, 9184-9195.

Estivill-Torrus, G., Pearson, H., van Heyningen, V., Price, D.J., and Rashbass, P. (2002). Pax6 is required to regulate the cell cycle and the rate of progression from symmetrical to asymmetrical division in mammalian cortical progenitors. Development *129*, 455-466.

Farah, M.H., Olson, J.M., Sucic, H.B., Hume, R.I., Tapscott, S.J., and Turner, D.L. (2000). Generation of neurons by transient expression of neural bHLH proteins in mammalian cells. Development *127*, 693-702.

Farkas, L.M., Haffner, C., Giger, T., Khaitovich, P., Nowick, K., Birchmeier, C., Paabo, S., and Huttner, W.B. (2008). Insulinoma-associated 1 has a panneurogenic role and promotes the generation and expansion of basal progenitors in the developing mouse neocortex. Neuron *60*, 40-55.

Fode, C., Ma, Q., Casarosa, S., Ang, S.L., Anderson, D.J., and Guillemot, F. (2000). A role for neural determination genes in specifying the dorsoventral identity of telencephalic neurons. Genes Dev *14*, 67-80.

Ge, W., He, F., Kim, K.J., Blanchi, B., Coskun, V., Nguyen, L., Wu, X., Zhao, J., Heng, J.I., Martinowich, K.*, et al.* (2006). Coupling of cell migration with neurogenesis by proneural bHLH factors. Proc Natl Acad Sci U S A *103*, 1319-1324.

Gong, S., Zheng, C., Doughty, M.L., Losos, K., Didkovsky, N., Schambra, U.B., Nowak, N.J., Joyner, A., Leblanc, G., Hatten, M.E.*, et al.* (2003). A gene expression atlas of the central nervous system based on bacterial artificial chromosomes. Nature *425*, 917-925.

Gorski, J.A., Talley, T., Qiu, M., Puelles, L., Rubenstein, J.L., and Jones, K.R. (2002). Cortical excitatory neurons and glia, but not GABAergic neurons, are produced in the Emx1-expressing lineage. J Neurosci *22*, 6309-6314.

Götz, M., and Barde, Y.A. (2005). Radial glial cells defined and major intermediates between embryonic stem cells and CNS neurons. Neuron *46*, 369-372.

Götz, M., and Huttner, W.B. (2005). The cell biology of neurogenesis. Nat Rev Mol Cell Biol *6*, 777-788.

Götz, M., and Sommer, L. (2005). Cortical development: the art of generating cell diversity. Development *132*, 3327-3332.

Götz, M., Stoykova, A., and Gruss, P. (1998). Pax6 controls radial glia differentiation in the cerebral cortex. Neuron *21*, 1031-1044.

Guillemot, F., Molnar, Z., Tarabykin, V., and Stoykova, A. (2006). Molecular mechanisms of cortical differentiation. Eur J Neurosci *23*, 857-868.

Guo, F., Maeda, Y., Ma, J., Xu, J., Horiuchi, M., Miers, L., Vaccarino, F., and Pleasure, D. (2010). Pyramidal neurons are generated from oligodendroglial progenitor cells in adult piriform cortex. J Neurosci *30*, 12036-12049.

Hartfuss, E., Galli, R., Heins, N., and Gotz, M. (2001). Characterization of CNS precursor subtypes and radial glia. Dev Biol *229*, 15-30.

Haubensak, W., Attardo, A., Denk, W., and Huttner, W.B. (2004). Neurons arise in the basal neuroepithelium of the early mammalian telencephalon: a major site of neurogenesis. Proc Natl Acad Sci U S A *101*, 3196-3201.

Haubst, N., Berger, J., Radjendirane, V., Graw, J., Favor, J., Saunders, G.F., Stoykova, A., and Gotz, M. (2004). Molecular dissection of Pax6 function: the specific roles of the paired domain and homeodomain in brain development. Development *131*, 6131-6140.

He, Z., Li, J.J., Zhen, C.H., Feng, L.Y., and Ding, X.Y. (2006). Effect of leukemia inhibitory factor on embryonic stem cell differentiation: implications for supporting neuronal differentiation. Acta Pharmacol Sin *27*, 80-90.

Hemavathy, K., Ashraf, S.I., and Ip, Y.T. (2000). Snail/slug family of repressors: slowly going into the fast lane of development and cancer. Gene *257*, 1-12.

Henke, R.M., Meredith, D.M., Borromeo, M.D., Savage, T.K., and Johnson, J.E. (2009). Ascl1 and Neurog2 form novel complexes and regulate Delta-like3 (Dll3) expression in the neural tube. Dev Biol *328*, 529-540.

Hevner, R.F., Hodge, R.D., Daza, R.A., and Englund, C. (2006). Transcription factors in glutamatergic neurogenesis: conserved programs in neocortex, cerebellum, and adult hippocampus. Neurosci Res *55*, 223-233.

Hevner, R.F., Shi, L., Justice, N., Hsueh, Y., Sheng, M., Smiga, S., Bulfone, A., Goffinet, A.M., Campagnoni, A.T., and Rubenstein, J.L. (2001). Tbr1 regulates differentiation of the preplate and layer 6. Neuron *29*, 353-366.

Hinds, J.W. (1972). Early neuron differentiation in the mouse olfactory bulb. II. Electron microscopy. J Comp Neurol *146*, 253-276.

Hirabayashi, Y., Itoh, Y., Tabata, H., Nakajima, K., Akiyama, T., Masuyama, N., and Gotoh, Y. (2004). The Wnt/beta-catenin pathway directs neuronal differentiation of cortical neural precursor cells. Development *131*, 2791-2801.

Hodge, R.D., Kowalczyk, T.D., Wolf, S.A., Encinas, J.M., Rippey, C., Enikolopov, G., Kempermann, G., and Hevner, R.F. (2008). Intermediate progenitors in adult hippocampal neurogenesis: Tbr2 expression and coordinate regulation of neuronal output. J Neurosci *28*, 3707-3717.

Ishibashi, M., Ang, S.L., Shiota, K., Nakanishi, S., Kageyama, R., and Guillemot, F. (1995). Targeted disruption of mammalian hairy and Enhancer of split homolog-1 (HES-1) leads to up-regulation of neural helix-loop-helix factors, premature neurogenesis, and severe neural tube defects. Genes Dev *9*, 3136-3148.

Joshi, A.A., Shattuck, D.W., Thompson, P.M., and Leahy, R.M. (2005). A framework for registration, statistical characterization and classification of cortically constrained functional imaging data. Inf Process Med Imaging *19*, 186-196.

Justice, N.J., and Jan, Y.N. (2002). Variations on the Notch pathway in neural development. Curr Opin Neurobiol *12*, 64-70.

Kriegstein, A.R., and Gotz, M. (2003). Radial glia diversity: a matter of cell fate. Glia *43*, 37-43.

LaBonne, C., and Bronner-Fraser, M. (2000). Snail-related transcriptional repressors are required in Xenopus for both the induction of the neural crest and its subsequent migration. Dev Biol *221*, 195-205.

Land, P.W., and Monaghan, A.P. (2003). Expression of the transcription factor, tailless, is required for formation of superficial cortical layers. Cereb Cortex *13*, 921-931.

Langer, E.M., Feng, Y., Zhaoyuan, H., Rauscher, F.J., 3rd, Kroll, K.L., and Longmore, G.D. (2008). Ajuba LIM proteins are snail/slug corepressors required for neural crest development in Xenopus. Dev Cell *14*, 424-436.

Lee, J.K., Cho, J.H., Hwang, W.S., Lee, Y.D., Reu, D.S., and Suh-Kim, H. (2000). Expression of neuroD/BETA2 in mitotic and postmitotic neuronal cells during the development of nervous system. Dev Dyn *217*, 361-367.

Lein, E.S., Hawrylycz, M.J., Ao, N., Ayres, M., Bensinger, A., Bernard, A., Boe, A.F., Boguski, M.S., Brockway, K.S., Byrnes, E.J., *et al.* (2007). Genome-wide atlas of gene expression in the adult mouse brain. Nature *445*, 168-176.

Li, H.S., Wang, D., Shen, Q., Schonemann, M.D., Gorski, J.A., Jones, K.R., Temple, S., Jan, L.Y., and Jan, Y.N. (2003). Inactivation of Numb and Numblike in embryonic dorsal forebrain impairs neurogenesis and disrupts cortical morphogenesis. Neuron *40*, 1105-1118.

Li, N., Zhao, C.T., Wang, Y., and Yuan, X.B. The transcription factor Cux1 regulates dendritic morphology of cortical pyramidal neurons. PLoS One *5*, e10596.

Li, W., Sun, G., Yang, S., Qu, Q., Nakashima, K., and Shi, Y. (2008). Nuclear receptor TLX regulates cell cycle progression in neural stem cells of the developing brain. Mol Endocrinol *22*, 56-64.

Liu, P., Jenkins, N.A., and Copeland, N.G. (2003). A highly efficient recombineering-based method for generating conditional knockout mutations. Genome Res *13*, 476-484.

Luskin, M.B., and Shatz, C.J. (1985). Studies of the earliest generated cells of the cat's visual cortex: cogeneration of subplate and marginal zones. J Neurosci *5*, 1062-1075.

Malatesta, P., Hartfuss, E., and Gotz, M. (2000). Isolation of radial glial cells by fluorescent-activated cell sorting reveals a neuronal lineage. Development *127*, 5253-5263.

Mallamaci, A., and Stoykova, A. (2006). Gene networks controlling early cerebral cortex arealization. Eur J Neurosci *23*, 847-856.

Manzanares, M., Locascio, A., and Nieto, M.A. (2001). The increasing complexity of the Snail gene superfamily in metazoan evolution. Trends Genet *17*, 178-181.

Marin, F., and Nieto, M.A. (2006). The expression of Scratch genes in the developing and adult brain. Dev Dyn *235*, 2586-2591.

Marin, O. (2003). Thalamocortical topography reloaded: it's not where you go, but how you get there. Neuron *39*, 388-391.

McConnell, S.K. (1995). Constructing the cerebral cortex: neurogenesis and fate determination. Neuron *15*, 761-768.

Meinhardt, H. (2001). Organizer and axes formation as a self-organizing process. Int J Dev Biol *45*, 177-188.

Metzstein, M.M., and Horvitz, H.R. (1999). The C. elegans cell death specification gene ces-1 encodes a snail family zinc finger protein. Mol Cell *4*, 309-319.

Misson, J.P., Edwards, M.A., Yamamoto, M., and Caviness, V.S., Jr. (1988). Mitotic cycling of radial glial cells of the fetal murine cerebral wall: a combined autoradiographic and immunohistochemical study. Brain Res *466*, 183-190.

Miyata, T., Kawaguchi, A., Okano, H., and Ogawa, M. (2001). Asymmetric inheritance of radial glial fibers by cortical neurons. Neuron *31*, 727-741.

Miyata, T., Kawaguchi, A., Saito, K., Kawano, M., Muto, T., and Ogawa, M. (2004). Asymmetric production of surface-dividing and non-surface-dividing cortical progenitor cells. Development *131*, 3133-3145.

Miyata, T., Kawaguchi, D., Kawaguchi, A., and Gotoh, Y. (2010). Mechanisms that regulate the number of neurons during mouse neocortical development. Curr Opin Neurobiol *20*, 22-28.

Miyata, T., Maeda, T., and Lee, J.E. (1999). NeuroD is required for differentiation of the granule cells in the cerebellum and hippocampus. Genes Dev *13*, 1647-1652.

Molyneaux, B.J., Arlotta, P., Menezes, J.R., and Macklis, J.D. (2007). Neuronal subtype specification in the cerebral cortex. Nat Rev Neurosci *8*, 427-437.

Morrison, S.J. (2001). Neuronal potential and lineage determination by neural stem cells. Curr Opin Cell Biol *13*, 666-672.

Mu, Y., Lee, S.W., and Gage, F.H. (2010). Signaling in adult neurogenesis. Curr Opin Neurobiol.

Mühlfriedel, S., Kirsch, F., Gruss, P., Chowdhury, K., and Stoykova, A. (2007). Novel genes differentially expressed in cortical regions during late neurogenesis. Eur J Neurosci *26*, 33-50.

Muyrers, J.P., Zhang, Y., and Stewart, A.F. (2001). Techniques: Recombinogenic engineering--new options for cloning and manipulating DNA. Trends Biochem Sci *26*, 325-331.

Muzio, L., DiBenedetto, B., Stoykova, A., Boncinelli, E., Gruss, P., and Mallamaci, A. (2002). Conversion of cerebral cortex into basal ganglia in Emx2(-/-) Pax6(Sey/Sey) double-mutant mice. Nat Neurosci *5*, 737-745.

Nadarajah, B., Alifragis, P., Wong, R.O., and Parnavelas, J.G. (2003). Neuronal migration in the developing cerebral cortex: observations based on real-time imaging. Cereb Cortex *13*, 607-611.

Nakakura, E.K., Watkins, D.N., Schuebel, K.E., Sriuranpong, V., Borges, M.W., Nelkin, B.D., and Ball, D.W. (2001a). Mammalian Scratch: a neural-specific Snail family transcriptional repressor. Proc Natl Acad Sci U S A *98*, 4010-4015.

Nakakura, E.K., Watkins, D.N., Sriuranpong, V., Borges, M.W., Nelkin, B.D., and Ball, D.W. (2001b). Mammalian Scratch participates in neuronal differentiation in P19 embryonal carcinoma cells. Brain Res Mol Brain Res *95*, 162-166.

Nieto, M., Monuki, E.S., Tang, H., Imitola, J., Haubst, N., Khoury, S.J., Cunningham, J., Gotz, M., and Walsh, C.A. (2004). Expression of Cux-1 and Cux-2 in the subventricular zone and upper layers II-IV of the cerebral cortex. J Comp Neurol *479*, 168-180.

Nieto, M.A. (2001). The early steps of neural crest development. Mech Dev *105*, 27-35.

Nieto, M.A. (2002). The snail superfamily of zinc-finger transcription factors. Nat Rev Mol Cell Biol *3*, 155-166.

Noctor, S.C., Flint, A.C., Weissman, T.A., Dammerman, R.S., and Kriegstein, A.R. (2001). Neurons derived from radial glial cells establish radial units in neocortex. Nature *409*, 714-720.

Noctor, S.C., Martinez-Cerdeno, V., Ivic, L., and Kriegstein, A.R. (2004). Cortical neurons arise in symmetric and asymmetric division zones and migrate through specific phases. Nat Neurosci *7*, 136-144.

Nowakowski, R.S., Caviness, V.S., Jr., Takahashi, T., and Hayes, N.L. (2002). Population dynamics during cell proliferation and neuronogenesis in the developing murine neocortex. Results Probl Cell Differ *39*, 1-25.

Nowakowski, R.S., and Rakic, P. (1979). The mode of migration of neurons to the hippocampus: a Golgi and electron microscopic analysis in foetal rhesus monkey. J Neurocytol *8*, 697-718.

O'Leary, D.D. (1989). Do cortical areas emerge from a protocortex? Trends Neurosci *12*, 400-406.

O'Leary, D.D., Chou, S.J., and Sahara, S. (2007). Area patterning of the mammalian cortex. Neuron *56*, 252-269.

O'Leary, D.D., and Koester, S.E. (1993). Development of projection neuron types, axon pathways, and patterned connections of the mammalian cortex. Neuron *10*, 991-1006.

Ochiai, W., Yanagisawa, M., Takizawa, T., Nakashima, K., and Taga, T. (2001). Astrocyte differentiation of fetal neuroepithelial cells involving cardiotrophin-1-induced activation of STAT3. Cytokine *14*, 264-271.

Ohtsuka, T., Sakamoto, M., Guillemot, F., and Kageyama, R. (2001). Roles of the basic helix-loop-helix genes Hes1 and Hes5 in expansion of neural stem cells of the developing brain. J Biol Chem *276*, 30467-30474.

Olson, J.M., Asakura, A., Snider, L., Hawkes, R., Strand, A., Stoeck, J., Hallahan, A., Pritchard, J., and Tapscott, S.J. (2001). NeuroD2 is necessary for development and survival of central nervous system neurons. Dev Biol *234*, 174-187.

Peinado, H., Portillo, F., and Cano, A. (2005). Switching on-off Snail: LOXL2 versus GSK3beta. Cell Cycle *4*, 1749-1752.

Pinon, M.C., Tuoc, T.C., Ashery-Padan, R., Molnar, Z., and Stoykova, A. (2008). Altered molecular regionalization and normal thalamocortical connections in cortex-specific Pax6 knock-out mice. J Neurosci *28*, 8724-8734.

Pinto, L., and Gotz, M. (2007). Radial glial cell heterogeneity--the source of diverse progeny in the CNS. Prog Neurobiol *83*, 2-23.

Qian, X., Shen, Q., Goderie, S.K., He, W., Capela, A., Davis, A.A., and Temple, S. (2000). Timing of CNS cell generation: a programmed sequence of neuron and glial cell production from isolated murine cortical stem cells. Neuron *28*, 69-80.

Quinn, J.C., Molinek, M., Martynoga, B.S., Zaki, P.A., Faedo, A., Bulfone, A., Hevner, R.F., West, J.D., and Price, D.J. (2007). Pax6 controls cerebral cortical cell number by regulating exit from the cell cycle and specifies cortical cell identity by a cell autonomous mechanism. Dev Biol *302*, 50-65.

Rakic, P. (1972). Mode of cell migration to the superficial layers of fetal monkey neocortex. J Comp Neurol *145*, 61-83.

Rakic, P. (1988). Specification of cerebral cortical areas. Science *241*, 170-176.

Rakic, P. (2002). Evolving concepts of cortical radial and areal specification. Prog Brain Res *136*, 265-280.

Rakic, P. (2003). Developmental and evolutionary adaptations of cortical radial glia. Cereb Cortex *13*, 541-549.

Rallu, M., Machold, R., Gaiano, N., Corbin, J.G., McMahon, A.P., and Fishell, G. (2002). Dorsoventral patterning is established in the telencephalon of mutants lacking both Gli3 and Hedgehog signaling. Development *129*, 4963-4974.

Reynolds, B.A., and Weiss, S. (1992). Generation of neurons and astrocytes from isolated cells of the adult mammalian central nervous system. Science *255*, 1707-1710.

Roark, M., Sturtevant, M.A., Emery, J., Vaessin, H., Grell, E., and Bier, E. (1995). scratch, a pan-neural gene encoding a zinc finger protein related to snail, promotes neuronal development. Genes Dev *9*, 2384-2398.

Ross, S.E., Greenberg, M.E., and Stiles, C.D. (2003). Basic helix-loop-helix factors in cortical development. Neuron *39*, 13-25.

Roybon, L., Deierborg, T., Brundin, P., and Li, J.Y. (2009). Involvement of Ngn2, Tbr and NeuroD proteins during postnatal olfactory bulb neurogenesis. Eur J Neurosci *29*, 232-243.

Saito, T., and Nakatsuji, N. (2001). Efficient gene transfer into the embryonic mouse brain using in vivo electroporation. Dev Biol *240*, 237-246.

Sanada, K., and Tsai, L.H. (2005). G protein betagamma subunits and AGS3 control spindle orientation and asymmetric cell fate of cerebral cortical progenitors. Cell *122*, 119-131.

Sasaki, S., Tabata, H., Tachikawa, K., and Nakajima, K. (2008). The cortical subventricular zone-specific molecule Svet1 is part of the nuclear RNA coded by the putative netrin receptor gene Unc5d and is expressed in multipolar migrating cells. Mol Cell Neurosci *38*, 474-483.

Sato, Y., Hirata, T., Ogawa, M., and Fujisawa, H. (1998). Requirement for early-generated neurons recognized by monoclonal antibody lot1 in the formation of lateral olfactory tract. J Neurosci *18*, 7800-7810.

Sauer, B. (1998). Inducible gene targeting in mice using the Cre/lox system. Methods *14*, 381-392.

Sauer, B., and Henderson, N. (1989). Cre-stimulated recombination at loxP-containing DNA sequences placed into the mammalian genome. Nucleic Acids Res *17*, 147-161.

Scardigli, R., Baumer, N., Gruss, P., Guillemot, F., and Le Roux, I. (2003). Direct and concentration-dependent regulation of the proneural gene Neurogenin2 by Pax6. Development *130*, 3269-3281.

Scardigli, R., Schuurmans, C., Gradwohl, G., and Guillemot, F. (2001). Crossregulation between Neurogenin2 and pathways specifying neuronal identity in the spinal cord. Neuron *31*, 203-217.

Schuurmans, C., Armant, O., Nieto, M., Stenman, J.M., Britz, O., Klenin, N., Brown, C., Langevin, L.M., Seibt, J., Tang, H., *et al.* (2004). Sequential phases of cortical

specification involve Neurogenin-dependent and -independent pathways. EMBO J *23*, 2892-2902.

Schuurmans, C., and Guillemot, F. (2002). Molecular mechanisms underlying cell fate specification in the developing telencephalon. Curr Opin Neurobiol *12*, 26-34.

Schwab, M.H., Bartholomae, A., Heimrich, B., Feldmeyer, D., Druffel-Augustin, S., Goebbels, S., Naya, F.J., Zhao, S., Frotscher, M., Tsai, M.J., *et al.* (2000). Neuronal basic helix-loop-helix proteins (NEX and BETA2/Neuro D) regulate terminal granule cell differentiation in the hippocampus. J Neurosci *20*, 3714-3724.

Schwab, M.H., Druffel-Augustin, S., Gass, P., Jung, M., Klugmann, M., Bartholomae, A., Rossner, M.J., and Nave, K.A. (1998). Neuronal basic helix-loop-helix proteins (NEX, neuroD, NDRF): spatiotemporal expression and targeted disruption of the NEX gene in transgenic mice. J Neurosci *18*, 1408-1418.

Sessa, A., Mao, C.A., Hadjantonakis, A.K., Klein, W.H., and Broccoli, V. (2008). Tbr2 directs conversion of radial glia into basal precursors and guides neuronal amplification by indirect neurogenesis in the developing neocortex. Neuron *60*, 56-69.

Seugnet, L., Simpson, P., and Haenlin, M. (1997). Transcriptional regulation of Notch and Delta: requirement for neuroblast segregation in Drosophila. Development *124*, 2015-2025.

Smart, I.H. (1973). Proliferative characteristics of the ependymal layer during the early development of the mouse neocortex: a pilot study based on recording the number, location and plane of cleavage of mitotic figures. J Anat *116*, 67-91.

Smart, I.H., Dehay, C., Giroud, P., Berland, M., and Kennedy, H. (2002). Unique morphological features of the proliferative zones and postmitotic compartments of the neural epithelium giving rise to striate and extrastriate cortex in the monkey. Cereb Cortex *12*, 37-53.

Spemann, H., and Mangold, H. (2001). Induction of embryonic primordia by implantation of organizers from a different species. 1923. Int J Dev Biol *45*, 13-38.

Stoykova, A., Treichel, D., Hallonet, M., and Gruss, P. (2000). Pax6 modulates the dorsoventral patterning of the mammalian telencephalon. J Neurosci *20*, 8042-8050.

Sur, M., and Rubenstein, J.L. (2005). Patterning and plasticity of the cerebral cortex. Science *310*, 805-810.

Tabata, H., Kanatani, S., and Nakajima, K. (2009). Differences of migratory behavior between direct progeny of apical progenitors and basal progenitors in the developing cerebral cortex. Cereb Cortex *19*, 2092-2105.

Tabata, H., and Nakajima, K. (2003). Multipolar migration: the third mode of radial neuronal migration in the developing cerebral cortex. J Neurosci *23*, 9996-10001.

Tarabykin, V., Stoykova, A., Usman, N., and Gruss, P. (2001). Cortical upper layer neurons derive from the subventricular zone as indicated by Svet1 gene expression. Development *128*, 1983-1993.

Tomioka, N., Osumi, N., Sato, Y., Inoue, T., Nakamura, S., Fujisawa, H., and Hirata, T. (2000). Neocortical origin and tangential migration of guidepost neurons in the lateral olfactory tract. J Neurosci *20*, 5802-5812.

Tuoc, T.C., Radyushkin, K., Tonchev, A.B., Pinon, M.C., Ashery-Padan, R., Molnar, Z., Davidoff, M.S., and Stoykova, A. (2009). Selective cortical layering abnormalities and behavioral deficits in cortex-specific Pax6 knock-out mice. J Neurosci *29*, 8335-8349.

Visel, A., Thaller, C., and Eichele, G. (2004). GenePaint.org: an atlas of gene expression patterns in the mouse embryo. Nucleic Acids Res *32*, D552-556.

Warming, S., Costantino, N., Court, D.L., Jenkins, N.A., and Copeland, N.G. (2005). Simple and highly efficient BAC recombineering using galK selection. Nucleic Acids Res *33*, e36.

Weinstein, D.C., and Hemmati-Brivanlou, A. (1999). Neural induction. Annu Rev Cell Dev Biol *15*, 411-433.

Wolfer, D.P., Henehan-Beatty, A., Stoeckli, E.T., Sonderegger, P., and Lipp, H.P. (1994). Distribution of TAG-1/axonin-1 in fibre tracts and migratory streams of the developing mouse nervous system. J Comp Neurol *345*, 1-32.

Wrobel, C.N., Mutch, C.A., Swaminathan, S., Taketo, M.M., and Chenn, A. (2007). Persistent expression of stabilized beta-catenin delays maturation of radial glial cells into intermediate progenitors. Dev Biol *309*, 285-297.

Wu, S.X., Goebbels, S., Nakamura, K., Kometani, K., Minato, N., Kaneko, T., Nave, K.A., and Tamamaki, N. (2005). Pyramidal neurons of upper cortical layers generated by NEX-positive progenitor cells in the subventricular zone. Proc Natl Acad Sci U S A *102*, 17172-17177.

Xu, Z.P., Dutra, A., Stellrecht, C.M., Wu, C., Piatigorsky, J., and Saunders, G.F. (2002). Functional and structural characterization of the human gene BHLHB5, encoding a basic helix-loop-helix transcription factor. Genomics *80*, 311-318.

Zhong, Y., Takemoto, M., Fukuda, T., Hattori, Y., Murakami, F., Nakajima, D., Nakayama, M., and Yamamoto, N. (2004). Identification of the genes that are expressed in the upper layers of the neocortex. Cereb Cortex *14*, 1144-1152.

Zimmer, C., Tiveron, M.C., Bodmer, R., and Cremer, H. (2004). Dynamics of Cux2 expression suggests that an early pool of SVZ precursors is fated to become upper cortical layer neurons. Cereb Cortex *14*, 1408-1420.

III. SUPPLEMENT

ABBREVIATIONS:

Short name	Full name
AB	antibody
AP	anterior-posterior
AVE	anterior visceral endoderm
bHLH	basic helix-loop-helix
BLBP	brain lipid binding protein
BMP	bone morphogenesis protein
BrdU	5-bromo-2-desoxy-uridine
BSA	bovine serum albumin
C-	carboxyl-
CC	corpus callous
cDNA	complementary desoxy-ribonucleic acid
CGE	caudal ganglionic eminence
ChIP	chromatin immunoprecipitation
CHORI	Children's Hospital Oakland Research Institute
cKO	conditional knockout
CNS	central nervous system
CP	cortical plate
cDNA	complementary DNA
CR	Cajal-Retzius
Cre	cyclization recombination
CV	cresylviolet
Dcx	doublecortin
DV	dorsal-ventral
DG	dentate gyrus
DIG	digoxygenin
DIV	days of *in vitro* culture
DAPI	4'-6'-diamidino-2-phenylindole
DEPC	diethylpyrocarbonate
DIG	digoxigenin
DIV	days in-vitro
DP	Dorsal pallium
DNA	desoxy-ribonucleic acid
DNase	desoxyribonuclease
DG	dentate gyrus
Div	days in vitro
DMEM	Dulbecco modified Eagle's minimal essential medium
dNTPs	desoxyribonucleotides
DOC	desoxycholate
DTT	dithiothreitol
E	embryonic day
EDTA	ethylenediaminetetracetic acid
EMT	epithelial-Mesenchymal Transition
EST	expressed sequence tags
FCS	fetal calf serum
FGF	fibroblast growth factor,
Flp	flippase recombination enzyme
Frt	flippase recognition target
GABA	γ- aminobutyric acid

GE	ganglion eminence
GFAP	glial fibrillary acidic protein
GFP	green fluorescent protein
GOF	gain of function
HBSS	Hank's balanced salt solution
HEPES	hydroxyethyl-piperazineethanesulfonic acid
HD-TF	Homeobox domain transcription factor
Hi	Hippocampus
ICC	Immuno-cytochemistry
IHC	Immuno-histochemistry
INM	internuclear migration
INs	Interneurons
IP	intermediate progenitor cell
IRES	internal ribosomal entry side
IPs	Intermediate progenitors
ISH	*In-situ* hybridization
IUE	*In-utero* electroporation
IZ	Intermediate zone
L	Layer
lacZ	β-galactosidase (gene)
LGE	Lateral ganglion eminence
loxP	locus of X-over P1
MEMFA	MOPS/EGTA/Magnesium sulphate/formaldehyde buffer
MGE	Media ganglion eminence
ML	medial-lateral
MZ	Marginal zone
N-	amino-
NBT/BCIP	nitro blue tetrazolium / bromo-chloro-indolyl phosphate
NCBI	National Centre for Biotechnology Information
NEO	neomycin
NEP	Neuroepithelial cell progenitor
NGS	Normal Goat Serum
NIH	National Institutes of Health
NLS	nuclear localization signal
OB	Olfactory Bulb
ORF	open reading frame
P	Postnatal Day
PAC	Prophage Artificial Chromosome
PAGE	polyacrylamide gel electrophoresis
PFA	paraformaldehyde
PBS	phosphate buffered saline
PCR	polymerase chain reaction
PDL	poly-D-lysine
PFA	paraformaldehyde
PP	Preplate
PSPB	Pallial-subpallial border
PTM	Post-translation modification
qPCR	Quantitative RT-PCR
RA	retinoid acid
RGC	Radial glia cell
RMS	Rostral migratory streams
RNA	ribonucleic acid
RNase	ribonuclease

RMS	rostral migratory stream
RNA	ribonucleic acid
Rpm	rounds per minute
RT	room temperature
RT-PCR	real time-polymerase chain
SDS	sodium dodecyl sulphate
Sey	Small eye
sFRP2	secreted frizzled-related protein 2
SEM	standard error of the mean
SEZ	subependymal zone
Shh	Sonic hedgehog homolog
shRNA	Short hairpin RNA interference
smRNA	Small modulatory RNA
SNAG	Snail and Gfi-1
SP	subplate
SVZ	subventricular zone
TBE	Tris-borate-EDTA
TCA	thalamo-cortical afferences
TE	Tris / EDTA (buffer)
TF	transcription factor
TK	thymidine kinase
Tris	tris(hydroxymethyl)aminomethane
U	unit
UTR	untranslated region
V	ventricle
VZ	Ventricular zone
WB	Western blot
WM	White matter
Wnt	wingless / int (genes in drosophila)
X-gal	bromo-chloro-indolyl-galactopyranoside

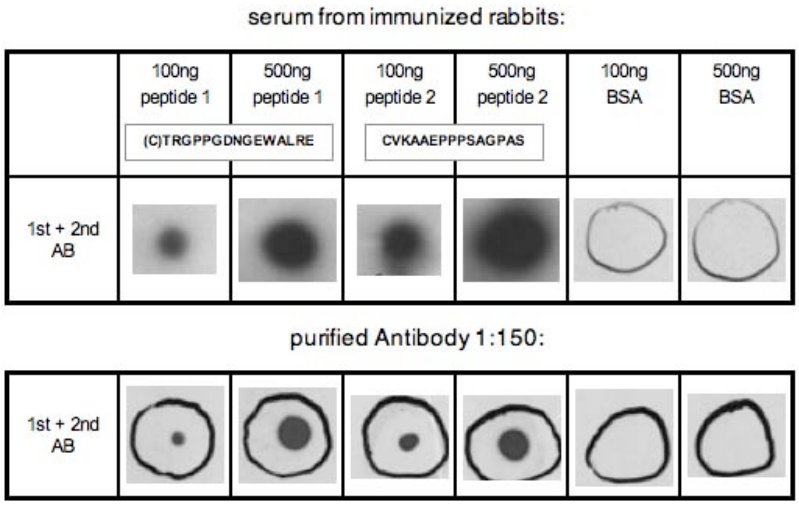

Figure 40: Dot-blot analysis on antigen peptide. Sera from rabbits were diluted 1:1 with PBS; a nitrocellulose membrane was spotted with Scrt2 peptide(s) or BSA at 100 and 500 ng and then blotted with diluted serum or purified antibody (1:150). Secondary antibody HRP-anti-rabbit was applied 1:10.000; dots were only secondary AB was applied were negative (negative control)

Gene		Identity (%)	
Species	Symbol	Protein	DNA
Mus musculus	**Scrt2**		
vs. Homo sapiens	SCRT2	93.1	91.5
vs. Rattus norvegicus	Scrt2	99.2	97.3
vs. Danio rerio	zgc:162551	62.1	66.7

Table 2: The homology of *Scrt2* between different vertebrates. Pair wise alignment scores (from NCBI-HomoloGene: 99867) for mouse Scrt2 mRNA and protein level are shown.

Figure 41: Western-blot analysis with two different Scrt2-antibodies on cortical extracts. Cortical tissiue from different developmental stages was isolated and protein extracts were prepared as described in 4.4.14 and used for SDS-PAGE and western blot (4.6.16). Primary α-Scrt2 antibodies were applied (rb 1:500), secondary

antibody α-rb-HRP (1:10.000). Note that the lab made antibody exclusively detected a peptide fragment of about 32 kDa, corresponding to Scrt2.2, while the AB from Santa Cruz exclusively detected a peptide fragment of about 50 kDa, corresponding to Scrt2.3.

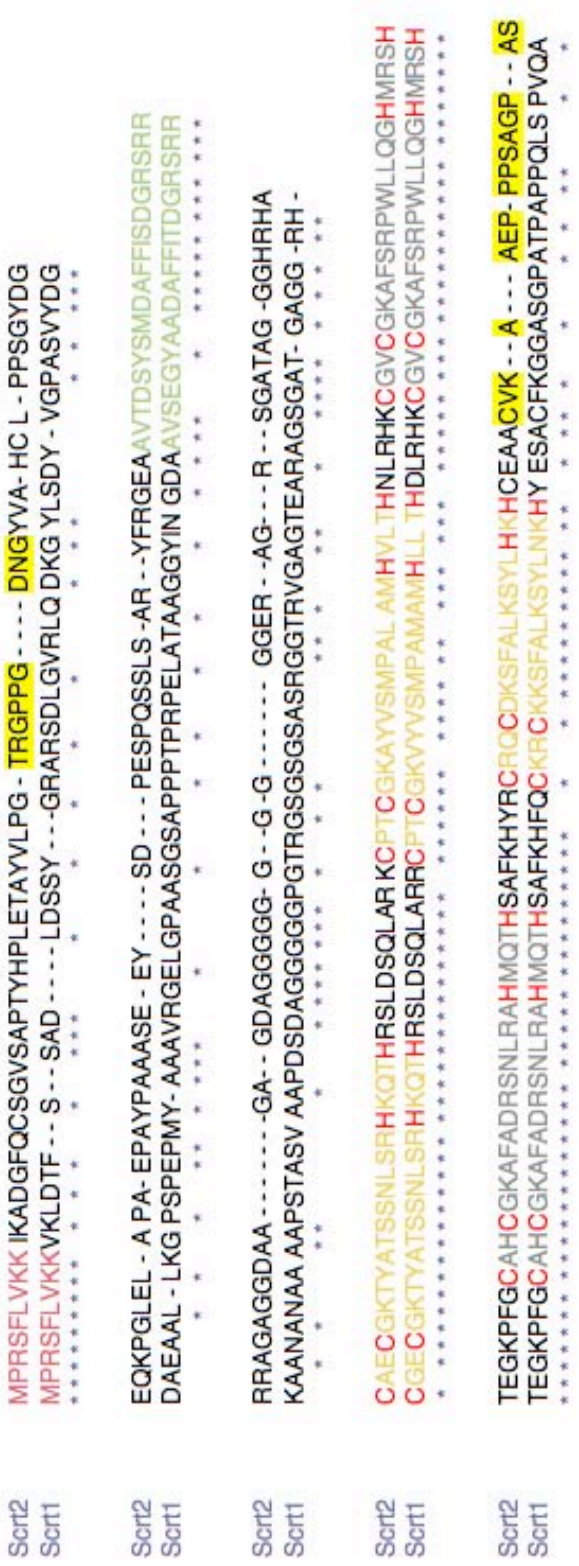

Figure 42: Amino acid wise alignment of the open reading frames (ORF) of mouse Scrt2 and Scrt1. The SNAG domain is highlighted in violet, the Scratch-specific zinc-finger in orange and the C_2H_2-superfamily common zinc-fingers in grey. The peptide sequences, marked in yellow indicate the epitopes that have been chosen to generate Scrt2-specific antibody.

Figure 43: Protein domains of predicted alternatively spliced transcripts of the *mScrt2* gene. The corresponding transcript-IDs and their nucleotide-size as well as their date of announcement in NCBI, the number of coding amino acids and the given name are shown in the upper row of each version. Homologous peptide domains present in an individual protein are indicated in the same cooler (A - H), as also used in figure 16.

Name: **opti-Scrt2.2** (976 bp)

ORF: 936 bp protein= 312 aa

Cloning sites: SacI / EcoRI

gcggccgcctcgag**gagctc**ATGCCTAGGAGCTTTCTGGTGAAGAAGATCAAGGCTGACGGCTTTCAGTGCTC
CGGAGTGTCCGCTCCCACCTACCACCCTCTGGAGACCGCCTACGTGCTGCCAGGAACACGCGGACCTC
CCGGCGATAACGGATACGTGGCCCACTGCCTGCCTCCTAGCGGATACGACGGAGAGCAGAAGCCCGG
ACTGGAGCTGGCTCCTGCCGAGCCTGCCTACCCTGCTGCCGCCTCCGAGGAGTACTCCGACCCTGAGT
CCCCCCAGTCTTCTCTGAGCGCCAGGTATTTCCGGGGCGAGGCTGCCGTGACCGACAGCTACAGCATG
GACGCCTTCTTCATCTCCGACGGAAGAAGCAGGAGGAGAAGAGCCGGCGCCGGAGGAGATGCCGCC
GGAGCTGGCGATGCCGGCGGAGGAGGCGGAGGAGGAGGCGGCGGCGAGAGAGCTGGAAGATCTGG
CGCCACCGCCGGCGGCGGCCACAGACACGCCTGTGCCGAGTGCGGAAAGACCTACGCCACAAGCAGC
AACCTGTCTAGGCACAAGCAGACACACCGGTCCCTGGATTCTCAGCTGGCTAGGAAGTGTCCCACATG
TGGAAAGGCCTACGTGTCCATGCCTGCCCTGGCTATGCACGTGCTGACCCACAATCTGAGACACAAGT
GCGGCGTGTGCGGCAAGGCCTTCTCCAGACCATGGCTGCTGCAGGGCCACATGCGCAGCCACACAGG
AGAGAAGCCCTTCGGATGCGCCCACTGTGGCAAGGCCTTTGCTGACAGGTCCAACCTGAGAGCCCAC
ATGCAGACACACAGCGCCTTCAAGCACTATAGATGCAGGCAGTGCGATAAGTCTTTCGCCCTGAAGTC
CTACCTGCACAAGCACTGCGAGGCTGCTTGCGTGAAGGCTGCTGAGCCTCCCCCCAGCGCCGGACCT
GCCTCCTGA**gaattc**ctcgaggcggccgc

Name: **opti-Scrt2.3** (1509 bp)

ORF: 1491 bp protein: 496 aa

Cloning sites: XhoI

ccg**ctcgag**ATGATGAAGAAAGAATCCCGTTCGTCCAGCCTGCTGGACATAGTGAACTCCTGGGACCTG
GCATGCGTGCCATATAAAGCGGGAAGTCGATCAGCCGAACATAGCTATAGCGACCGTCTGTGTGCAC
GGCGTCGCCGACGTCGCCGGCGCCGTCGCAGAGCGCGCGCGGCCCCCGAGCCAGAACCCCGCCCCTC
ACCCCCGCGTCGCCTGCGTGGACGCCCACCCGCAGGCAGCTGCCCAGTGCTGAAACCGGCACCCACA
GCGAATCGTGCCGGCCGTCCCCCGCCCCCGCCAGGACTCCCCTGTCCAGCAAGCCCGCCGCCGGGTTG
TACCATGCCCCGGAGCTTCCTGGTGAAGAAGATTAAAGCGGACGGCTTTCAATGTTCGGGTGTGAGC
GCGCCCACCTACCACCCGCTGGAAACAGCGTATGTGCTGCCCGGTACCCGCGGACCACCCGGTGATAA
TGGCGAGTGGGCGCTGCGTGAAGGTAGCGGTGGCAGCCCCACATGGGCGGCAGCGGGAAACCGCGG
TGGCGATGTACGTGGTCGCGAGCATCCCCGCGACTTCCAGAGAACAGGTCGGGCGGGCCTGGGTCTG
GGACGAACTAAGGAATCAGGCCGCGTCGGTAGCTCCCGTTCACATGCCCCCATAGGCACCCTGAAGG
TTGTGGCGTTAGAGTACGGTTGGAGTTACGTCGCCCACTGTCTGCCGCCATCGGGTTATGATGGAGA
ACAGAAACCGGGTCTGGAGCTGGCACCGGCGGAACCGGCATACCCCGCCGCGGCCAGCGAGGAGTAT
TCCGACCCCGAATCACCCCAGTCGAGCCTGTCAGCACGTTACTTTCGAGGCGAGGCCGCAGTTACCGA
CTCCTACAGCATGGATGCGTTCTTCATCAGCGACGGTCGTTCTAGACGACGCCGTGCGGGCGCCGGT
GGAGACGCGGCCGGAGCCGGTGACGCCGGCGGCGGGGGTGGCGGTGGCGGCGGAGGAGAGCGTGC
AGGCCGTTCCGGTGCCACGGCGGGCGGCGGCCATCGTCACGCCTGCGCGGAGTGCGGTAAAACATAC
GCCACAAGCAGCAATCTGAGCCGGCATAAGCAGACACATCGCAGCCTGGATTCGCAGCTGGCCCGCA
AGTGTCCGACCTGCGGGAAGGCCTACGTGAGCATGCCCGCACTGGCCATGCATGTGCTGACCCATAA
TCTGCGTCATAAGTGCGGAGTGTGTGGCAAAGCCTTCAGCCGTCCCTGGCTGCTGCAGGGTCATATG
CGCTCCCATACGGGTGAAAAGCCGTTTGGTTGTGCCCACTGCGGCAAGGCATTTGCCGATCGTAGCA
ATCTGCGGGCACACATGCAAACCCACTCAGCCTTCAAACACTACCGTTGTCGTCAGTGTGATAAGTCA
TTCGCGCTGAAGAGCTACCTGCATAAGCACTGTGAAGCGGCCTGCGTGAAAGCGGCCGAGCCCCCAC
CGTCTGCGGGTCCGGCAAGCTGA**ctcgagc**gg

Figure 44: Codon-optimized DNA-sequences of the used *Scrt2.2* and *Scrt2.3* open reading frames. The nucleotide size and the resulting number of amino acids are shown in the top of the two ORFs; the small letters indicate the additional nucleotides encoding recognition sites (in bold) of the restriction enzyme used for cloning. Start and stop codons are underlined.

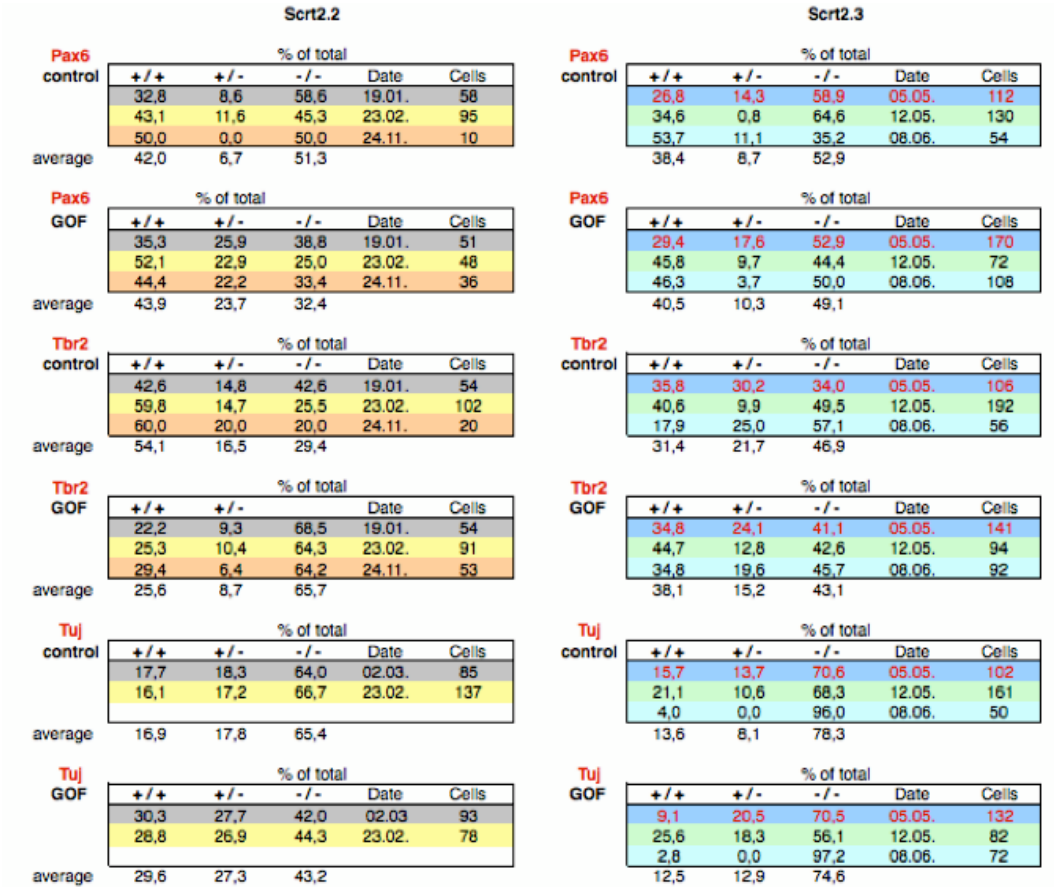

Scrt2.2

		% of total			
Pax6 control	+/+	+/-	-/-	Date	Cells
	32,8	8,6	58,6	19.01.	58
	43,1	11,6	45,3	23.02.	95
	50,0	0,0	50,0	24.11.	10
average	42,0	6,7	51,3		

		% of total			
Pax6 GOF	+/+	+/-	-/-	Date	Cells
	35,3	25,9	38,8	19.01.	51
	52,1	22,9	25,0	23.02.	48
	44,4	22,2	33,4	24.11.	36
average	43,9	23,7	32,4		

		% of total			
Tbr2 control	+/+	+/-	-/-	Date	Cells
	42,6	14,8	42,6	19.01.	54
	59,8	14,7	25,5	23.02.	102
	60,0	20,0	20,0	24.11.	20
average	54,1	16,5	29,4		

		% of total			
Tbr2 GOF	+/+	+/-		Date	Cells
	22,2	9,3	68,5	19.01.	54
	25,3	10,4	64,3	23.02.	91
	29,4	6,4	64,2	24.11.	53
average	25,6	8,7	65,7		

		% of total			
Tuj control	+/+	+/-	-/-	Date	Cells
	17,7	18,3	64,0	02.03.	85
	16,1	17,2	66,7	23.02.	137
average	16,9	17,8	65,4		

		% of total			
Tuj GOF	+/+	+/-	-/-	Date	Cells
	30,3	27,7	42,0	02.03	93
	28,8	26,9	44,3	23.02.	78
average	29,6	27,3	43,2		

Scrt2.3

		% of total			
Pax6 control	+/+	+/-	-/-	Date	Cells
	26,8	14,3	58,9	05.05.	112
	34,6	0,8	64,6	12.05.	130
	53,7	11,1	35,2	08.06.	54
	38,4	8,7	52,9		

		% of total			
Pax6 GOF	+/+	+/-	-/-	Date	Cells
	29,4	17,6	52,9	05.05.	170
	45,8	9,7	44,4	12.05.	72
	46,3	3,7	50,0	08.06.	108
	40,5	10,3	49,1		

		% of total			
Tbr2 control	+/+	+/-	-/-	Date	Cells
	35,8	30,2	34,0	05.05.	106
	40,6	9,9	49,5	12.05.	192
	17,9	25,0	57,1	08.06.	56
	31,4	21,7	46,9		

		% of total			
Tbr2 GOF	+/+	+/-	-/-	Date	Cells
	34,8	24,1	41,1	05.05.	141
	44,7	12,8	42,6	12.05.	94
	34,8	19,6	45,7	08.06.	92
	38,1	15,2	43,1		

		% of total			
Tuj control	+/+	+/-	-/-	Date	Cells
	15,7	13,7	70,6	05.05.	102
	21,1	10,6	68,3	12.05.	161
	4,0	0,0	96,0	08.06.	50
	13,6	8,1	78,3		

		% of total			
Tuj GOF	+/+	+/-	-/-	Date	Cells
	9,1	20,5	70,5	05.05.	132
	25,6	18,3	56,1	12.05.	82
	2,8	0,0	97,2	08.06.	72
	12,5	12,9	74,6		

Figure 45: Clonal-pair analysis of cortical progenitor divisions. On the left is shown the analysis under *Scrt2.2*-GOF condition, on the right the analysis of *Scrt2.3*-GOF. Each individual experiment is displayed by the same colour code and the IHC- staining is shown as blocks. The values of each row present the percental portions of all analysed GFP+ cell pairs per IHC-condition. These data present the raw data, prove of significance is included in the diagrams of figures 27 and 28 respectively.

INDEX OF FIGURES / TABLES

Fig. 1: The primary brain vesicles……2
Fig. 2: Early signalling centres in the telencephalon……2
Fig. 3: Patterning of the telencephalon……3
Fig. 4: Origins and migrational pathways of cortical neurons……4
Fig. 5: Progenitor cell divisions and neurogenesis in the embryonic neocortex……6
Fig. 6: Generation and identity of neocortical layers……8
Fig. 7: Lineage restricted genes in subpopulation of cortical projection neurons and their corresponding progenitors……9
Fig. 8: Evolution C2H2 zinc finger transcription factors and structural / functional domains of Scratch proteins……13
Fig. 9: mScrt2 expression in the embryonic mouse brain……16
Fig. 10: *Pax6*-dependent down-regulation of in *mScrt2* in the embryonic cortex……17
Fig. 11: TFs Scrt2 and Ngn2 show similar regionalized pattern defects in the *Pax6* deficient cortex……17
Fig. 12: Scrt2 protein expression in the late embryonic and postnatal cortex……18
Fig. 13: *mScrt2* expression in the postnatal brain……19
Fig. 14: Scrt2 expression in GABAergic interneurons and newly post-mitotic granular cells in the IGL of the cerebellum……20
Fig. 15: Structure of the provisional mouse Scratch2 transcript……20
Fig. 16: Predicted mScrt2 isoforms encoded by alternatively spliced *Scrt2* transcripts……22
Fig. 17: The principle of the Cre-loxP based strategy for conditional *mScrt2* activation in transgenic mice……23
Fig. 18: Functional analysis of the *Scrt2.2-pJoJo* construct……24
Fig. 19: Cre-mediated recombination in *Scrt2-pJoJo;Emx1Cre* double transgenic mice……25
Fig. 20: Cre-mediated lacZ-reporter expression in brains of *Scrt2.2-pJoJo* mice……26
Fig. 21: Over expression of *mScrt2* in the generated *Scrt2.2;Emx1Cre* transgenic mice……27
Fig. 22: Decreased cortical thickness in *Scrt2.2* double transgenic brains at P10……28
Fig. 23: Decreased presentation of mature astrocytes in the postnatal cortex (P10) in *Scrt2.2*-GOF brains……29
Fig. 24: Early phenotype (E12.5) of *Scrt2.2-pJoJo;Emx1Cre* cortex……31
Fig. 25: Cortical phenotype of *Scrt2.2-pJoJo;Emx1Cre* mice at E16.5…… 33
Fig. 26: Principle of the clonal-pair analysis……36
Fig. 27: Clonal-pair types, analyzed by IHC-staining……37
Fig. 28: *In-vitro* clonal-pair analysis after in-vivo *mScrt2.2*-GOF……38
Fig. 29: Focal *mScrt2.2*-overexpression in cortical progenitors using *in-utero* electroporation ……39
Fig. 30: Accumulation of targeted cells with GFP+/scrt2.2 expression vector In the SVZ of the developing cortex……40

Fig. 31: Impaired cell migration after *Scrt2.3* expression in cortical progenitors……..41
Fig. 32: Postnatal phenotype in the cortex after ectopic expression of *mScrt2.3* in RGPs……....43
Fig. 33: Schematic cascade of early events in *Xenopus* neurogenesis…….44
Fig. 34: *mScrt2.2*-GR expands the neural plate and inhibits neuronal commitment at the open neural plate stage…….....45
Fig. 35: At the tail bud stage, *mScrt2.2*-GR reduces the number of differentiating neurons anteriorly 46
Fig. 36: *mScrt2.2*-GR affects neural marker gene expression in neuralized *Xenopus* animal caps…..47
Fig. 37: Construction and functional analysis of the *Scrt2* conditional knock out vector…….....49
Fig. 38: Targeting of the *Scrt2* genomic locus with the cKO construct in ES cells……....51
Fig. 39: Generation of the *Scrt2* conditional knockout vector via recombineering…….....70
Fig. 40: Dot-blot analysis on antigen peptides……....102
Fig. 41: Western blot analysis with two different Scrt2-antibodies on cortical extracts……..102
Fig. 42: Amino acid wise alignment of the open reading frames of mouse Scrt2 and Scrt1 ……103
Fig. 43: Protein domains of predicted alternatively spliced transcripts of the *mScrt2* gene……..104
Fig. 44: Codon-optimized DNA-sequences of the used *Scrt2.2* and *Scrt2.3* open reading frames….105
Fig. 45: Clonal-pair analysis of cortical progenitor divisions……..106

Tab. 1: Summary of the regulatory effects in gene expression in *Scrt2.2*-GOF condition……..…….34
Tab. 2: The homology of Scrt2 between different vertebrates……....……102

IV. ACKNOWLEDGEMENTS

First of all, I like to express my gratitude to my supervisor, PD. Dr. Anastassia Stoykova for giving me the opportunity to work on this project and allowing me to expand my knowledge in the fascinating field of neurobiology. She gave me the possibility to develop my own ideas and to establish new approaches in the lab. Furthermore I am thankful for all the helpful discussions we had.

I thank the members of my thesis committee, Prof. Tomas Pieler and Prof. Klaus Armin Nave for the time they devoted to this project with critical comments and for the valuable discussions we had during our meetings. Finally, I thank Prof. Michael Hörner, Prof. Ernst Wimmer and Dr. Till Marquardt, who kindly agree to join my examination board.

I thank my collaborators, Dr. Barbara Rust and Dr. Kris Henningfeld for their performance of the Xenopus experiments.

Furthermore I want to thank the students of the CMPB program for their nice scientific and social co-operations.

My gratitude goes to all members of the department Molecular Cell Biology, especially to Dr. Tran Chong Tuoc and Dr. Anton Tonchev for supply of protocols, material and knowledge.

Special thanks go to Alexander Klimke, Simon Kordovich, Tamara Rabe and Marco Tylkowski for sharing excitement and frustration, successes and failures and their encouragement - as colleagues and friends.

I want to thank Dr. Yvonne Uerlings for providing me her recombineering experience, which enabled me to generate successfully a cKO-construct.

I appreciate technical assistance as well as motivating words of Martina Daniel and technical help with *in-utero* electroporation from Silke Schlott.

I am also grateful to Heike Fett and Christian Dietl from the BTL for maintenance and provision of mice as well as to Sahrif Mansur and Ulrich Franke for ES-cell electroporation and transfer.

I am thankful to Yvonne and Tamara for comments and correction on this script.

I am extremely grateful to my Dad for believing in me and for supporting my ambitions throughout my life.

And the best at the end: Frank, I thank you so much for your love and any kind of encouragement during these sometimes difficult years. You spend a lot of time, power and patrol ;-) allowing us to be together although 360 km separated to do my research. ♥

V. CURRICULUM VITAE

CURRICULUM VITAE

Personal data

Name:	Vanessa Paul
Date of birth:	April 18th 1981
Place of birth:	Menden, Germany
Nationality:	German

Academic Education

10/2001 - 12/2005	Biology studies, Ruhr-University Bochum, Germany
01/2005 - 12/2005	Diploma thesis, Ruhr-University Bochum, Germany Dept. Biochemistry II Receptor Biochemistry Head: Prof. Dr. Michael Hollmann
12/2005	Diploma examination; final grade 1.3
Since 06/2006	Research assistant, Max Planck Institute for Biophysical Chemistry, Dept. Molecular Cell Biology / Research Group Developmental Biology
09/2006 - 09/2010	PhD student of the Göttingen Graduate School for Neurosciences and Molecular Biosciences (GGNB); Program of the DFG Research Centre Molecular Physiology of the Brain (CMPB)

Work Experience

10/2003 - 01/2004	Student assistance; Ruhr-University Bochum, Germany, Dept. Biochemistry II
2007 - 2010	Tutor of the annual lecture course (1 week) of the International Max Planck Research School “Neuroscience” (MSc/PhD)

Contact Details

Department Molecular Cell Biology
Max Planck Institute for Biophysical Chemistry
Am Fassberg 11
37077 Göttingen, Germany
Phone: + 49 551 2011469
E-mail: vpaul@gwdg.de